HAW HAMBURG

CC4E

MASTERTHESIS

Analysis of the Impact of Household Heat Pumps and Photovoltaics on the Electricity Distribution Grid in Hamburg

Nicholas Tedjosantoso

Fakultät Life Sciences
Department Umwelttechnik

Faculty of Life Sciences
Department of Environmental Engineering

Nicholas Tedjosantoso

Analysis of the Impact of Household Heat Pumps and Photovoltaics on the Electricity Distribution Grid in Hamburg

Masterarbeit eingereicht im Rahmen der Masterprüfung
im Studiengang Renewable Energy Systems
am Department Umwelttechnik und Verfahrenstechnik
der Fakultät Life Sciences
der Hochschule für Angewandte Wissenschaften Hamburg

Betreuender Prüfer: Prof. Dr. Hans Schäfers
Zweitgutachter: M.Sc. Martin Grasenack

Eingereicht am: 22.01.2024

Title of the Master Thesis

Analysis of the Impact of Household Heat Pumps and Photovoltaics on the Electricity Distribution Grid in Hamburg

Keywords

Residential PV System, Residential Heat Pump, Battery Storage, Thermal Storage, Electricity Grid, Electrical Demand Time Series, Heat Demand Time Series, Linear Programming, ALKIS, LoD2, Census

Abstract

In this work, a model is developed to analyze the impact of household heat pumps and photovoltaics on the electricity distribution grid in Hamburg. Referring to existing studies and tools, this thesis first estimates the future heat and electricity demand, as well as the electricity generated by PV, for residential buildings in Hamburg. Based on a set of criteria, a specific energy system is then assigned to each building. Using this information as input, the total electricity demand is subsequently calculated using a linear optimization model. In this study, a total of 229,119 building objects are assessed. To evaluate the impact different combinations of technologies can have on the electricity distribution grid, the results are aggregated based on their approximate location in relation to the grid areas. Finally, two indicators, namely: full load hours and the ratio between the peak demands in positive (energy taken from the grid) and negative (energy fed into the grid) directions, are derived from the aggregated results to provide a simplified assessment of the grid situation.

Table of Contents

List of Figures

List of Tables

List of Acronyms

AdV	Working Committee of the Surveying Authorities of the States of the Federal Republic of Germany	*Arbeitsgemeinschaft der Vermessungsverwaltungen der Länder der Bundesrepublik Deutschland*
ALKIS	Authoritative Real Estate Cadastre Information System	*Amtliches Liegenschaftskatasterinformationssystem*
BSW	Ministry of Urban Development and Housing	*Behörde für Stadtentwicklung und Wohnen*
CAD	computer aided design	-
CHP	combined heat and power	-
COP	coefficient of performance	-
DAHV	daily accumulated heat volume	-
DSO	distribution system operator	-
EEHH	Renewable Energies Hamburg Cluster	*Cluster Erneuerbare Energien Hamburg*
EFH	Single-family house	*Einfamilienhaus*
WPG	Heat Planning Act	*Wärmeplanungsgesetz*
EEG	Renewable Energy Act	*Erneuerbare-Energien-Gesetz*
FfE	Research Center for Energy Economics e.V.	*Forschungsstelle für Energiewirtschaft e.V.*
GIS	Geographical Information System	-
GMH	Large multi-family building	*Großes Mehrfamilienhaus*
AGEB	Working Group on Energy Balances	*Arbeitsgemeinschaft Energiebilanzen e.V.*
HH	High-rise building	*Hochhaus*
IWU	-	*Institut Wohnen und Umwelt*
LoD2	3D Lod2 City Model	*3D-Gebäudemodell LoD2*
LP	linear programming	-
MFH	Multi-family building	*Mehrfamilienhaus*
MILP	Mixed-Integer Linear Programming	-
FLH	full load hour	-
MV	medium-voltage	-
NUTS	Classification of Territorial Units for Statistics	-
LoD	level of detail	-
PV	Photovoltaic	-
RDV	relative daily variation	-
RH	Row-house	*Reihenhaus*
RHV	relative hourly variation	-
SIZEP	Sizing Evaluation Step	-
SLP	Standard Load Profiles	-
SVG	scalable vector graphics	-

TSO	transmission system operator	-
TUM	Technical University of Munich	*Technische Universität München*

List of Symbols

α	azimuth	$^\circ$
η_{AC2BAT}	AC to battery efficiency	$\%$
η_{BAT2AC}	battery to AC efficiency	$\%$
η_{PV2AC}	PV to AC efficiency	$\%$
η_{PV2BAT}	PV to battery efficiency	$\%$
$\eta_{TES,c}$	thermal storage charge efficiency	$\%$
$\eta_{TES,d}$	thermal storage discharge efficiency	$\%$
γ	tilt angle	$^\circ$
σ_{BAT}	battery daily self discharge rate	$\%$
σ_{TES}	thermal storage daily self discharge rate	$\%$
θ_amb	ambient temperature	C
a	building footprint area	m^2
A_{ref}	reference area for heat demand calculation	m^2
A_{type}	building use specific coefficient	-
b_H	heating line offset	-
B_{type}	building use specific coefficient	-
C_{BAT}	maximum battery capacity	*kWh*
COP	coefficient of performance	-
C_{type}	building use specific coefficient	-
D_{type}	building use specific coefficient	-
$h(\theta, type)$	daily normalized profile value	C
k_{hp}	heat pump utilization factor for heat demand	-
$k_{hp,c}$	heat pump utilization factor for thermal storage	-
L_d	annual average heat load	*W*
L_d	daily average heat load	*W*
L_h	hourly average heat load	*W*
b_W	hot water line offset	-
m_H	heating line gradient	-
m_W	hot water line gradient	-
P_{hp}	maximum heat ouput of heat pump	*kW*
PR	performance ratio	-
s	number of storeys	-
s_a	additional storey due to heated attic	-
T	set of all discrete periods of time	-
t	discrete time period	-
T_{sink}	sink temperature	$^\circ C$

T_{source}	source temperature	$°C$
W_{BAT}	energy stored in battery	kWh
$W_{BAT,c}$	energy charged into battery	kWh
$W_{BAT,d}$	energy discharged from battery	kWh
$W_{BAT,d,grid}$	energy discharged from battery for electricity grid	kWh
$W_{BAT,d,TES}$	energy discharged from battery for thermal storage	kWh
W_c	energy demand for compressor	kWh
W_{el}	electricity demand	kWh
$W_{el,max,n}$	peak electricity value in negative direction	kWh
$W_{el,max,p}$	peak electricity value in postive direction	kWh
$W_{el.heater}$	heat supply from electrical heater	kWh
$W_{el.heater,c}$	heat supply from electrical heater for thermal storage	kWh
$W_{el,hp}$	electricity demand from heat pump	kWh
$W_{el,limit}$	maximum electricity demand allowed during optimization	kWh
$W_{el,total}$	total electricity demand	kWh
$W_{el,total,n}$	total electricity demand in negative direction	kWh
$W_{el,total,p}$	total electricity demand in postive direction	kWh
$W_{grid,BAT}$	energy from the grid to charge battery	kWh
$W_{grid,TES}$	energy from the grid to charge thermal storage	kWh
W_{hp}	useful heat energy from heat pump	kWh
W_{pv}	PV generation	kWh
$W_{pv,BAT}$	PV generation for battery	kWh
$W_{pv,grid}$	PV generation for grid feed in	kWh
$W_{pv,TES}$	PV generation for thermal storage	kWh
W_{TES}	energy stored in thermal energy storage	kWh
$W_{TES,c}$	energy charged into thermal energy storage	kWh
$W_{TES,d}$	energy discharged from thermal energy storage	kWh
$W_{TES,max}$	maximum energy stored in thermal energy storage	kWh
W_{th}	heat demand	kWh

1 Introduction

According to a newly published report from the United Nations' Intergovernmental Panel on Climate Change (IPCC) from March 20, 2023, emissions of greenhouse gasses must decrease now and will need to be cut by approximately half by 2030 to realistically reach the goal of limiting global warming to 1.5 °C [1]. This urgent need to reduce greenhouse gas emission is also reflected in the German climate policy, where emissions are to be reduced by at least 65% by 2030 and by at least 88% by 2040 (compared to 1990) [2]. In Figure 1.1 the greenhouse gas emissions of Germany (in CO_2 equivalents) from the year 1990 up to 2022 is shown.

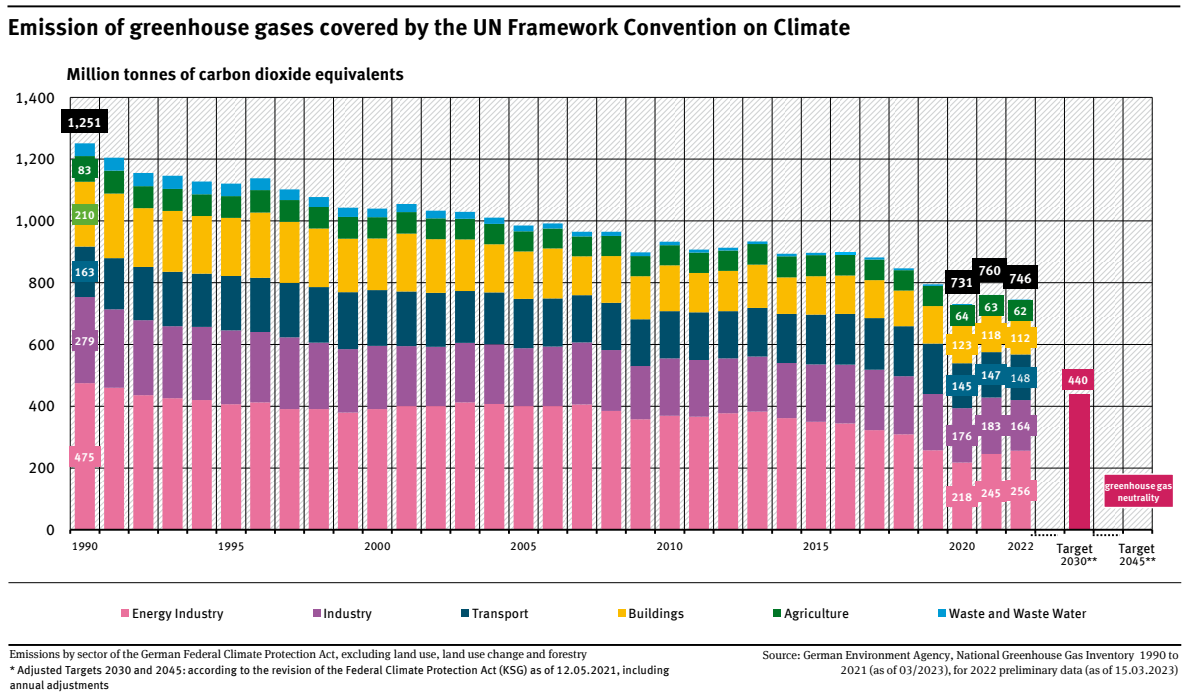

Figure 1.1: Greenhouse gas emissions in Germany by sector from 1990 to 2022 [3].

From Figure 1.1 it is also clear that while a downward trend can be observed along the years, it is currently not enough to reach the climate reductions goals in 2030. Out of the different sectors, it can also be seen that the highest emission is caused by the energy industry with around 34% of the total emission. This highlights the urgent need for energy generation from renewable sources. Historically, electricity generation in Germany was dominated by large thermal power plants fueled with nonrenewable sources, namely natural gas, coal, and nuclear power, all under the premise of cost minimization. The prominence

of electricity generation from renewable sources came about following a paradigm shift towards climate-friendly generation starting in the early 2000s. This shift initiated a transition in electricity generation away from roughly 300 large thermal power plants to currently over one million decentralized renewable generation plants [4]. In the first half of 2023, the majority of the electricity generated in Germany and fed into the grid came from renewable energy sources, accounting for 53.4% of the total generation [5].

In an urban environment such as the Free and Hanseatic City of Hamburg, the focus lies primarily on solar generation technologies such as PV (Photovoltaic) for energy supply. Coincidentally, one of the largest PV potential in Hamburg lies on roofs of residential buildings [6]. Given the relatively simple installation process and the maturity of the solar industry, there has been a growing interest in PV systems, especially rooftop PV [7], in recent years [8]. However, a rapid and uncontrolled increase of PV penetration may compromise grid stability [8], [9]. Considering Hamburg's reliance on PV, especially rooftop systems, it is essential to examine the effects of widespread decentralized PV systems on the electricity distribution grid. Due to the decentralized nature of PV generation, the analysis should also be conducted using high spatial resolution.

Behind the industry and transportation sectors, where emission reductions are often challenging [10], [11], the building sector is responsible for approximately 15% of the total greenhouse gas emissions. In Hamburg, this proportion increases to around 25%, second only to the industrial sector (28%) [12]. This underscores the significance of the building sector in achieving the emission goals of both Germany and Hamburg. Despite the imperative to reduce greenhouse gas emissions, the final energy consumption in households has increased by approximately 2.3% compared to the year 1990 [13]. To better understand how energy is consumed on average in private households, the final energy consumption is categorized based on its usage in Figure 1.2

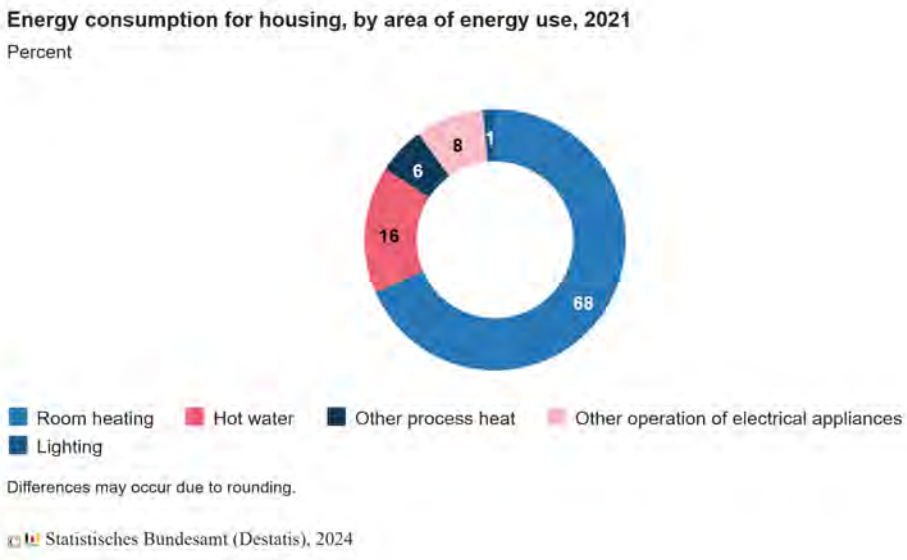

Figure 1.2: Energy consumption for housing, by area of energy use, 2021 [14].

From Figure 1.2 it is evident that the overwhelming majority of the energy consumed in households is

used for heating purposes. To better understand the potential for reducing greenhouse gas emissions in household energy consumption, Figure 1.3 presents the energy sources for this consumption. Despite the sharp decrease in the usage of mineral oil over the years, roughly 58% of the end energy consumption comes from conventional sources [15]. Heat supply in private households represents therefore an important lever to successfully achieve the climate protection goals.

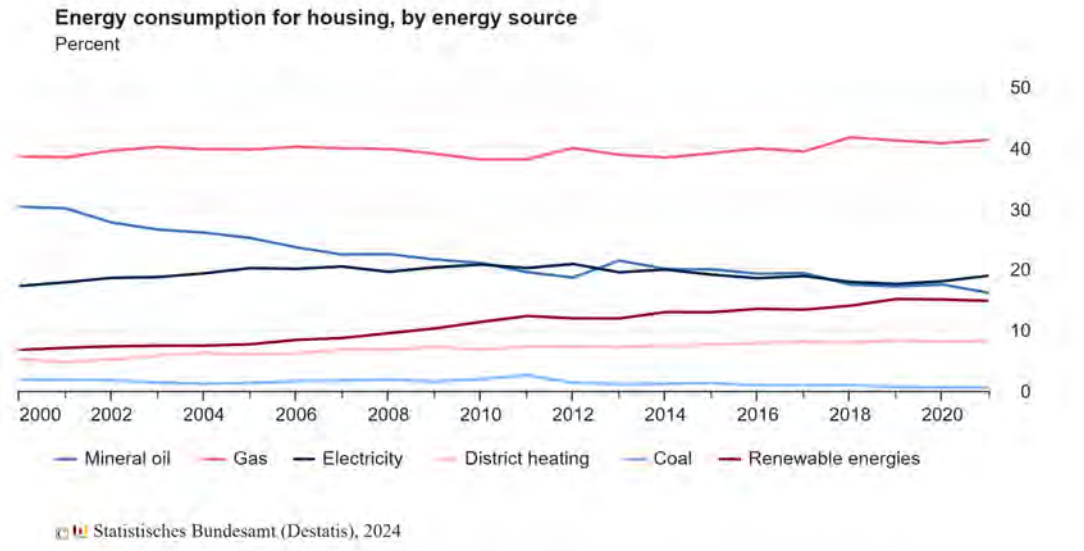

Figure 1.3: Energy consumption for housing, by energy source [15].

In 2023, approximately 31% of residential buildings in Hamburg are connected to a district heating network, a figure significantly higher than the countrywide average of 6% [16]. For regions, where district heating is not technically or financially feasible, climate friendly alternative heating technology has to be assessed. With a view of the current climate target, heat pump is often seen as an ecologically feasible option. Furthermore, the symbiotic relationship between heat pump and PV has also been well documented in the literature [17]. In an urban environment such as Hamburg, heavily reliant on solar generation from PV, this symbiotic relationship is of high importance. Additionally, heat pumps have demonstrated a relatively high degree of public acceptance [18], evident in the sharp rise in demand for residential heat pumps in recent years [19]. Despite the promising nature of heat pump, the additional load on the electricity grid caused by the electrification of the heat demand cannot be ignored.

Contrary to the interconnected nature of the electricity grid, the heat demand from residential buildings is typically not connected to one another, except for cases involving a district heating network. For this reason, high spatial resolution is required to assess the feasibility of a highly decentralized heating system based on heat pumps.

1.1 Objective

Based on the above-mentioned reasons, the idea of analyzing the effect of heat pumps and PV systems for residential buildings towards the electricity distribution grid was developed. Using this idea as a foundation, the following objectives are derived:

- Estimate the heat and electricity demand of every residential building in Hamburg
- Estimate the potential of rooftop PV of every residential roof surface in Hamburg
- Analyze the feasibility of heating supply based on heat pumps
- Analyze the effect of heat pumps and PV systems on the electricity distribution grid

In addition to these objectives, the decision to simulate each individual building is also made. Therefore, the method develop in this work has to be somewhat efficient in term of computational time.

1.2 Thesis Outline

This work is essentially divided into three main segments. The first segment begins with a short literature overview over the methods used in the literature to analyze the effects of the aforementioned technologies on the electricity distribution grid (Chapter 2). The segment then continues with a brief overview of the fundamentals used in developing the methodology presented in this thesis (Chapter 3). The first segment then concludes with a brief overview of the external datasets used in this work (Chapter 4). The core segment begins with Chapter 5, in which the individual steps taken to develop the model are presented. Subsequently, plausibility checks are conducted to estimate the extent of errors made using the presented method (Chapter 6). Following that, the results generated using the developed method are shown and discussed in chapter 7. The final segment (Chapter 8) summarizes the results of this work and provides an outlook on possibilities for improving, optimizing, and expanding the methodology outlined in this thesis.

2 State of the art

To assess the relevance of the aforementioned objective, a literature regrading the effects from the combination of heat pump and PV system on the electricity grid is conducted.

In recent years, it is evident from the literature that low carbon technologies, such as PV, heat pumps, batteries and hot water tanks, have been a focal topic of numerous research projects [20]–[23]. This trend can also be observed in Germany through the Energy Research Programme (*Energieforschungsprogramm*), currently is in 7th iteration [24]. Despite the differences in methods and scope, a consensus regarding the importance of sector coupling for the decarbonization of the energy system can be found [25].

From the literature, it is widely known that the use of sector coupling to decarbonize the heat sector often occurs at the distribution level, e.g., individual buildings or districts [20], [21]. However, the consideration of flexibility options often occurs on a centralized or aggregated level [20], [21], [25], [26]. This lack of granularity may limit the conclusion regarding the effect sector coupling can have on the electricity distribution grid.

To combat this issue, a tool was developed in the research project eGo^n to investigate the effects of sector coupling on the electrical grid with a comparatively high spatial resolution [27], [28]. Nonetheless, due to complexity of the generated model, a reduction method is employed to reduce the spatial complexity of the model. Since this project aims to study the whole region of Germany, the accuracy of the reduced model is assumed to be high enough [29], [30].

Due to the special situation of Hamburg as a state city, the usage spatial aggregation, as described in eGo^n, may lead to disproportionate high losses in accuracy. This is mainly attributed to the characteristic of Hamburg, where, based on the NUTS (Classification of Territorial Units for Statistics), its region are not split further. Considering the aforementioned reason along with the considerably smaller scope of this thesis as compared to the eGo^n, the decision made in this work to work on a new high spatially resolved model specific to Hamburg, which builds upon parts of the assumptions and methods developed in eGo^n.

3 Fundamentals

In this chapter, a brief overview of the basics upon which this master thesis is built is presented. It begins with a concise explanation of the typical methodology used to model energy demand. Following that, a brief overview of the technologies of a residential heating system used in this work is presented. Subsequently, a brief introduction regarding a PV system is provided. The chapter then continues with a brief description of the electricity system and its electricity grid. To conclude the chapter, a small introduction towards optimization and LP (linear programming) is provided."

3.1 Energy Demand Modeling

With the ever-increasing importance of the building sector for the climate protection goals [31], numerous building energy models have been developed along the years to better understand the role of buildings in climate protection [32]. Depending on chosen approach, the models can be classified into either top-down or bottom-up model [33]. Within top-down models building stocks are often regarded as a black box, and their energy consumption is estimated by establishing correlations between consumption at an aggregated level and relevant variables. On the other hand, bottom-up models estimate the energy consumption of individual or groups of buildings. More precisely, the bottom-up models can be distinctly categorized into either statistical or engineering-based methods. [32]–[34]. In the following both variants of bottom-up models are explained further, as both approaches are used in this thesis.

A Bottom-up statistical building energy model uses on historical measurement data as an input for a mathematical model, mostly based on regression analysis, to estimate the energy consumption of the considered buildings. [32], [35]. Despite the often higher accuracy of this approach, the downsides of such an approach have to be considered. Apart from the inherent dependency on site-specific measurement data, statistical models often lacks transparency [36]. In the context of this thesis, this approach is indirectly employed, as electrical load profiles generated using a statistical bottom-up approach developed in [37] are used in Chapter 5.3. This statistical model is used as one of the inputs to estimate the electricity load profile of each and every residential building in Hamburg.

Engineering-based methods, on the other hand, do not rely on measurement data as the energy consumption are estimated using physics-based calculation or simulation [33], [34]. Depending on the aggregation process, two major types of engineering-based bottom-up models can be identified, namely: the building by building approach and the archetype approach [32], [34], [38]. The building-by-building method involves simulating the energy consumption of each individual building separately. The archetype approach on the other hand uses specific building types ("archetypes") to represent a cohort of buildings [32]. Due to the nature of the archetype approach, it is often utilized in large-scale analyses where comprehensive building information, such as insulation details, is not available for each building [39].

Within this work, the bottom-up archetype approach is utilized in Chapter 5.2 using the TABULA reference method [40], [41]. Using this method, the annual heat demand of each residential building in Hamburg can be estimated.

3.2 Heating System

Within this work, a building is assumed to either be connected to a district heating network or have a single specific heating system. In the context of this thesis, a heating system always comprises of a heat pump, electrical heater, and a thermal energy storage. In the following, a brief overview of the technologies considered in this work to meet the heat demand of a building is provided.

3.2.1 District Heating

The term district heating refers to the supply of hot water and space heating energy to buildings via an underground pipeline network [42]. A district heating system mainly consists of three primary components: heat source, distribution network, and end-users (consumers) [43].

Heat Source

One of the major advantages of district heating networks is the flexibility of the heat sources, allowing the integration of a variety of centralized and decentralized sources [42], [43]. For economic reasons, heat is primarily supplied by centralized CHP (combined heat and power) plants, supported by peak-load boilers [44]. Due to the flexibility of district heating networks, it is also possible to integrate waste heat from industrial processes, waste recycling, or wastewater treatment, as well as heat from renewable sources [42]–[44]. In Germany, the majority of fuels used to generate district heating are still fossil fuels, while around 18% of total generation comes from renewable energy sources [45]. In Hamburg, a share of 20.2% of renewable energy is reported [46].

Heat Distribution Network

The second component is the heat distribution network that transports the energy from the heat source to the customers. In the distribution network, hot water is typically used as the heat transfer medium. Through an insulated pipe system, heat is distributed to the customer, where a heat exchanger is used to transfer the required amount of heat. The cooled heat transfer medium then flows back to the heat source to begin the cycle once again [43]. Due to the high costs of the heat distribution networks, the viability of district heating solutions is often limited by the heat density of the potential heat supply area [47].

End-users

In principle, any building can be linked to a district heating network, given the availability of a compatible building system [48]. Figure 3.1 provides an overview of the most important terms for heat transfer from district heating. As this work considers only a simplified approach regarding the connection between district heating networks and individual buildings (see chapters 4.6 and 5.7), further explanations of the components are omitted from this thesis and can be found in the literature (e.g. [48]).

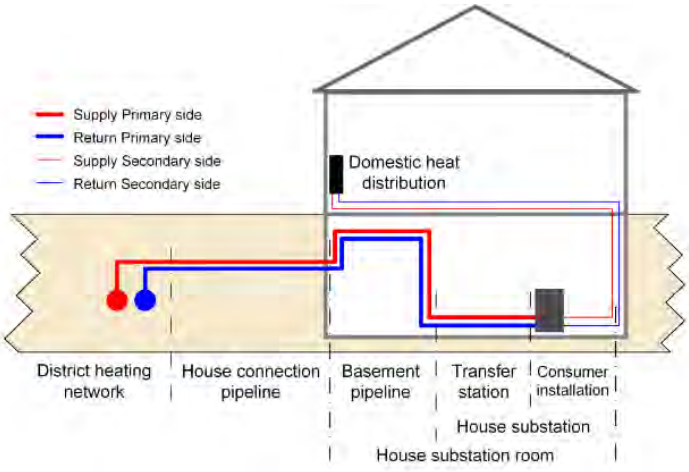

Figure 3.1: Overview of house connection for district heating [48].

In recent years, district heating has been identified as one of the key technologies in the urban heating transition toward a climate-neutral heating supply [49]. In Hamburg, district heating has also been identified as one of the most important levers for the CO2 reduction path in all sectors [50].

3.2.2 Heat Pump

Generally speaking, heat pumps are systems in which pumps are used to generate useful heat from a low-temperature source. The generated heat can then be utilized for numerous applications, including space heating, domestic hot water supply, or process heat. Heat pumps can be generally differentiated into three kinds [51]:

- compression heat pumps
- absorption heat pumps
- adsorption heat pumps

Currently, compression-based and absorption-based heat pumps are the most commonly used systems in the market [52]. In the following, the operating principle of compression heat pumps is explained.

Compression Heat Pumps

Essentially, compression-based heat pumps can be seen as refrigerators operating in reverse. Figure 3.2 provides an overview of the operating principle of compression heat pumps. In the evaporator, a refrigerant is first vaporized using heat extracted from a low-temperature heat source. The refrigerant in the gaseous form is then compressed using a compressor and raised to a higher pressure and temperature level. The generated heat is dissipated in another heat exchanger, the condenser, where it can be utilized for various purposes. In the liquefied state, the refrigerant is now expanded via an expansion valve, causing it to cool down and finally return to the evaporator to begin the next cycle [51], [53].

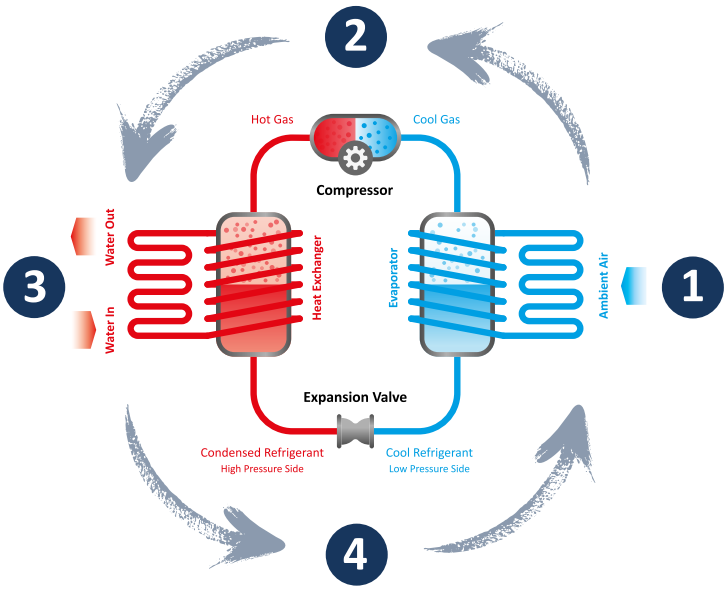

Figure 3.2: Operating principle of compression heat pump [54].

Coefficient of Performance (COP)

The performance of a heat pump is defined by its COP (coefficient of performance). This coefficient describes the efficiency of a heat pump and is defined as the ratio between the useful heat W_{hp} and the required energy for compressor W_c. As the heat output taken from the environment heat output is not taken into account, the COP of a heat pump is is always greater than 1 [51].

$$COP = \frac{W_{hp}}{W_c} \tag{3.1}$$

COP	coefficient of performance
W_{hp}	useful heat energy from heat pump
W_c	energy demand for compressor

As the amount of energy needed for the compressor depends on the amount of heat available from the environment, the calculated COP is normally related to a specific operating condition [55]. The COP is later used in Chapter 5.8 to estimate the electricity demand of the heat pump.

3.2.3 Electrical Heater

Electric heating systems generate heat from electric current. Heat is generated in an electrical resistor, which is heated by the flow of electricity. Different concepts exist in the market for generating heat from electricity [56]. In the following, several relevant concepts commonly used in the residential sector are discussed.

Electric Heating Rods

In the residential sector, electric heating rods are used in conjunction with a storage tank for generating heat energy for space heating and domestic hot water. Heating rods consist of several interconnected heating elements, depending on the required output. When current flows through the heating rod, heat is generated due to the high ohmic resistance, and it is then transferred to the medium being heated. This technology is particularly suitable to work in combination with other heating technologies. User This type of electrical heater is often cited to have a thermal efficiency close to 100%, as all incoming electricity is converted to heat. [56].

Electric Flow Heaters

In contrast to heating rods, electric flow heaters do not require a storage tank and can be directly integrated into the heating or domestic hot water circuit. They consists of a pressurized tube, with one inlet and one outlet nozzle, which together form the flow tube. Water flowing through the tube is then heated by heating elements inside the flow tube. Similar to heating rods, this type of system is often mentioned to have a thermal efficiency close to 100% [56].

Electric Surface Heating Systems

Another option for generating heat from electricity is the usage of electric surface heating systems. In the context of residential buildings, this concept is also often referred to as electric underfloor heating systems. In accordance with DIN EN 50559, such concept offers a well-established alternative to conventional water-based heating systems. Due to the even heat distribution over the floor surface, heat savings of up to 10% are possible [56]. As this concept is not designed to also provide heat required for domestic hot water, electric underfloor heating systems are not considered in this thesis.

3.2.4 Thermal Energy Storage

In the course of the energy transition, heat storage is a key component for a modern and sustainable energy supply through the decoupling of heat generation from heat consumption. Based on the physical principle used, thermal energy storage system can be differentiated into three types [56]:

- sensible heat storage
- latent heat storage
- thermochemical heat storage

Among the available technologies, sensible heat storage is currently commercially available, while latent and thermochemical heat storage methods are predominantly in the developmental stage [57]. For this reason, only sensible heat storage is considered in this work.

Sensible Heat Storage

Heat storage in a sensible heat storage system is achieved by heating a storage medium. The amount of energy stored depends on the specific heat capacity of the storage medium. For short-term storage, many sensible heat storage systems are operated with water due to its low costs and high specific heat capacity [56], [58].

Due to the relatively high temperature differences between the storage medium and the environment, heat losses plays an integral part in this type of storage. Additionally, the heat losses of a storage tank also depends on the shape of the storage tank and the type of insulation used. With the help of appropriate thermal insulation, the associated heat losses can be reduced [56], [58]. The heat losses considered in this work are further explained in Chapter 5.5.3 and subsequently utilized as an input in Chapter 5.8.

3.3 Photovoltaic (PV) System

In the following section, a brief overview of both PV systems and battery storage systems is provided. The section begins with a simplified explanation of a PV system, covering several important aspects of such a system. To conclude this section, an introduction to a battery storage system in the context of a PV system is presented.

3.3.1 PV System

PV modules enable the direct conversion of solar radiation into electrical energy. This is based on the photoelectric effect, in which photons are absorbed within a PV module, and electrons are released in the process. PV modules are produced using semiconductor materials such as silicons. The PV modules provide direct current, which can later be converted into alternating current using an inverter. The performance of PV modules depends on various factors, such as the quality and purity of the semiconductor material and the size of the PV modules. Currently, a PV module has a power density of approximately

200 W/m^2 and a typical size of 1.6 m^2. The entirety of the PV module, inverter, and other peripherals is referred to as a PV system [6].

The amount of energy generated from a PV system depends on several technical framework conditions. In the following, some of the most important points are presented.

Azimuth and Tilt Angle

As the PV generation profile of a particular system depends on the solar radiation, which depends on position of the sun, the performance of a PV system is highly influenced by its azimuth α and tilt angle γ. The solar azimuth can be described as the angle between the geographic north and the vertical circle passing through the center of the sun, wherein tilt angle is the vertical angle between the horizontal and the array surface [51], [59]. In the Northern Hemisphere, azimuth is often calculated from the south for solar applications, this orientation may maximize the received solar radiation [60]. To avoid misunderstandings, this work utilizes north azimuth (0° = North, 90° = East, 180° = South, 270° = West).

Shadings

Within a PV system, shadings are to be avoided wherever possible, as even partial shading can lead to disproportionately high losses [51]. Based on the source, a distinction is made between external shading (due to buildings, trees, etc.) and self-shading. Due to the detrimental effect of shadings, future sources of shading should also be taken into account in planning [6].

PV System and Performance Ratio

As previously mentioned, a PV system is made up not only of PV modules but also of different components that fulfill various roles. Since most of these components are electrically connected to the PV modules, proper planning of these components is crucial for the performance of a PV system due to the potential losses that may occur [61]. To evaluate the performance of a PV system, a parameter called PR (performance ratio) is often used. PR is a globally recognized performance parameter of a PV system and represents the actual energy generated by the PV system to its expected energy. In simpler terms, the Performance Ratio (PR) serves as an indicator of the losses that occur within the system [62].

3.3.2 Battery Storage System

Due to the decreasing rate of feed-in-tariff, recent increases in electricity prices, and the intermittency of PV generation, an increase in the adoption of battery storage systems into PV systems can be seen in recent years [63]–[65]. Historically, the price of battery storage systems is often cited as one of the limiting factors for the integration of batteries into PV system [63], [66]. Fueled by recent developments, mass production, and further advancements in the field, the price of battery storage unit has significantly decreased over the years, leading to the higher adoption rate of batteries in PV systems [67], [68].

Out of the different technologies available in the market, four concepts have been shown to be suitable for residential PV systems, namely: lead-acid batteries, lithium-ion batteries, sodium sulphur batteries, and vanadium redox batteries [63]. Compared to other technologies, lithium ion batteries are shown to have higher efficiency and longer lifetime, while retaining high energy density [57], [63]. Outside of solar applications, lithium-ion batteries are also often regarded as the most prominent battery technology due to their significant role in electric vehicles [69]–[71]. Due to the prominence of lithium-ion batteries in the market, this technology is used in this thesis.

3.4 Electricity System

In the following section, a brief overview of the structure of the electricity system and the electricity grid is provided. This section begins with a simplified explanation of the electricity system. Following this, the structure of the electricity grid in Germany is touched upon. Finally, the challenges arising in the electricity grid due to the increasing integration of renewable energy sources are briefly discussed.

3.4.1 Electricity System

Electricity system can be roughly defined as the the entirety of all systems required for the generation, transmission and distribution of electrical energy [72]. An electrical system does not comprise only of the physical infrastructure but also of the underlying electricity market [73]. Figure 3.3 provides a schematic overview of an electricity system.

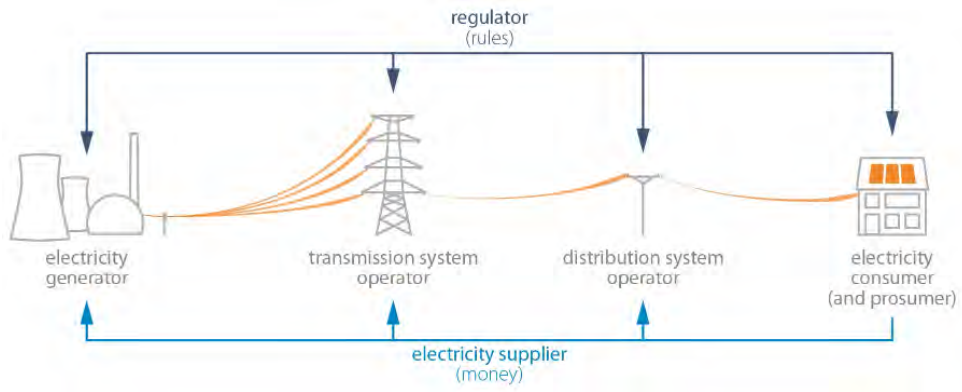

Figure 3.3: Schematic overview of the electricity system [73].

The physical side of the electricity system, which refers to the flow of electricity, comprises of electricity generators and its transportation system. Depending on its goal, the system is typically differentiated into systems designed for long-distance transmission and distribution system [73]. The physical grid (also often called the electricity grid) is explained further in chapter 3.4.2. Generally speaking, the electricity market deals with the cash flow of the electricity system [73]. As economic aspects are not considered in this work, further explanations regarding the electricity market are omitted.

3.4.2 Electricity Grid

The German electricity grid is one of the most important electricity grids in Europe and dates back to a time when the electricity supply was dependent on a few centrally controlled large power plants [72]. Furthermore, the German grid is a part of the European synchronous grid, which connects the electricity grid of more than 20 countries in continental Europe [72], [74]. As previously mentioned, the electricity grid can be seen as a network that connects electricity generators with customers through the transmission and distribution grids [73].

As previously mentioned, the electricity grid in Germany is differentiated into the transmission grid and distribution grid. Figure 3.4 provides a simplified representation of the structure of the electricity grid. Also seen in the figure is the categorization of the grid depending on its voltage level. Electricity is transmitted between voltage levels using transformer substations.

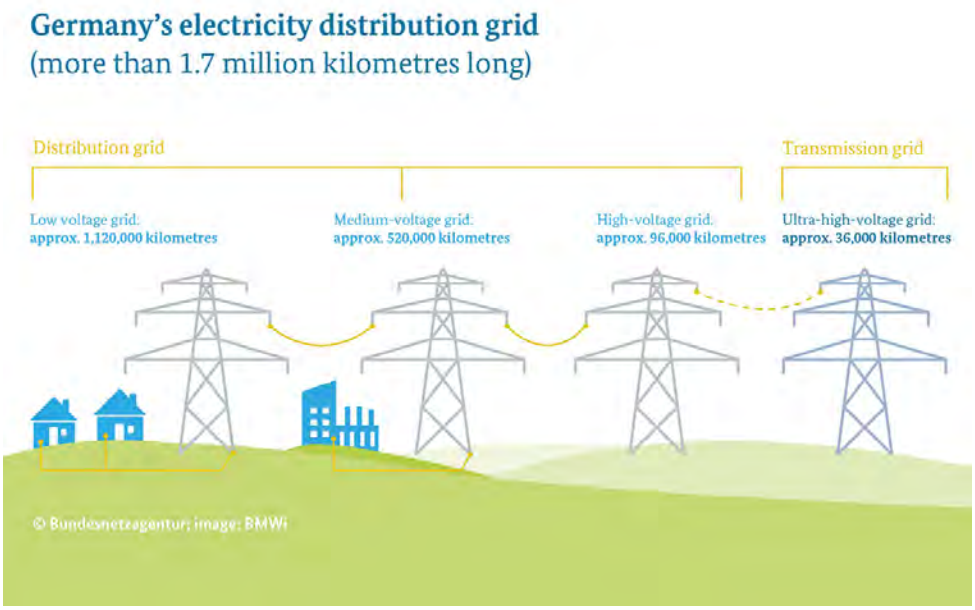

Figure 3.4: Germany's electricity distribution grid [75].

Transmission Grid

The transmission grid, also known as the transport grid, is utilized to transport electrical energy over long distances. Moreover, to minimize transmission losses, energy is transmitted at very high voltages [76]. Transmission grids in Germany and neighboring European countries typically operate as systems based on three-phase current at 220 and 380 kV. Grids at this voltage level are also often referred to as ultra-high-voltage grids [72], [75], [76].

At this voltage level, only large thermal power plants and, more recently, large wind farms are connected, with no loads present [72], [77]. The operation of the transmission grid falls under the responsibility of

the TSOs. The transmission grids of all interconnected partners form the European interconnected grid [74], [76].

Distribution Grid

A distribution grid is used to distribute electrical energy to end consumers and is managed by DSO, of which 866 exist in Germany [73], [78], [79]. The distribution grid comprises of the 110 kV high-voltage, 10 kV medium-voltage, and 400 V low voltage grid [72], [78], [80].

High-voltage Grid The high-voltage grid in Germany spans roughly 95,000 kilometers [79]. These grids primarily receive their energy upstream from the transmission grid through a transformer substation and serve as a redistribution system at the regional level. Additionally, high-voltage grids supply electricity directly to large industrial consumers and are used to feed electricity from smaller power plants, wind farms, and large PV parks [81], [82].

Medium-voltage Grid The medium-voltage grid represents the second level of the distribution grid and receives energy from the high-voltage grid and/or from decentralized installed capacities, such as small PV plants or wind parks [81], [82]. Through the medium-voltage grid, electricity is distributed at the local level in urban and rural areas, with industrial and commercial sites often directly connected at this voltage level [72], [82], [83]. In densely populated areas, underground cables are predominantly used, whereas overhead lines are often found in rural areas [84]. In total, the length of the medium-voltage grid in Germany amounts to roughly 530,000 km [79].

Low voltage Grid The low voltage grid represents the lowest voltage level of the electrical energy supply, connecting end consumers, private households, and small commercial and industrial sites to the electricity grid [85]. At this voltage level, electrical energy is provided upstream from higher voltage grids or is received from small-scale decentralized sources, such as rooftop PV systems [83]. In total, the low voltage grid in Germany has an approximate length of 1,570,000 km [79].

3.4.3 Challenges due to Renewable Energy Integration

Within the electricity system, the supply and demand of electricity must be equal at all times, as imbalances can lead to grid instabilities and in extreme cases blackouts [73]. Compared to other European Countries, Germany's electricity grid is characterized by a high level of stability and reliability [86]. In the wake of the increasing decentralized and variable electricity generation due to the expansion of renewable energy systems, new challenges have to be addressed to ensure the stability of the grid [87]. In the following, a number of challenges that are relevant to this thesis are discussed.

Variable Generation and Flexibility

Historically, imbalances in the electricity grid were primarily attributed to unplanned and unpredictable loads. However, with the advent of the energy transition, greater emphasis has been placed on the variability associated with generation from renewable energy sources [87], [88]. Consequently, there is an increasing need for system flexibility to cope with the additional variability and uncertainty introduced by renewable energies [88], [89].

Residual Loads and Grid Congestion

Residual load is defined as the difference between actual consumption and generation from non-dispatchable renewable energy sources [82]. Depending on the level of renewable feed-in, two challenging situations may arise: high and low residual load.

At times of high residual load, indicating low electricity from renewable sources, flexible power generation is required to meet energy demand. Currently, this flexibility is predominantly provided by conventional power plants [90], [91]. This has sparked discussions regarding the role of flexible conventional power plants in supporting the integration of renewable sources into existing infrastructure [90], [92], [93].

In contrast, low residual load (or even negative) occurs during times of high electricity generation from renewable sources. Depending on the available capacity of the electricity grid, this situation can lead to grid congestion. Grid congestion arises when the demand for transmission exceeds the available capacity for electricity transmission [90], [94].

In the transmission grid, an example of grid congestion occurs during periods of strong wind. This is attributed to the prevalence of wind turbines in the north and east of Germany and the simultaneous high electricity demand in the southern and western regions, necessitating the transportation of wind power over long distances [94], [95]. Grid congestion can also manifest locally in the distribution level due to the increasing amount of decentralized PV and wind power plants. The growing penetration of these technologies amplifies power flow in lower voltage levels [96]. In cases of grid overload, electricity must be transferred to higher voltage levels, a phenomenon commonly known as reverse power flow. As the electrical grid was historically designed without the consideration of bidirectional flow of electricity, reverse power flow introduces additional challenges in maintaining the stability of the grid [82], [97]–[99].

Consideration of the Challenges in this Thesis

In the literature, a considerable number of options are available to improve flexibility within the grid [100]. As this thesis aims to analyze the impact of heat pumps and PV in a residential context, the consideration of flexibility is limited to the potential of sector coupling in individual residential buildings.

The spatial resolution used in this work, namely individual buildings, is chosen based on considerations related to grid congestion. However, to study the effects on the distribution grid in Hamburg, aggregation is required. This aggregation is done at the medium-voltage level due to the availability of the dataset.

3.5 Optimization

In the course of the energy transition, there has been an ever-increasing emphasis on achieving a high share of generation from renewable sources while simultaneously minimizing its costs [101]. Such a problem is often framed as an optimization problem, falling under the branch of applied mathematics known as operations research. An optimization problem is commonly defined as the use of specific methods where the objective is to minimize or maximize a particular characteristic, such as cost, in which its variations are limited by an objective function. The setup of an optimization problem involves not only the mathematical formulation of the objective function but also the formulation of a set of constraints [102]–[104]. In the following a simplified mathematical representation of an optimization problem is presented.

In general, an optimization model consists of an objective function F that is to be maximized or minimized. The value of the objective function depends on the decision variables x_1 up to x_n, which, in turn, are subject to constraints g_i [102]–[104].

$$z = F(x_1, ..., x_n) \tag{3.2}$$

$$gi(x_1, ..., x_n) \begin{cases} \geq \\ = \quad b_i \forall i \in m \\ \leq \end{cases} \tag{3.3}$$

Among the various types of optimization, this thesis focuses on a specific sub-type known as linear programming.

3.5.1 Linear Programming (LP)

LP utilizes a mathematical model to describe a specific problem, where all mathematical functions (objective function and constraints) are linear. The significance of linear programming in real-world applications cannot be understated, given that many practical problems, including energy system models, can be effectively modeled as linear optimization problems [103], [105]. This development is further driven by the prevalence of a remarkably efficient optimization method known as the simplex method, allowing the solving of large linear programming problems [103].

As this thesis aims to optimize individual residential buildings for the whole region of Hamburg, considerations have to be made regarding the required computational time. Therefore, the CPLEX commercial solver, which is based on the simplex algorithm, is used within this thesis [106]. The decision to use a commercial solver instead of open-source solvers is partly based on publicly available benchmarks, which highlight the current discrepancy in terms of computational speed between the solvers [107], [108]. While it is clear that the models used for these benchmarks are significantly larger and more complex than the LP model used in this thesis, it is assumed that the difference in solving speed is also present in smaller models. Despite this, the development of open-source solvers should not be ignored, as the availability of high-performance open-source solvers can enhance the accessibility of energy modeling tools [107], [109]

4 Data

In this chapter, a brief overview is provided regarding the external datasets used in this study. In Figure 4.1 a simplified workflow showing where each of the external datasets are used in this work is provided. Additionally, this section addresses the constraints and considerations arising from the combination of diverse datasets.

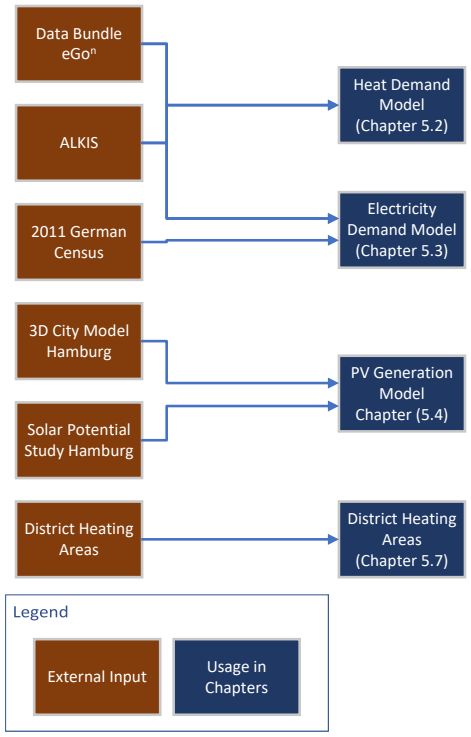

Figure 4.1: Overview of the usage of external datasets

4.1 2011 German Census

In accordance to an EU regulation from 2008, a population, building and housing census was carried out in Germany in 2011 [110]. The results of this census are publicly available in different aggregation levels. The data are either aggregated based on its region (from NUTS-1 (Classification of Territorial Units for Statistics) up to the municipality level) or its geographical grid (either 1km x 1km or 100m x

100m areas) [111]. Also stated in the EU regulation is the obligation for its member states to conduct a census every ten years. Due to the corona virus pandemic, the census was postponed to 2022. The results of census 2022 are scheduled to be published in 2024 [112], [113]. Within this work, the census data set is used in Chapter 5.3 to approximate the electrical load profile for each city district.

4.2 ALKIS

ALKIS (Authoritative Real Estate Cadastre Information System - *Amtliches Liegenschaftskatasterinformationssystem*) is the standardized national data model developed by AdV (Working Committee of the Surveying Authorities of the States of the Federal Republic of Germany - *Arbeitsgemeinschaft der Vermessungsverwaltungen der Länder der Bundesrepublik Deutschland*), in which formerly separately kept real estate books and real estate maps are combined [114]. ALKIS data set for Hamburg is continuously updated at the beginning of each quarter and is publicly available [115]. For this work, ALKIS data set from April 2023 is used.

Among all of the datasets available within ALKIS, two objects are of particular interest for this work: buildings and addresses. In ALKIS building are differentiated between main and secondary buildings, where only main buildings are assigned a particular address. Secondary buildings, on the other hand, are assigned a pseudo number, which points to a particular main building [116]. Using these pseudo numbers, an address can be indirectly assigned to secondary buildings using the connection between secondary and main buildings.

Within this work, the method used to approximate the heat demand for each residential building in Hamburg (Chapter 5.2) is based on ALKIS data set. Furthermore, ALKIS data set is also used in Chapter 5.3 together with census data set to generate city district specific electricity load profile.

4.3 3D City Model Hamburg

The 3D city model of Hamburg is publicly available in three versions, which differ in terms of their LoD (level of detail): LoD1, LoD2, and LoD3. These levels represents different accuracy levels, with higher levels offering greater precision and higher structural complexity. Figure 4.2 provides a representation of a building in the different level of detaillevel of details.

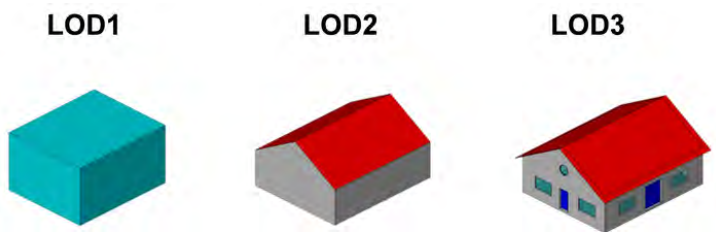

Figure 4.2: Representation of the same building in the Levels of Detail 1-3. [117]

This study uses the 3D city model of Hamburg with the level of detail LoD2 from April 2023. This decision is made considering the availability of LoD3 dataset and the superior accuracy of LoD2 compared to LoD1 [117], [118]. In the LoD2 model, the laser data obtained from aerial surveys of all roof surfaces is examined, and the data is used to assign standardized roof shapes to corresponding buildings. The modeled buildings utilize building floor plan from ALKIS, pointing to the connection between the two datasets [119].

Within this work, the LoD2 data set is utilized to examine the available roof surfaces on every residential building in Hamburg for the utilization of PV (Chapter 5.4).

4.4 Solar Potential Study Hamburg

For the analysis of PV potential on residential buildings in Hamburg, solar potential study in Hamburg commissioned by the EEHH (Renewable Energies Hamburg Cluster - *Cluster Erneuerbare Energien Hamburg*) is used in this work. The solar potential study utilizes a public database to generate hourly weather data for a 20-year period, covering January 1, 2001, to December 31, 2020. The weather data is then used to generate hourly PV generation time series for the 20-year period as an intermediate result [6]. Both datasets (weather data and hourly PV generation) have been made available by the authors of the study. In Chapter 5.4, this data set is used to estimate the amount of electricity generated by PV for each residential building in Hamburg.

4.5 Data Bundle eGo^n

The research project eGo^n aims to investigate the effects of sector coupling on the electrical grid and the benefits of new flexibility options. As a part of the open-source and open-data principles followed in this project, descriptions regarding the datasets used in the project have been made publicly available. Due to the nature of required datasets, not every data set can be automatically downloaded from its sources. For this reason, a section of the required datasets has been published under open data license [28], [120]. Among the published datasets, two in particular, namely: the household electricity load profile (Chapter 5.3) and the intra-day heat load profile (Chapter 5.2), are used in this work.

4.6 District Heating Areas

As a part of the study carried out by BSW (Ministry of Urban Development and Housing - *Behörde für Stadtentwicklung und Wohnen*) of the Free and Hanseatic City of Hamburg to examine whether and how climate-neutral housing can be achieved in Hamburg by 2045, an assessment of the feasibility of district heating based on linear heat density was conducted for each building block. The building blocks are categorized as follows [121]–[123]:

- Existing district heating area
- Potential area for district heating expansion

- Potential area for decentralized heating network
- Decentralized heating supply

For the purpose of this work, the aforementioned data set has been made available by the author of the study. It is utilized in Chapter 5.7 to approximate the availability of district heating for residential buildings in Hamburg.

4.7 Limitations and Considerations

In this section, a brief consideration of the limitations occurring due to the different datasets are shown.

4.7.1 Consistency of Datasets

As this thesis aims to study the interaction between differently energy sources, it is highly important that the same data basis used for heat calculation (Chapter 5.2) is also used for electrical (Chapter 5.3) and PV (Chapter 5.4) time series calculations. As both heat and electrical time series calculation is based on ALKIS, it is unproblematic. PV on the other hand utilizes LoD2 (3D Lod2 City Model) (Chapter 4.3). Despite LoD2 of Hamburg being based on ALKIS, a difference regarding data availability can be observed. Some building objects that are modeled in ALKIS are not modeled in the 3D city model.

Due to the above mentioned reasons, the principle of least common denominator is applied in this thesis whenever necessary. Using this principle, only building objects that exist in both ALKIS and LoD2 are considered. Building objects that exist in only one of the datasets are excluded. As a result, 6110 building objects (residential and non-residential), representing roughly 2% of the total number of buildings in ALKIS, must be excluded.

4.7.2 Outdated Datasets

As mentioned above, the census data set of Germany was last updated in 2011. For the analysis of building objects (ALKIS and LoD2), on the other hand, data sets from April 2023 are used. This discrepancy in time may lead to inevitable errors, when these datasets are utilized together.

4.7.3 Accuracy of Datasets

As mentioned earlier in Chapter 4.3, the geometry of roof surface in LoD2 is approximated based on a aerial survey. This inherently leads to inaccuracies, which are in the range of approximately ±1m. Furthermore, due to the use of standardized roof types, deviations in roof shapes are also to be expected for buildings with complex roof shapes [119]. However, due to the lack of data available for comparison, the error caused due to inaccuracy of the data set cannot be quantified in this work.

5 Methodology

In this chapter, the methodology developed in this work is explained. This chapter begins with a general description of the workflow implemented in this thesis. After that, each component of the workflow is explained in greater detail. The chapter ends with description of the energy optimization model used in this thesis.

5.1 Energy System Workflow

A simplified workflow of the methodology used in this thesis is given in Figure 5.1. The dark orange rectangles represents the input data required in this workflow. These data are either provided directly from external sources or derived from a combination of various datasets. The blue rectangle refers to intermediate results at the building level, while the gray rectangle indicates the final results at the MV grid level

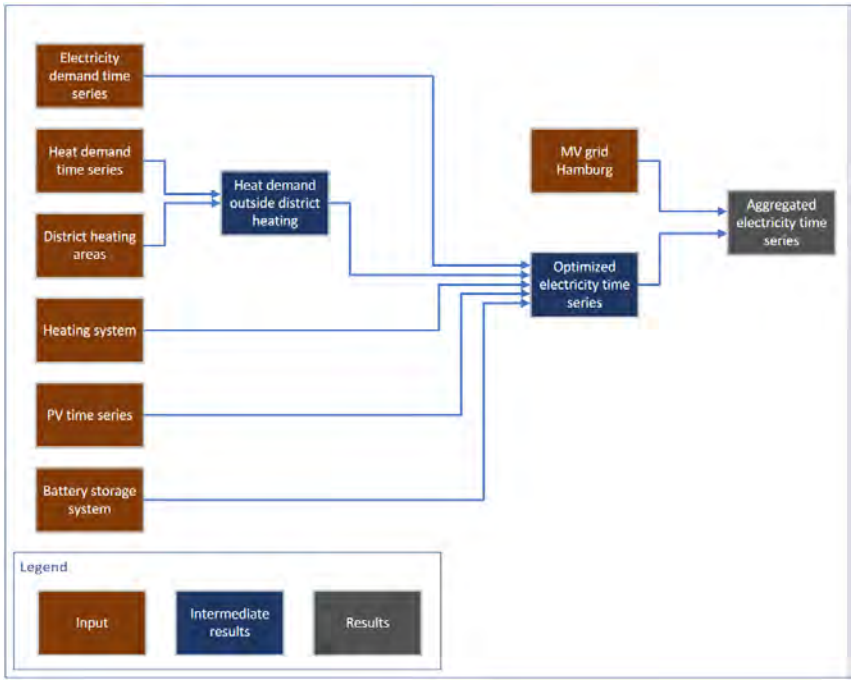

Figure 5.1: Overview of the methodology

Within this thesis, the energy flow of a building is represented by its electricity (Chapter 5.3), heat (Chapter 5.2), and PV (Chapter 5.4) time series. Depending on its location, the occurring heat demand is met using either district heating (Chapter 5.7) or the building heating system (Chapter 5.5). The size of the battery storage system (Chapter 5.5) is determined based on the capacity of the PV installation. These information then serve as inputs for a mathematical optimization model (Chapter 5.8). Finally, the results are aggregated based on the MV distribution grid (Chapter 5.6). Following [124] and [125], the year 2011 is chosen as the representative weather year.

5.2 Heat Demand Model

This section describes the methodology used to create a heat demand profile for all residential buildings in Hamburg. The method used is a combination of a top-down and bottom-up approach and is highly influenced by the methodology presented in [126], [127] and [125]. The combined methodology begins with the calculation of reference area for residential buildings out of building objects from ALKIS and IWU (*Institut Wohnen und Umwelt*) building archetype. Using the calculation method from TABULA, the annual heat consumption can be calculated. This annual value is then further disaggregated into hourly time series

5.2.1 Identification and Classification of Residential Living Area

The modeling of heat demand profile begins with the identification of residential buildings and their reference area. For this purpose, the methods used for the creation of heat cadastre Hamburg (*Wärmekataster Hamburg*), where individual buildings are assigned to a specific building archetype, are taken as reference [127], [128]. In this step, building objects out of ALKIS along with its relevant attributes are used as baseline information.

Building Archetypes

As a part of TABULA, a European project aimed at creating a harmonized structure for European building typologies, a residential building typology for Germany was developed by IWU using a sample study of residential building stocks in Germany. Three specific attributes, namely: construction year, construction type, and renovation level, are used to classify a building into a specific energetic archetype [128], [129]. This typology is chosen considering the following facts:

- Recommended classification methodology given by the EU Energy Efficiency Directive EED [130]
- Established and well known method in Germany [126], [127], [131], [132]

An overview of the IWU archetypes used in this thesis is presented in Table 5.1. For each of these archetypes, a specific yearly heat demand (space heating and domestic hot water) can be calculated using a specific ”reference building”. Additionally, IWU also provide a correction function to reduce the discrepancy between ”consumption” and ”demand” [40].

Table 5.1: Overview of IWU typology types [128]

Construction Year	Construction epoch	Construction Types				
... 1859	A	EFH	-	MFH	-	-
1860 ... 1918	B	EFH	RH	MFH	GMH	HH
1919 ... 1948	C	EFH	RH	MFH	GMH	-
1949 ... 1957	D	EFH	RH	MFH	GMH	-
1958 ... 1968	E	EFH	RH	MFH	GMH	HH
1969 ... 1978	F	EFH	RH	MFH	GMH	HH
1979 ... 1983	G	EFH	RH	MFH	-	-
1984 ... 1994	H	EFH	RH	MFH	-	-
1995 ... 2001	I	EFH	RH	MFH	-	-
2002 ... 2009	J	EFH	RH	MFH	-	-
2010 ... 2015	K	EFH	RH	MFH	-	-
2016 ...	L	EFH	RH	MFH	-	-

EFH = Single-family house
RH = Row-house
MFH = Multi-family building
GMH = Large multi-family building
HH = High-rise building

Another important attribute of the IWU typology is the renovation level. Due to the lack of the data availability regarding building's renovation level within ALKIS, only renovation level of "0" or "baseline" out of the three available renovation levels of the IWU archetype is used in this thesis. It is important to note that, within this context, the term "baseline" denotes the current predominant energetic state in which a specific archetype is to be found. Nevertheless, relying on the assumption of baseline renovation level may lead to an overestimation of the heat demand, considering that approximately 1% of the buildings in Hamburg undergo energetic renovation each year [123].

Archetype Assignment

Ignoring renovation level, two distinct attributes are still required to assign each building object to a particular energetic archetype. This section deals with the assignment of construction epoch and construction type using the available ALKIS attributes.

Construction Epoch From Table 5.1 it is shown that building construction year provides important information to classify each buildings to its corresponding energetic archetypes. However, due to the variability in data quality, using ALKIS as a data source for construction year comes with its own challenges. A quick analysis of the data set reveals that roughly one third of the residential buildings in Hamburg do not posses this information. To tackle this problem, the method described in [127], [128] is used.

For buildings with missing construction year, new generic archetypes are generated for each of the construction types. The annual heat demand of these generic archetypes is calculated using the mean value of all heat demands for the particular construction type from all available construction epochs up to I. For example, the specific annual heat demand of the new generic RH is equal to the arithmetic mean of RH-B up to RH-I. Construction epoch I is used as cut-off due to the obligation to document the construction year, which was introduced after the year 1998 [128].

Construction Type Similar to the construction year, ALKIS also includes construction type as an attribute of the building object. This attribute, called *Bauweise*, can be roughly translated to construction type. However, the construction types defined in the IWU typology differ from the ones defined in ALKIS. To systematically assign the different constructions types, assignment rules from [128] is used. This assignment rule makes use of a further ALKIS building attribute, namely: number of storeys above ground. The overall assignment rule for every attribute combinations is shown in Table 5.2

Table 5.2: IWU - ALKIS construction type assignment rule. Adapted from [128]

Epoch	*Bauweise*	*Bauweise* Code	Number of Storeys	IWU Type
A	*Freistehendes Einzelgebäude*	1100	$\leq$ 2, else regarded as missing *Bauweise*	EFH
	Doppelhaushälfte	2100		
	Reihenhaus	2200		
	Freistehender Gebäudeblock	1200	Any	MFH
	Haus in Reihe	2300		
	Gruppenhaus	2400		
	Gebäudeblock in geschlossener Bauweise	2500		
	Missing Bauweise	-	1,2	EFH
			$>$ 2	MFH
B, C, D	*Freistehendes Einzelgebäude*	1100	$\leq$ 2, else regarded as missing *Bauweise*	EFH
	Doppelhaushälfte	2100		RH
	Reihenhaus	2200		
	Freistehender Gebäudeblock	1200	$\leq$ 4	MFH
	Haus in Reihe	2300		
	Gruppenhaus	2400	$\geq$ 5	GMH
	Gebäudeblock in geschlossener Bauweise	2500		
	Missing Bauweise	-	1,2	EFH
			3,4	MFH
			$\geq$ 5	GMH
E,F	*Freistehendes Einzelgebäude*	1100	$\leq$ 2, else regarded as missing *Bauweise*	EFH
	Doppelhaushälfte	2100		RH
	Reihenhaus	2200		
	Freistehender Gebäudeblock	1200	$\leq$ 5	MFH

	Haus in Reihe	2300		
	Gruppenhaus	2400	6,7,8	GMH
	Gebäudeblock in geschlossener Bauweise	2500	> 8	HH
	Missing Bauweise	-	1,2	EFH
			3,4,5	MFH
			6,7,8	GMH
			> 8	HH
G, H, I, J, K, L	*Freistehendes Einzelgebäude*	1100	$\leq$ 2, else regarded as missing *Bauweise*	EFH
	Doppelhaushälfte	2100		RH
	Reihenhaus	2200		
	Freistehender Gebäudeblock	1200	any	MFH
	Haus in Reihe	2300		
	Gruppenhaus	2400		
	Gebäudeblock in geschlossener Bauweise	2500		
	Missing Bauweise	-	1,2	EFH
			> 2	MFH
Missing	*Freistehendes Einzelgebäude*	1100	$\leq$ 2, else regarded as missing *Bauweise*	EFH
	Doppelhaushälfte	2100		RH
	Reihenhaus	2200		
	Freistehender Gebäudeblock	1200	≤ 5	MFH
	Haus in Reihe	2300		
	Gruppenhaus	2400	6,7,8	GMH
	Gebäudeblock in geschlossener Bauweise	2500	> 8	HH
	Missing Bauweise	-	1,2	EFH
			3,4,5	MFH
			6,7,8	GMH
			> 8	HH

Reference Area

After the assignment of ALKIS to IWU archetype, the reference area for the calculation of the building specific annual heat demand needs to be determined. The calculation is based on building footprint area and number of storeys. This calculation is then further refined using additional building attributes and cadastral objects.

Building Use Within ALKIS, each of the building objects is assigned to one of the 232 possible building uses. However, due to the occurrence of mixed-use buildings in ALKIS, additional assumptions and

simplifications are required to determine the share of residential area for these mixed-use buildings. For this purpose, the assumptions regarding the share of residential area for each building use, as outlined in [128], are implemented. Table 5.3 provides an overview of all building uses and their share of residential area. Building uses that are not shown in Table 5.3 are assumed to have zero residential area.

Table 5.3: Residential share assumption. Based on [128]

ALKIS Name	ALKIS Code	Share of Residential Area
Wohngebäude	1000	100%
Wohnhaus	1010	100%
Bauernhaus	1221	100%
Wohngebäude mit Handel und Dienstleistungen	1120	100% - ground floor area
Wohn- und Geschäftsgebäude	1123	100% - ground floor area
Wohngebäude mit Gemeinbedarf	1110	50%
Wohn- und Verwaltungsgebäude	1121	50%
Wohn- un Bürogebäude	1122	50%
Wohngebäude mit Gewerbe und Idustrie	1130	50%
Wohn- und Betriebsgebäude	1131	50%
Land- und forstwirtschaftliches Wohngebäude	1210	50%
Land- und forstwirtschaftliches Wohn- und Betriebsgebäude	1220	50%
Wohn- und Wirtschaftsgebäude	1222	50%
Gemischt genutztes Gebäude mit Wohnen	1100	15%
Gebäude für Handel und Dienstleistung mit Wohnen	2310	15%
Gebäude für Gewerbe und Industrie mit Wohnen	2320	15%

Roof Type Another important aspect in the calculation of reference heating area is the consideration of heated attics in residential buildings. Since there is no geometric information available in ALKIS building objects, assumptions and simplifications using building roof type, as described in [128], are implemented. Table 5.4 provides an overview of roof types, where heated attic could appear.

Further rules are then implemented for these four different roof types. Both mansard roofs and half-hip roof are assumed to always have heated attic. Gable/Saddle roof and hip roof are considered to have heated attic when the building in question are assigned to one the following IWU archetypes: EFH-A,

Table 5.4: Overview of roof types with possibility of heated attic [116], [128]

ALKIS Code	ALKIS Name	Translated Name
3100	*Satteldach*	Gable/Saddle Roof
3200	*Walmdach*	Hip Roof
3300	*Krüppelwalmdach*	Half-hip Roof
3400	*Mansardendach*	Mansard Roof

EFH-B, EFH-C, EFH-D, EFH-E, RH-B, RH-C, RH-D, RH-E or MFH-A. In the case of a heated attic, the heated floor area will then be increased by 75% of the building footprint area [128].

Building Parts Building parts are used within this work to account for building objects with "complex" building shapes. Figure 5.2 illustrates an example of the connection between building and its building parts. As shown in the figure, building parts can be used to describe parts of a building with a significant difference in shape within the same building. Building parts typically have a number of storeys separate from the main building. This additional information can then be utilized to either increase or decrease the overall heating reference area [116], [128].

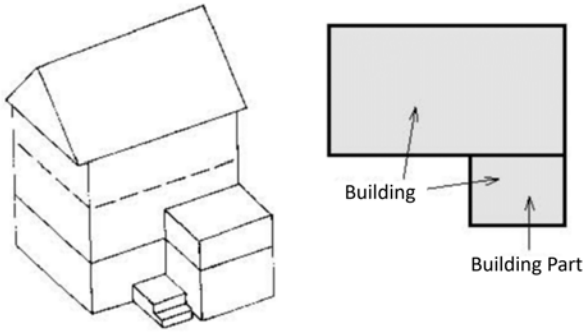

Figure 5.2: Example of connection between building and building parts in ALKIS [116]

An overview of all building parts considered in this model is shown in Table 5.5. In contrast to the clear number of storeys for lower and higher parts of the building, passageways are usually not assigned a number of storeys. Therefore, as a simplification, passageways are assumed to have one storey in height. This assumption is based on the directive on areas for the fire department (*Richtlinie über Flächen für die Feuerwehr*), which specifies a minimum clearance height of 3.5m for passageways [133].

Reference Area Calculation For the calculation of reference area for heating, it is important to note, that there is no single uniform definition. Depending on the reference and available data set, different calculation methods, such as volume-based calculation from DIN V 18599-1 [134] or area-based calculation from VDI 3807-2 [135]) can be used. Within this work, area-based calculation using

Table 5.5: Overview of building parts

ALKIS Code	ALKIS Name	Translated Name
1100	*Geringergeschossiger Gebäudeteil*	Lower storey building part
1200	*Höhergeschossiger Gebäudeteil*	Higher storey building part
2610	*Durchfahrt im Gebäude*	Passageway through building
2620	*Durchfahrt an überbauter Verkehrsstraße*	Passageway on built-over road

building footprint area and number of storeys, as described in [128] is used. The following formula 5.1 and 5.2 illustrate how the reference area is calculated in this thesis.

$$A_{ref} = a(s + s_a) \tag{5.1}$$

$$s_a = \begin{cases} 0.75 & \text{for building with heated attic} \\ 0 & \text{for building without heated attic} \end{cases} \tag{5.2}$$

A_{ref}	reference area for heat demand calculation
a	building footprint area
s	number of storeys
s_a	additional storey due to heated attic

In case of a building with building part(s), the total reference area is equal to the sum of all reference areas from each of the components. Using figure 5.3 as an example, the overall reference area is equal to the sum of $A_{ref,A}$ and $A_{ref,B}$.

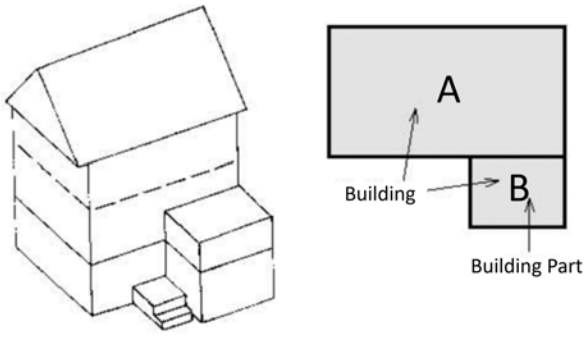

Figure 5.3: Example building for reference area calculation. Based on [116]

5.2.2 Annual Heat Demand Calculation

This section deals with the conversion of IWU building typology to energetic values. The conversion makes use of the TABULA reference method, which in turn uses the IWU typology and its subsequent reference building [40], [41].

TABULA Calculation Method

The TABULA calculation method can be described as a modified approach to DIN 4108 with additional consumption correction function [126]. The consumption correction is based on metered data, from which a function is derived. This function is then used to transform the computed heat demand into an estimate of the heat consumption. The use of a function rather than a simple factor is also beneficial as the discrepancy between consumption and demand is not linear. The function is derived out of a sample of 1702 buildings [40], [126] and it is shown in Figure 5.4.

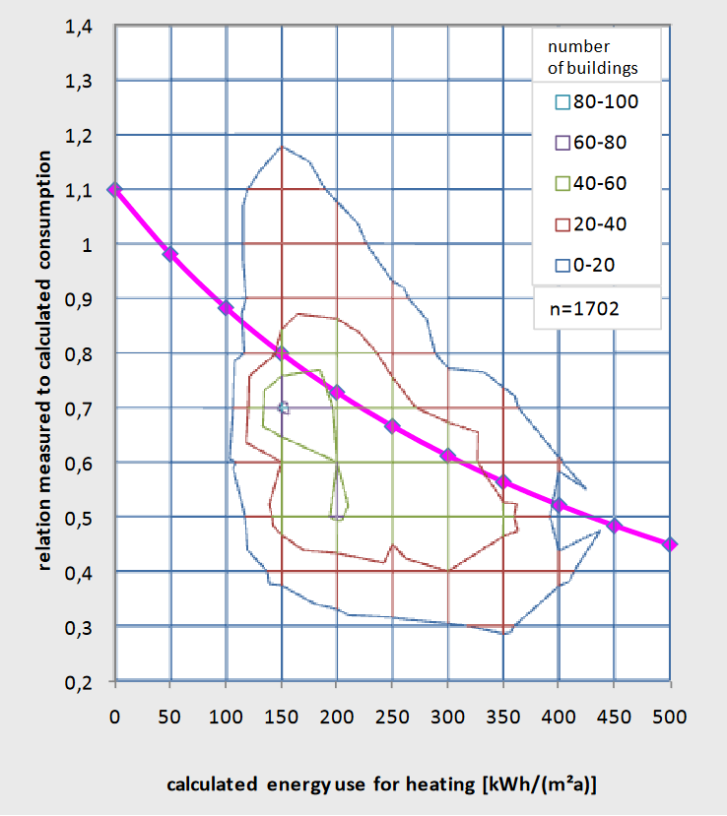

Figure 5.4: Consumption correction function [40]

Furthermore, the results of the calculated heat demand depend highly on the climate data set and its temperature assumptions. For this thesis, heating limit temperature is set at 12°C with an indoor temperature of 19°C. In the literature both 19°C and 20°C indoor temperature can be considered as standard values. As within this work no differentiation can be made between heated and unheated spaces in a building,

the use of 20°C indoor temperature may lead to disproportionately large heat demand. As a compromise 19°C is used instead. [126]. Furthermore, the use of a single temperature value for all building types may lead to both under- and overestimation of the heat demand for different building types. Nevertheless, these inaccuracies are accepted, as a more detailed calculation would require investigating each building separately, which is beyond the scope of this work.

As this thesis only deals with residential buildings in Hamburg, the weather station Hamburg *Fühlsbüttel* is chosen. Using the above mentioned temperature assumptions, relevant long-term average (2003-2022) of the relevant climate parameters are generated using degree days tool from IWU [136]. Table 5.6 provides an overview of the used climate parameters. For every other required parameters, TABULA standard values and standard values from IWU reference buildings are used. The resulting annual specific heat consumption can be seen in Table 5.7.

Table 5.6: Overview of climate parameters

Parameter	Value	Units
Heating Days	214	d
Average External Air Temperature	5.3	°C
Indoor Temperature	19	
Heating Limit Temperature	12	
Solar Gains Horizontal	375	$kWh/m^2 * a$
Solar Gains East	274	
Solar Gains South	428	
Solar Gains West	265	
Solar Gains North	172	

Table 5.7: Calculated specific heat consumption in $kWh/m^2 * a$

Contruction epoch	Construction Types				
	EFH	RH	MFH	GMH	HH
A	177.53	-	288.25	-	-
B	173.44	199.33	179.47	142.78	-
C	154.35	156.95	223.35	174.31	-
D	174.31	191.52	200.27	171.06	-
E	171.69	110.76	147.82	151.10	124.11
F	145.46	139.73	155.65	130.38	125.67
G	113.38	139,34	131.45	-	-
H	124.72	99.77	134.93	-	-
I	98.18	74.63	90.30	-	-
J	75.36	66.51	61.41	-	-
K	91.07	79.70	80.74	-	-
L	78.47	68.61	54.40	-	-
Missing	148.12	139.00	172.39	153.93	124.89

5.2.3 Generation of Hourly Heat Profile

Since TABULA calculation method only provides an annual characteristic value for the archetypes, further steps are needed to disaggregate it into load profile with the desired resolution. This section covers the steps taken to disaggregate the annual value into hourly value.

Daily Heat Value

The calculated annual profile is initially disaggregated into daily values using the *SigLinDe* function described in [137]. This function is based on the standard load profiles for gas (utilizing the *Sigmoid* function) from TUM (Technical University of Munich - *Technische Universität München*) [138] and its further development into *SigLinDe* by FfE (Research Center for Energy Economics e.V. - *Forschungsstelle für Energiewirtschaft e.V.*) [139]. Since both [138], [139] deal with gas profiles, the assumption is made that the heat profile is identical to the gas profile in its shape.

Both *Sigmoid* and *SigLinDe* utilize daily ambient mean temperature and building use specific coefficients A,B,C,D to calculate a daily normalized profile value. This value can then be multiplied with annual heat value and weekday factor to calculate its daily heat value [137]. For residential buildings, [138] concludes that no significant dependency exists between heat value and weekday factor, meaning that the weekday factor can be ignored for residential buildings. Similar results can also be found in English Homes [140]. Equation 5.3 shows the mathematical formulation of the *Sigmoid* function.

$$h(\theta, type) = \frac{A_{type}}{1 + \left(\frac{B_{type}}{\theta_{amb} - 40}\right)^{C_{type}}} + D_{type} \tag{5.3}$$

$h(\theta, type)$	daily normalized profile value
θ_amb	ambient temperature
A_{type}, B_{type}, C_{type}, D_{type}	building use specific coefficient

The *Sigmoid* function exhibits noticeable deviations in practice, especially for very cold ambient temperatures when compared to measured values. This discrepancy serves as motivation for the further development of the function by FfE. *SigLinDe* consists of a combination of *Sigmoid* function and two linear components, namely: heating line (*Heizgeraden*) and hot water line (*Warmwassergerade*). Both heating and hot water lines are described using a gradient and offset. The *Sigmoid* coefficients A,B,C,D are further used and in part modified [139]. The *SigLinDe* profile is then calculated according to equation 5.4.

$$h(\theta, type) = \frac{A_{type}}{1 + \left(\frac{B_{type}}{\theta_{amb} - 40}\right)^{C_{type}}} + D_{type} + \max \begin{pmatrix} m_H \theta_{amb} + b_H \\ m_W \theta_{amb} + b_W \end{pmatrix} \tag{5.4}$$

$h(\theta, type)$	daily normalized profile value
$\theta_a mb$	ambient temperature
A_{type}, B_{type}, C_{type}, D_{type}	building use specific coefficient
m_H	heating line gradient
b_H	heating line offset
m_W	hot water line gradient
b_W	hot water line offset

Figure 5.5 visualizes both *Sigmoid* and *SigLinDe* profiles for different ambient temperatures. As mentioned above, the difference lies mainly on the tail ends of the function. For residential buildings, both *Sigmoid* and *SigLinDe* are only differentiated between EFH and MFH.

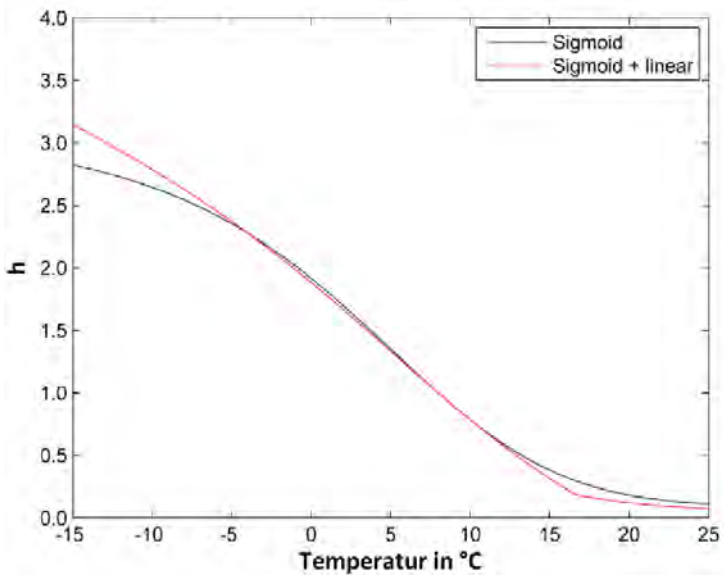

Figure 5.5: Comparison between *Sigmoid* and *SigLinDe* profile [139]

Intra Day Profiles

To further increase the temporal resolution of the building heat model, the generated daily profile needs to be further disaggregated into an hourly profile. In this work, the method described in [125], [141] and used in ego^n project [27] is implemented to generate a pool of intra day profiles.

For this method, a synthetic hourly heat demand profile, which has been generated using a closed source load profile generator developed in [142], is utilized. The load profile generator has the capability to generate load profiles of electricity, space heating, and domestic hot water for individual households [125], [142]. As part of the data bundle for ego^n project (chapter 4.5), a set containing 1259 heat demand profiles for EFH and MFH has been published under an open data license. [120]. Using these heat demand profiles, a pool of intra day profiles is generated [125], [141].

The intra day profile pool comprises of 24-hour profiles, with each profile representing specific temperature classes and building type [141]. In this context, temperature class refers to the temperature range, in

which the average daily temperature lies. For this purpose, the temperature classification approach used in [143] is applied. Table 5.8 provides an overview of the temperature classification.

From 1259 heat demand profiles, roughly 460,000 intra-day profiles can be generated and classified per temperature class and building type. The accumulated individual intra-day profile is then normalized to its sum [125], [141].

Table 5.8: Temperature classification [143]

Temperature Class	Temperature Range
1	-20°C to -15°C
2	-14°C to -10°C
3	-9°C to -5°C
4	-4°C to -0°C
5	1°C to 5°C
6	6°C to 10°C
7	11°C to 15°C
8	16°C to 20°C
9	21°C to 25°C
10	26°C to 40°C

5.2.4 Heat Profile Calculation

To use *SigLinDe* profile and intra day profile pool, each residential building has to be classified as either EFH or MFH. The IWU archetypes, on the other hand, differentiate between five possible construction types. To address this discrepancy, the following assumption is made: building type EFH is further used for RH, while MFH is further used for both GMH and HH.

For the disaggregation of the annual heat value, ambient temperature data set from solar potential study Hamburg (Chapter 4.4) is used. Using the temperature data set, the daily average ambient temperature and its temperature class is calculated. The average temperature is subsequently used to compute the ratio of the demand on a given day to the annual demand.

One intra day profile is then selected from the profile pool for each temperature class, with each profile corresponding to the particular building type. This is done using the assumption that the heating pattern within a particular temperature class does not vary.

The hourly heat profile per building can then be calculated for each day using the combination of specific annual heat value from TABULA, daily heat ratio from the *SigLinDe* function, temperature class specific intra day profile and building reference area.

5.3 Electrical Demand Model

This section describes the methodology used to create electrical load profile for all residential buildings in Hamburg, which uses [125] as an inspiration. This methodology utilizes census data set together with ALKIS to generate characteristic load profiles that are specific to each city district. The calculated reference area from 5.2.1 is then used together with the characteristic load profiles and a scaling factor to calculate the building specific electrical load profile.

5.3.1 Generation of Base Load Profiles

In Germany, grid planing and modeling of electrical demands have traditionally relied on SLP (Standard Load Profiles). However, SLPs for electricity are currently based on measurements in the 1980s, which may differ from the current load profile. Another issue with SLPs are the inherent lack of variance for each of the modeled load profiles, raising concerns about the statistical validity of the load profiles. For residential purposes, currently only one profile exists [125], [144]–[148].

For this work, instead of the aforementioned SLP, load profiles generated using a statistical bottom-up approach developed in [37] are used. The statistical model considers different household types, their behavior, and their appliances, with appliances and their load profiles being selected in an arbitrary manner. In total, 12 household types are available for selection (Table 5.9). These household types are based on household compositions defined in Eurostat [37], [149].

Table 5.9: Household types considered in [37]

Household Type	Inhabitants Type	ID
Single	Retiree	SR
	Adults without children	SO
	Adults with children	SK
Couple	Retiree	PR
	Adults without children	PO
	Adults with one child	P1
	Adults with two children	P2
	Adults with three or more children	P3
Others	Retiree	OR
	Adults without children	O0
	Adults with one child	O1
	Adults with two or more children	O2

Sets of 2511 and approximately 100,000 different profiles have been published under open data license as a part of data bundle for ego^n project (Chapter 4.5) [120]. To reduce computational time, this thesis utilizes the set of 2511 profiles rather than the 100,000 generated profiles.

5.3.2 Census Data Preparation

As mentioned earlier, the generated profiles are classified based on household and inhabitant types. To use the generated profile, household information with the highest spatial resolution possible is needed. For this purpose, census data from 2011 German census is used (Chapter 4.1. The census data set is well known and is regularly used in numerous projects [27], [150], [151]

The preparation of census data in this work is based on [125]. In this work, two different types of census data set are used. The first census data set contains details about the amount of individuals residing in households, categorized by household type, household size, and age within each NUTS 1-region. The second data set contains information on households by family type or household size on cell level (100m x 100m). To generate household information with additional detail regarding its inhabitants on cell level, both census datasets are merged [125]. Due to different definitions of household types between Eurostat and the census, it is necessary to process and reorganize the census data set to ensure compatibility with the demand profiles [149], [152].

Census Data Preparation on NUTS-1 Level

Census data on the NUTS-1 level classifies households into five types: singles (S*), couple without children (P*), couple with children (P+), single parent (S+), and multi-person household without a core family (M*). Given that the Census data on the NUTS-1 level lacks sufficient details to differentiate M* based on the number of children present in the household, this cluster is represented by only adults and retirees. Using information regarding household size, 10 distinct categories can be derived from the aforementioned household types [125]. The newly created categories are selected in such a way that they are comparable to household types of the above-mentioned load profiles (Table 5.9). Table 5.10 provides an overview of the categories.

Table 5.10: Census household categories (NUTS-1) [125]

Household Type	Household Category	ID
S*	Single retiree	SR
	Single adults	SO
S+	Single with children	SK
P*	Retiree couple	PR
	Adult couple	PO
P+	Couple with 1 child	P1
	Couple with 2 children	P2
	Couple with 3 or more children	P3
M*	Multi-household retiree	OR
	Multi-household adult	O*

As the load profiles generated by [37] is based on household classification from [149], children (age $<$15) need to be excluded from the calculation. In this work, retirees are assumed to be at least 65 years

old. The number of people living in the 10 distinct categories can then be derived. As the obtained values represent the amount of inhabitants living in each categories, further steps are required to derive the number of households.

By dividing the number of inhabitants with the average amount of people living in each category, the amount of households can be calculated. For single and couples, the calculation is trivial due to the exclusion of children. For multi-households, the assumption made in [125] is used. Using census values on cell level, the weighted average number of people not residing in single or couple households is calculated for the corresponding NUTS-1 area. This value is then used as an approximation to calculate the number of households for category OR and O* (Table 5.10).

Census Data Preparation on Cell Level

At the cell level, census data contains household information with a high spatial resolution. However, in this spatial resolution data gaps and discrepancy exist due to confidentiality reasons [125], [153], [154]. Cells with unacceptable deviation due to confidentiality reasons are excluded from further steps. Figure 5.6 shows exemplary census cells for selected regions of Hamburg.

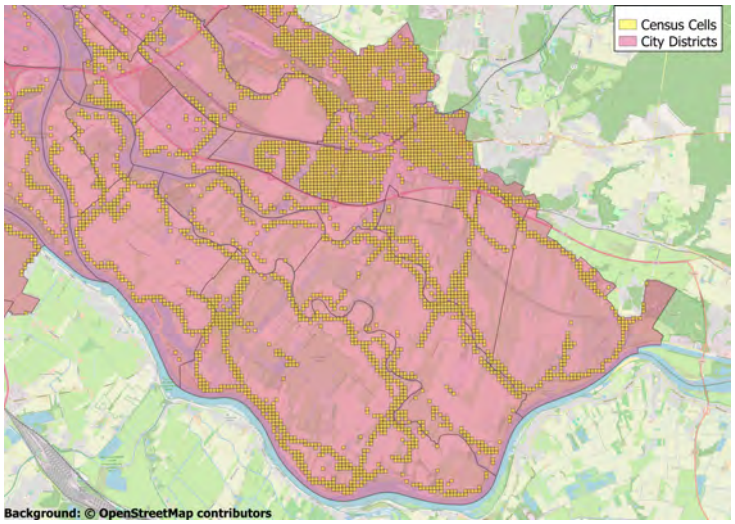

Figure 5.6: Census cells for selected region of Hamburg

Among the populated cells, a significant portion contains incomplete household information. These cells can be split into two categories, namely: cells with the total number of households but no household type (case number 1) and cells without both the total number of households and household types (case number 2). Cells falling into case number 2 (1750 cells, representing roughly 7% of cells containing complete information) are excluded from further calculation.

For cells falling into the first case (1353 cells, representing roughly 5% of cells containing complete information), these cells are first enriched with information of its corresponding city district from ALKIS. Using ”complete” cells from the same city district, the average distribution of household types for cells with the same total amount of household is calculated. If no matching cells are found within the city district, ”complete” cells from the NUTS-1 area are utilized instead. The average share is then multiplied

by the total number of households and rounded up to the nearest integer. Any deviation in the sum of household types from the rounded sum is adjusted by adding or subtracting the difference from a randomly selected household type to maintain the total number of households per cell.

Census and ALKIS

For the calculation of the city district specific characteristic load profiles, the total living space for each census cells needs to be calculated using ALKIS building objects. For this purpose, it is imperative to understand how census cells and ALKIS building objects are related to each other. [126] points out that census uses building entrances rather than individual building for its data collection. Within ALKIS building entrances are represented by an object called georeferenced addresses [116].

Figure 5.7 shows exemplary the relation between census cell and ALKIS. According to census, the cell on bottom right has 12 ”buildings”. According to ALKIS the aforementioned cell contains only three buildings. This clearly indicates that census uses individual addresses as the basis for its data collection. This also means that a census cell is populated when an address point (or by proxy a building) can be located.

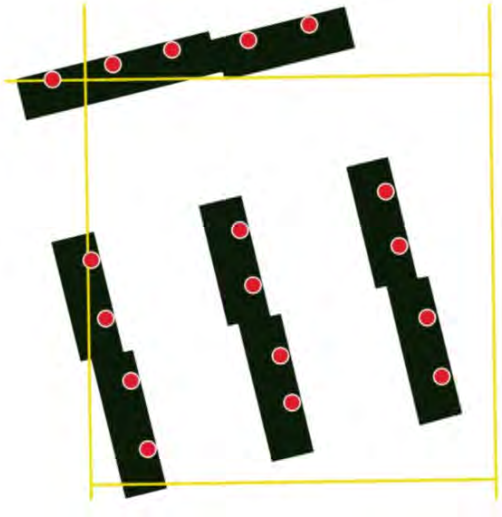

Figure 5.7: Example of relation between ALKIS building and census cells [126]. Black rectangles represent ALKIS building. Yellow squares represent census cells. Red dots represent ALKIS georeferenced address points.

To ensure continuity between all datasets used in this thesis, further considerations are needed for the ”prepared” census cells. Using the principle of least common denominator between ALKIS and LoD2, the amount of ”valid” building objects considered in this thesis is reduced. This, in turn, affects which census cells are to be considered in this thesis. To accommodate these restrictions, only census cells with a georeferenced address point, where the corresponding building(s) exist in both ALKIS and LoD2, are considered in further steps.

Refinement of Census Cells

As opposed to the census data set on NUTS-1, census cells only differentiate between five household types. The usage of load profiles from 5.3.1 however requires further refinement of these information. In this work, census cells are refined using proportionate allocation as described in [125].

For every single household within a census cell, a household category is selected at random. The selection is weighted using the distribution of household categories within a household type in NUTS-1. Figure 5.8 exemplifies how proportionate allocation is implemented. Using the distribution in NUTS-1 (60% SR and 40% SO), single households in census cells are refined. As the selection for each household is done randomly, different cells with an equal amount of household types may receive different amount of household categories. Nevertheless, the total sum of each household category in every cell will mirror the distribution observed at the NUTS-1 level.

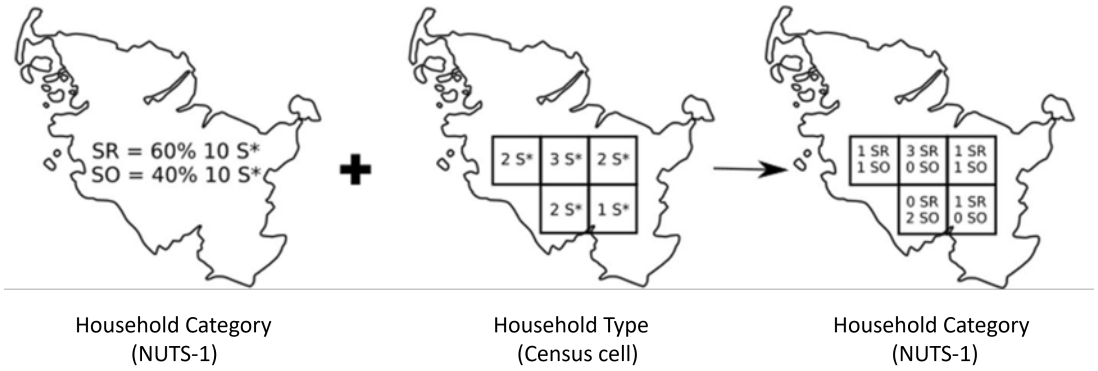

Figure 5.8: Exemplary refinement of census cells using proportionate allocation. Adapted from [125].

5.3.3 Base Load Profiles Allocation

Before the allocation of load profiles, the discrepancy between household types in Table 5.9 and household categories in Table 5.10, concerning multi-household (M*), needs to be addressed. As no differentiation regarding amount of children in O* category (Table 5.10) can be made, household types O0, O1 and O2 (Table 5.9) are therefore aggregated into a single new household type as a simplification. This means that for category O*, load profiles of type O0, O1, and O2 are available for selection. For the allocation, profiles are sampled in random in a way, that no single variation of a profile occurs more than once within a single cell. This variation can nevertheless still be utilized in other cells.

5.3.4 Reference Area Allocation

To generate city district specific electrical load profile, it is required to calculate how much living area exists within a census cell. Regarding living area, the methodology described in Chapter 5.2.1 is once again utilized. From Chapter 5.3.2 however, it is known that the census methodology utilizes building address point for data collection as opposed to individual buildings. Out of this, the possibility arises that an individual building is connected to multiple census cells due to multiple address points within the building in question.

An example of the aforementioned problem can be seen in figure 5.7. In this figure, five address points are assigned to the building on the top side. The building in question intersects with four different census cells, while the address points are located in two different census cells. As a result, a key question emerges regarding the allocation of shares of building living area towards census cells.

[126] addressed this issue by aggregating census cells so that the address points of a building object consistently fall within the same aggregated census cells. However, since the objective of this proposed method is to allocate building information, such as ownership, from census cells to building objects, it is not considered aligned with the goals of this chapter. This method does not provide clarity for the allocation of living area to census cells. Furthermore, the creation of aggregated cells could complicate the task of assigning census cells to city districts, as aggregated cells may cover multiple city districts. In this case, disaggregation would once again be required.

This thesis addresses this problem by assuming that every address point of a building holds an equal proportion of living space. Using example from Figure 5.7, 20% of the living area of the uppermost building is then assigned to one census cell, while the remaining portion is allocated to another cell. As the aim of this step is to generate a city district specific electrical load profile, the mistake due to inaccurate allocation of shares into address points is asummed to be negligible. It is also assumed that this error is less significant compared to the mistake resulting from a substantial difference in the publication dates (ALKIS being from 2023, while the census data is from 2011).

5.3.5 Census Cells and City Districts

For the placement of census cells into city districts, the city district data set from ALKIS *Stadtteile* is used. For most of the census cells, this process is trivial as the cell in question lies completely within the border of the city district. For cells at the edge of the border, however, further considerations are needed. In this thesis, the allocation of city district is done using the center point of the cell. Figure 5.9 shows exemplary the implementation of this assumption. Each of the census cells are allocated into a particular city district depending on the location of the center point.

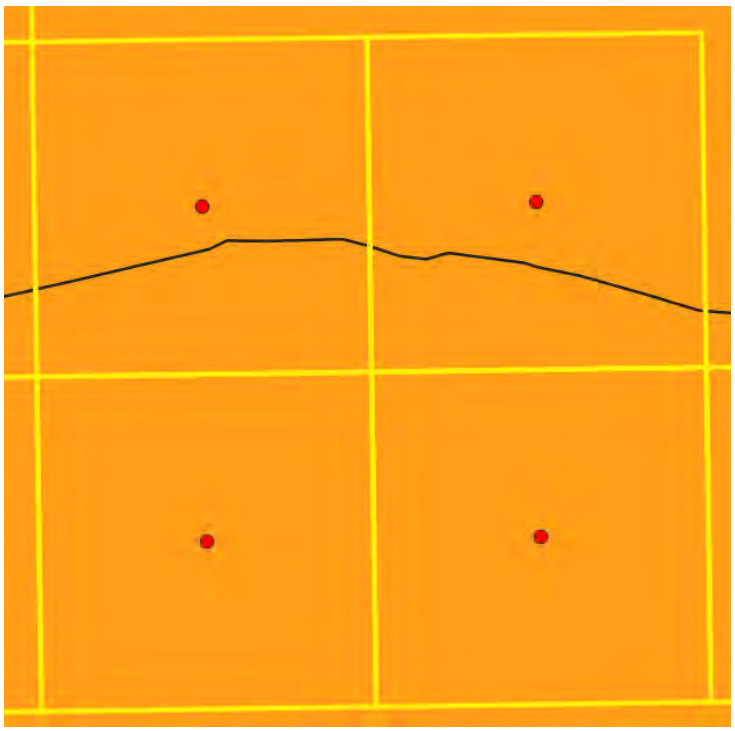

Figure 5.9: Exemplary placement of city district and census cells. Orange area represents city district. Yellow squares represent census cells. Red dots represent center point of the cell.

5.3.6 Characteristic Load Profiles per City District

For the calculation of characteristic load profiles per city district, remaining census cells are aggregated depending on their city district. For each city district, the sum of all base load profiles assigned to census cells within the district is then divided by the sum of all residential living areas (Chapter 5.2.1).

In Figure 5.10 the calculated city district load profiles for Lokstedt and Neuengamme are compared to dynamic household SLP [155]. The load profiles exhibit a general trend of peaks in certain hours during the day and a lower overall peak in summer times. Compared to the SLP, the presented method shows steeper gradients, higher peaks, and smaller base loads. These differences are further discussed in Chapter 6.5. Nonetheless, the general pattern of the city district load profiles is comparable to the SLP. As the goal of city district load profiles is to introduce variability to different districts, this method is assumed to be suitable.

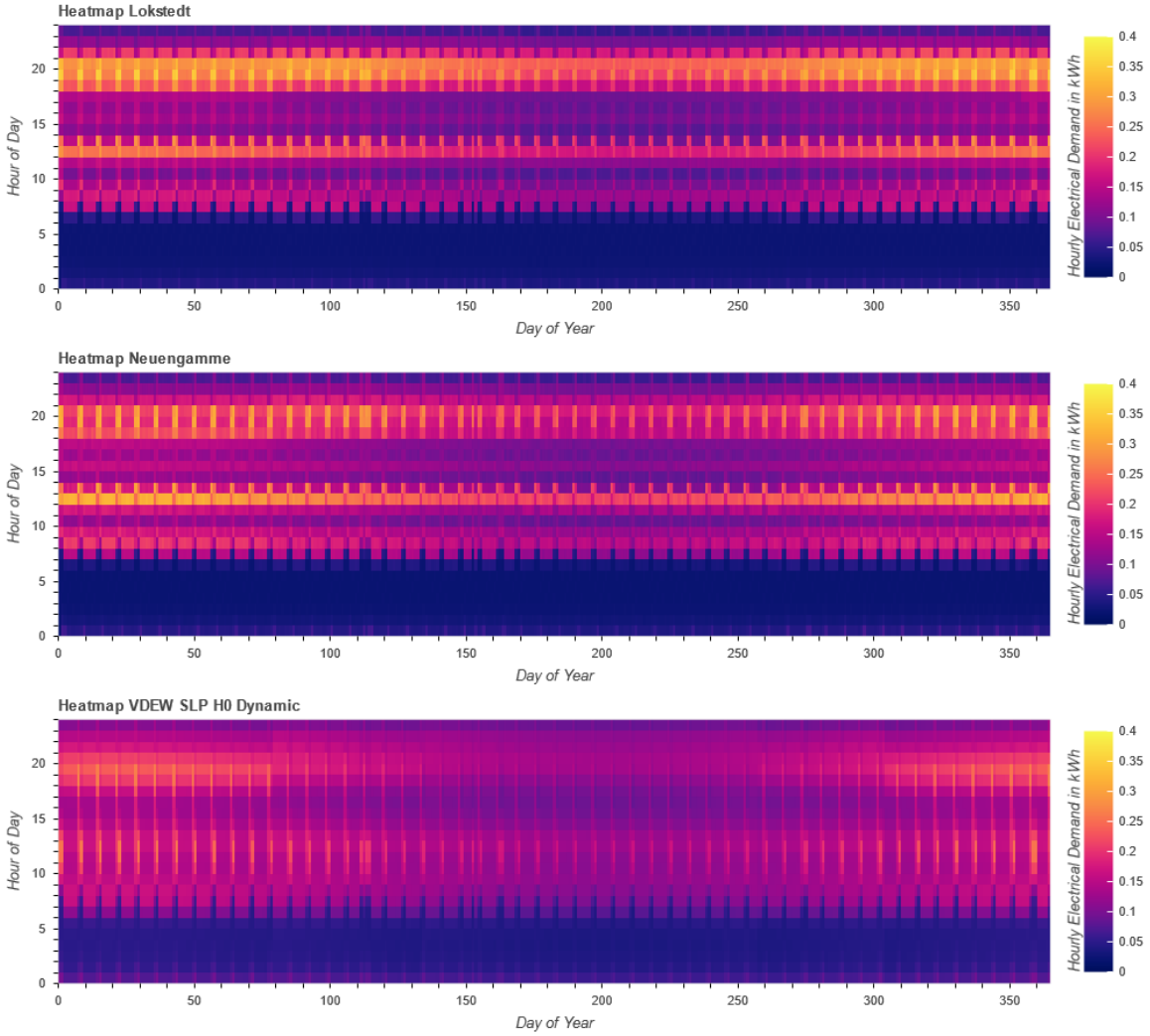

Figure 5.10: Comparison between VDEW dynamic household load profile [155] and city district load profile for Lokstedt and Neuengamme. All profiles are normalized to 1 MWh

5.3.7 Building and City District

As mentioned in Chapter 5.3.2 and illustrated in Figure 5.7, multiple address points can be assigned to a single building object. As a result, it is possible for a single building to be assigned to multiple city district due to its address points. Figure 5.11 provides an example of this case. This issue is addressed in this thesis using the assumption that a building object can only be assigned to a single city district. The assignment of city district is done using the highest intersection area with building footprint area.

On the other hand, it is also possible for a building object to not be assigned any address points, which refers to buildings that are neither a main building nor a secondary building. For these buildings, centroid

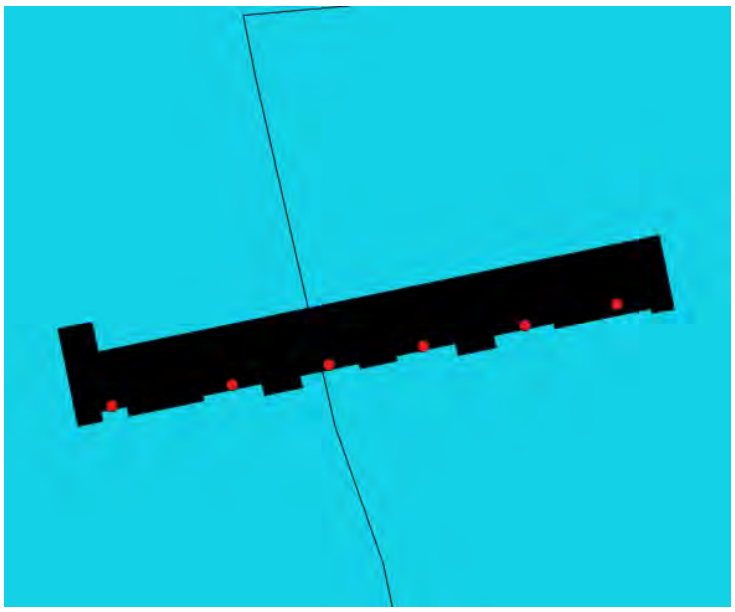

Figure 5.11: Example of relation between ALKIS building and city districts. Black rectangles represent ALKIS building. Red dots represent ALKIS georeferenced address points. Teal area represents city districts

of the building footprint area is used for the allocation of city districts.

Since the districts of Waltershof and Altenwerder predominantly comprise of port and industrial areas, buildings located within these districts are excluded from further consideration.

5.3.8 City District Scaling Factor

As a result of the census data set available at the time of writing this work, the generated city district load profiles are based on household information from the year 2011. As more than a decade has passed since the census data set was published, it is reasonable to assume that the structure of households in Hamburg has changed [156], [157]. To better model the current electrical demand, scaling factors specific to each city district are introduced.

To begin, the annual electrical demand per city district is calculated using the total living area within the district and its characteristic load profile. The resulting annual demand is then multiplied by the aforementioned factor to meet the assumed annual demand of that year. The assumed annual demand is calculated using a combination of statistics of household structures in Hamburg from year 2022 and average electricity demand per household by household size (without electrical heating) from year 2021 (Figure 5.12)[157], [158].

The statistics of household structures in Hamburg provide, for each city district, the total amount of households, the average household size, the amount of one person households, and the percentage share of household sizes. The statistics differentiate between one, two, three, and four or more persons in a household. As the amount of single households are given, the percentage share is combined with the

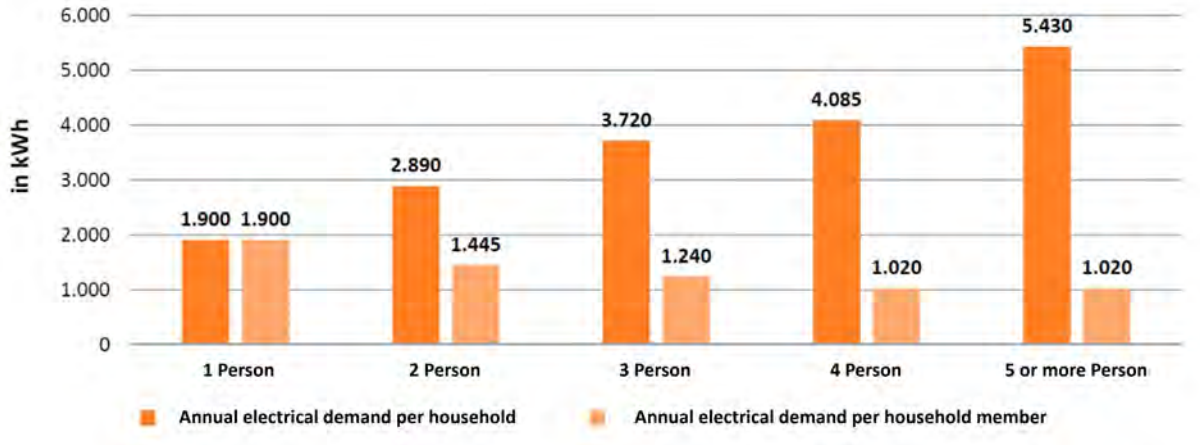

Figure 5.12: Average electricity demand per household by household size (without electrical heating) 2021 [158]

remaining amount of households to approximate the amount of the remaining household types. These values are then rounded to the nearest integer. In cases where the sum of the approximated values deviates from the set value, the difference is adjusted by addition or subtraction from randomly selected types. The random selection is weighted using the average share of each type.

Since the statistics does not differentiate further between four or more person per household, the average amount of inhabitants of this household type needs to approximated. For this approximation, the total amount of inhabitants in the city district is required. This can be estimated using the average household size and the total amount of households. It is important to note that the statistics are generated using standardized household generation process HHGen and only present a realistic description of households in Hamburg [157].

This uncertainty can also be seen in the approximated household size for households with four or more inhabitants, with some districts receiving values smaller than four. As the correctness of the statistics is out of the scope of this work, these values are accepted. To accommodate these values, adjustments to average electrical demand values from Figure 5.12 are required. The necessary annual values are then created using linear interpolation.

Furthermore, the districts of Waltershof and Finkenwerder, Neuland and Gut Moor, Altenwerder and Moorburg, as well as Kleiner Grasbrook and Steinwerder are each considered together in the statistics [157].

5.3.9 Building Specific Electrical Load Profile

The calculation of building specific electrical load profile is done using the reference area from Chapter 5.2.1, the specific load profile from Chapter 5.3.6 and the scaling factor from Chapter 5.3.8.

5.4 Photovoltaic Generation Model

This section describes the methodology used to generate time series data for rooftop PV systems in every building in Hamburg. The approach utilized in this study builds upon methodologies and findings from solar potential study Hamburg [6]. This section begins with the calculation of roof areas for all ”valid” residential buildings in Hamburg. Subsequently, roofs are categorized based on their relevant characteristics. These characteristics are then employed to assess the feasibility of PV on the roofs. Results from [6] are then utilized to calculate the PV generation profile for each suitable roof. The calculated profiles are then aggregated to generate pv generation profile for each building.

5.4.1 Building Roof Surfaces

As mentioned before in previous sections, some residential building objects are excluded to ensure continuity between the models used in this work. This refers to exclusions due to mismatch of ALKIS and LoD2 (Chapter 4.7), no residential living area (Chapter 5.2.1), and city districts of Waltershof and Altenwerder (Chapter 5.3.7).

For every ”valid” residential building, LoD2 data set is used as an approximation of the actual shape of each roof. Within LoD2, each roof is modeled separately, which means that a single building can have multiple roofs assigned to it. Each of the roofs can also have different roof types. Figure 5.13 shows an example of different roof configurations. This figure also shows that the edges and vertices of each roof are clearly defined.

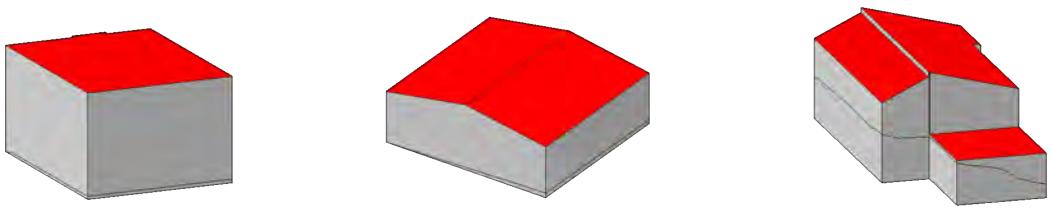

Figure 5.13: Examples of LoD2 building model

Using the vertices, the resulting area for each individual roof can be calculated. These vertices can, on top of that, be used to find the normal vector of the plane, which is an integral characteristic for the utilization of PV on roof surfaces. From the normal vector, two crucial parameters can be calculated, namely: tilt angle and surface azimuth. Due to the precision of LoD2 model, there are instances where the vertices result in a non-planar plane. Figure 5.14 provides an example of a non-planar surface. The nonplanarity of the surface can be directly noticed, as the plane can be seen as two triangles with different normal vectors.

To address non-planar surfaces, this work introduces an original method for generating a planar representation using the vertices, centroid, and normal vector of the original surface. This method builds upon

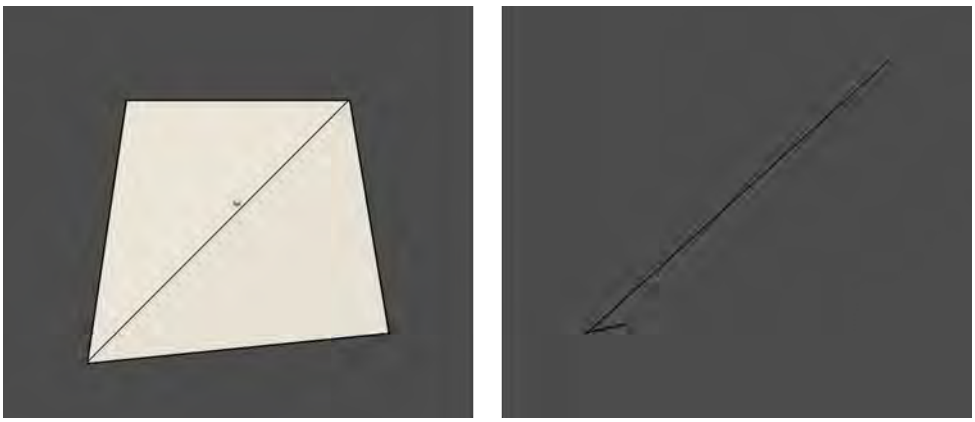

Figure 5.14: Example of non planar roof surface. Circle represents centroid.

a small subset of helper algorithms developed within the framework of the ”Large-scale 3D Geospatial Data for Urban Analytics” project [159]. First, a representative normal vector for the plane is calculated. Using the centroid and the approximated normal vector, a ”secondary” plane is generated. Following these steps, the original vertices are projected onto the secondary plane. The resulting plane out of the projected vertices is then used to calculate tilt angle, surface azimuth and surface area. Figure 5.15 shows the result of this simplification.

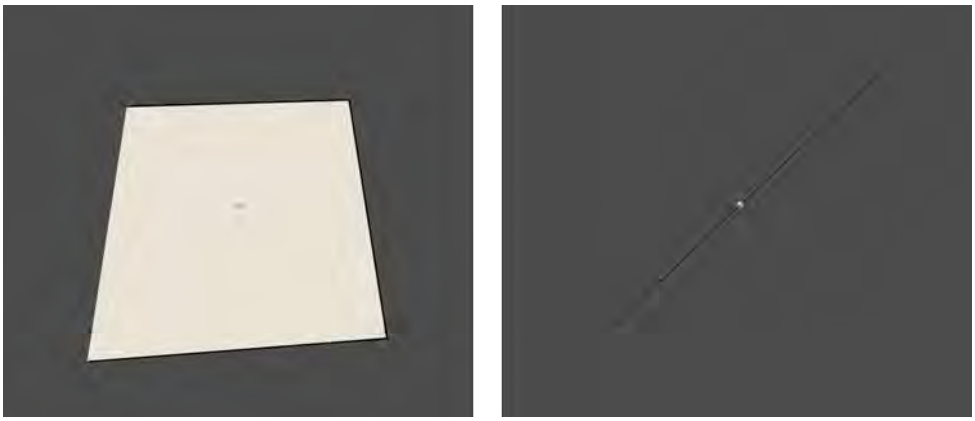

Figure 5.15: Simplified non planar roof surface. Circle represents centroid.

5.4.2 Classification of Roof Surfaces

As this thesis aims to utilize results from the solar potential study Hamburg, adjustments to tilt angle and surface azimuth are needed. Within the solar potential study, solar outputs are calculated for different combinations of tilt angle and azimuth. For tilt angle steps of five degrees are used while steps of ten degrees are used for surface azimuth [6]. To accommodate this, both tilt angle and surface azimuth are rounded to the nearest step.

5.4.3 Suitability of Roof Surfaces

To find roof areas that are suitable for PV utilization, a plethora of constraints has to be accounted for. These can for example be regulatory requirements, but also economic efficiency considerations, sociocultural or ecological factors [6]. Since the amendment of Hamburg's climate protection law (*Hamburgischen Klimaschutzgesetz* (HmbKliSchG)), one of the most important regulations that directly affect Hamburg residents are the obligation to install PV systems on Hamburg's roofs (*PV-Pflicht*) [160].

Using this regulation and assumptions made in solar potential study Hamburg for realizable potentials, suitable roofs are approximated. As this thesis does not carry out detailed examination of each buildings, constraints that require individual examination of the buildings, such as costs of the system, period of use, and building statics, are not considered. In the following, each of the constraints used in this thesis are explained.

Minimum Roof Areas

As system cost depends highly on the individual situation of the buildings, this constraint cannot be applied in general manner for all building objects. To approximate the economic feasibility of PV installation, available roof areas are used as a proxy.

The first restriction is the gross roof area available for each building. Buildings with gross roof area smaller than 50 m^2 are exempt from the solar obligation and are assumed to have no PV system [161]. For every other building, the suitability of every continuous section of the roof is examined. It is then differentiated between flat roofs (tilt angle equals zero) and tilted roofs. Flat roofs with a surface area smaller than 20 m^2 and tilted roofs with a surface area smaller than 10 m^2 are also excluded [161].

Minimum Irradiation Level

Another constraint that influences the economic viability of PV installation is the expected yield of the system. In the solar obligation, it is considered economically unjustifiable for buildings with gross floor area of up to 150 m^2 if the annual solar irradiation is more than 30% lower than the maximum annual solar irradiation on an optimally aligned and unshaded PV system [161].

In solar potential study Hamburg, this constraint is approximated using the comparison between long term average annual solar yield. Rather than only applying it only to building up to 150 m^2 gross floor area, the annual yield constraint is used for every roof surfaces. Additionally, the minimal annual yield is set to 80% of the optimal configuration, providing a buffer compared to the legal requirement [6].

Figure 5.16 shows the long term average annual PV solar yield depending on the tilt angle and azimuth. The percentage range for Hamburg spans from 24% (90° tilt angle at 10° azimuth) to 100% (40° tilt angle at 200° azimuth). From this figure, it an be clearly seen that flat roofs in Hamburg receive enough irradiation, while no general statement can be said for tilted roofs.

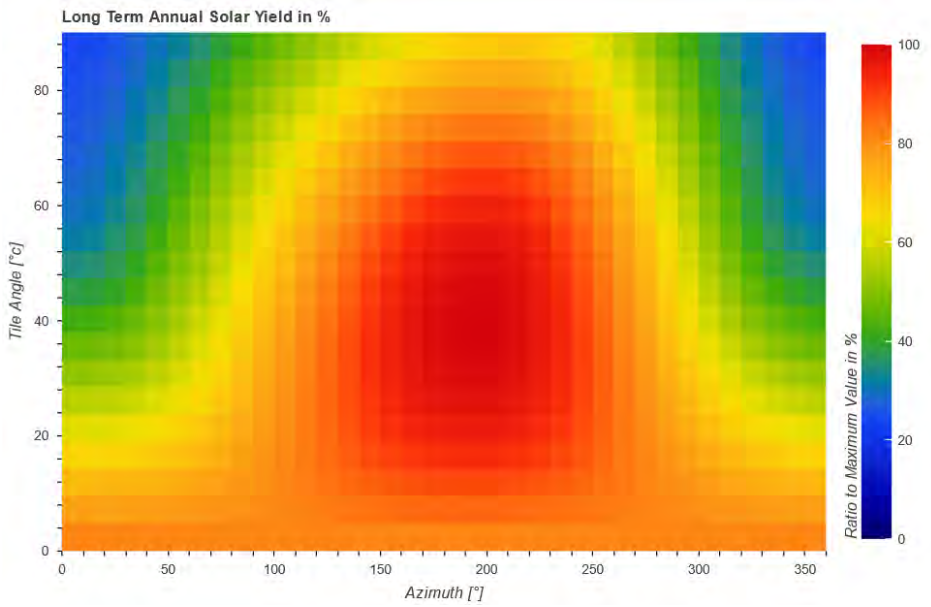

Figure 5.16: Ratio of Long term average annual PV solar yield to the maximum solar yield in Hamburg [6]. 0° Azimuth represents north.

5.4.4 Roof Utilization Factor

Roof surfaces can be covered with different proportions of PV modules. To model these proportions, the roof utilization factor is taken into account. The extent to which roof surfaces can be utilized for PV modules varies significantly for each building depending on the tilt angle, orientation and the type of surface. In this thesis the simplification used in the solar potential study Hamburg is applied. For flat roofs, a utilization factor of 80% is implemented, while 60 % is set for tilted roofs [6].

5.4.5 PV Module Assumption

As previously mentioned, the orientation and tilt angle of a PV system play a huge role in terms of energy yield. With roof-parallel installation on tilted roofs, the inclination and alignment of the PV modules are fixed by the roof. For flat roofs, on the other hand, the inclination and orientation of the PV modules can optimized to maximize yield or achieve the desired daily or seasonal distribution. In this thesis, PV modules on flat roofs are modeled with 15° inclination and an east/west orientation. PV modules in this configuration provide more electrical energy at times when there is an increased demand for electrical energy (mornings and evenings) [6].

Due to the high variability of roof dimensions, simplifications are needed to determine the amount of installed PV power for each roof surface. In this thesis, a power density of 200 $\frac{W}{m^2}$ is used to quantify the PV potential [6]. Using this simplification, individual examination of the roof surface can be omitted.

5.4.6 Performance Ratio

To realistically model PV generation, losses that occurs in the system, such as shading and electrical losses (for example due to inverter) have to be taken into account. Due to the nature of these losses, a detailed consideration of the losses would require individual examination of not only the PV system but also the site-specific weather situation (such as cloud cover). As these type of analysis are outside of the scope of this work, the consideration of PV losses in this thesis is simplified using performance ratio. For all PV systems a performance ratio of 80% is assumed. This assumption is in line with the value used in [6] and reported in [162]. This performance ratio is then applied for each time step.

5.4.7 Building Specific PV Generation Profile

For each building, the PV generation profile can now be calculated using the steps described in the previous sections. Using the vertices from LoD2, the relevant parameters for PV utilization can be derived for each roof surface (Chapters 5.4.1 - 5.4.2). Depending on the derived characteristics, assumptions are made regarding the feasibility (Chapters 5.4.3 - 5.4.4) and configuration (5.4.5) of the PV system. Using PV generation profile generated as a part of solar potential study Hamburg and assumptions regarding performance ratio (Chapter 5.4.6), the generation profile of each roof surface and subsequently of each building can be calculated [6].

5.5 Building Energy Model

The section aims to answer the question of how the energy demand and supply for both heat and electricity are matched on a building level. This section begins with the description of the building energy system modeled in this thesis. For every component used in the model of the building energy system, the methodology used for sizing and its corresponding assumptions are provided.

5.5.1 Overview of the Building Energy System

In recent years, the role of buildings in maintaining the stability of a the electrical grid has been ever increasing. Traditionally, buildings were assumed to have a passive role in the day-to-day operation of the electric grid. Due to factors such as the wide-spread implementation of renewable-energy-source, including electric storage, the role of buildings for the stability of the electrical grid has changed significantly [163], [164]

In this thesis, the following assumptions are made to model the electrical energy system of a building:

- Every building is connected to the electrical grid
- Buildings with PV installed are assumed to have a battery storage system
- Battery can be charged using both the electrical grid and PV

The assumptions regarding heating system of a building is differentiated depending on the availability of district heating for the particular building. In the case of district heating, the assumption is made that the heat demand of the building can be fully provided by district heating at all times. For buildings without connection to district heating, the following assumptions are made:

- Every building has one thermal energy storage system
- Heat is provided using the combination of an air sourced heat pump and an electrical heater
- Thermal energy storage can be charged using both the heat pump and the electrical heater

Figure 5.17 shows a simplified representation of the model used for the building energy system.

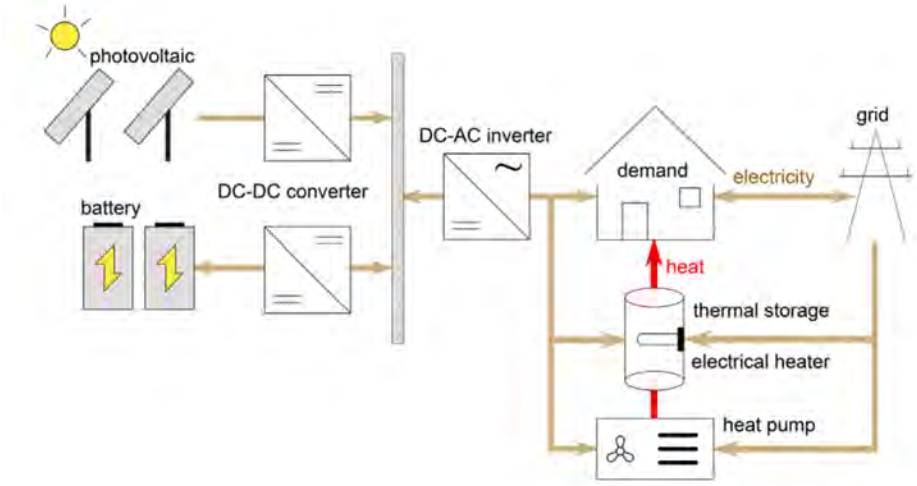

Figure 5.17: Building energy system. Adapted from [165]

5.5.2 Battery Storage System

Determining the size of the battery storage is a critical aspect in designing a PV system. From a life cycle cost perspective, the costs of battery storage often significantly impacts the economic feasibility of such a system [166], [167]. In the literature, the battery is often sized using a ratio between installed PV power in kW and battery capacity in kWh [168]. As costs of battery storage systems have evolved rapidly over the past several years, these price developments need to be considered in the approximation of the battery size [169]. In this thesis, the size of a battery is approximated using a ratio of 1.5 $\frac{kWp}{kWh}$. This ratio has been calculated using methods described in [170] considering future economic projections and a degree of self sufficiency of 0.5.

Despite the recent improvements in battery storage systems, it is important not to overlook the losses that occur within a battery storage system. Figure 5.18 provides an overview of the energy conversion paths for the battery in this thesis. For each of the paths, a constant efficiency value out of [171] is assumed. Furthermore, a daily self discharge rate of 0.17% is used in this thesis [57]. Table 5.11 provides an overview of the battery losses used in this thesis.

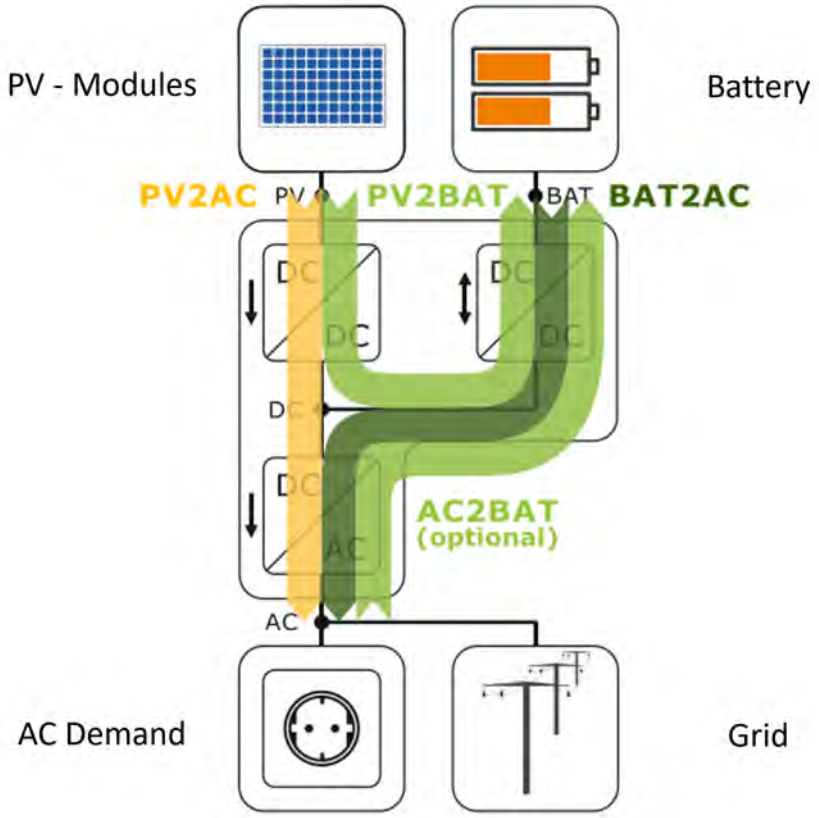

Figure 5.18: Energy conversion paths for battery storage. Adapted from [171]

Table 5.11: Assumptions regarding battery losses [57], [171]

Loss Type	Value	Source
PV2BAT	95.8%	[171]
PV2AC	96.2%	[171]
BAT2AC	95.5%	[171]
AC2BAT	95.3%	[171]
Daily self discharge	0.17%	[57]

5.5.3 Heating System Sizing

As shown in Figure 5.17, within this thesis, the combination of heat pump, electrical heater and thermal energy storage is used to model the heat supply for buildings with no connection to district heating. This assumption is influenced by the newly approved Building Energy Act (*Gebäudeenergiegesetz* - GEG), where every newly installed heating system is required to be powered by at least 65% renewable energy [172].

Similar to the sizing of the battery storage system, the heating system also needs to be sized accordingly to ensure cost-effective operation. In the literature, this step is typically done using a mathematical optimization [173]–[175]. As this thesis does not aim to find the best sizing method for heat pump systems, optimizing the size of the heating system on building level is deemed to be outside of the scope of this thesis. As a simplification, the SIZEP (Sizing Evaluation Step) described in [176] to estimate the capacity and power of a thermal energy storage is used instead.

SIZEP relies solely on time-series data (historical heat load) to approximate the capacity of thermal energy storage independently of the heat source. For this approximation, three descriptive parameters are derived out of the time-series, namely: RHV (relative hourly variation), RDV (relative daily variation), and DAHV (daily accumulated heat volume). This method is originally developed to be used in combination with CHP plants [176]. The equations used to calculate these parameters are given below

$$RHV = \frac{|L_h - L_d|}{L_a} \cdot 100 \tag{5.5}$$

$$RDV = \frac{0.5 \cdot \sum_{t=1}^{24} |L_h - L_d|}{L_a \cdot 24} \cdot 100 \tag{5.6}$$

$$DAHV = 0.5 \cdot \sum_{t=1}^{24} |L_h - L_d| \tag{5.7}$$

L_d annual average heat load
L_h hourly average heat load
L_d daily average heat load
t discrete time period

Using the first parameter RHV, the variation of the heat load in each hour of the year can be characterized to provide an approximation of the power required for thermal energy storage to eliminate the hourly load variation in a day. To take outliers into consideration, the value of the 99th percentile, instead of the highest RHV value, is utilized [176]. This value is then multiplied with the annual average heat load to determine the heating load of the heat pump. This calculation is based on the assumption that the thermal power of the thermal energy storage is equal to the heating load of the heat pump.

The second parameter, RDV, provides an approximation of the minimum capacity of the thermal energy storage system to eliminate heat load variations in the system. On the other hand, DAHV quantifies the necessary thermal storage capacity to ensure the continuous operation of the CHP plant throughout the entire year. While both RDV and DAHV provides an approximation for the capacity of thermal energy storage system, the value calculated using DAHV considers only the thermal load over 24 consecutive hours [176]. In this thesis, the capacity of thermal storage is approximated using DAHV rather than RDV to ensure a higher degree of reliability. Similar to RHV, the value of the 99th percentile is used instead of its highest value to consider outliers.

Similar to battery storage system, the consideration of losses that occur within the thermal storage system is simplified using a number of constant values. This simplification is used as a detailed calculation of the losses requires further information, such as temperature of the storage medium, insulation materials and shape of the storage [177], [178]. Such an analysis would then require a detailed examination, which

is outside of the scope of this work. Table 5.12 provides an overview of the losses considered in this thesis.

Table 5.12: Thermal storage losses [57]

Loss Type	Value
Charge efficiency	90%
Discharge efficiency	90%
Daily self discharge	0.5%

Within this work, heat pumps are modeled using a coefficient of performance (COP) that varies with the temperature, as the COP of a heat pump depends highly on the temperature of its heat source. To model this temperature dependency, the formula provided in [179] for air sourced heat pumps is used in this thesis. As this thesis only considers air sourced heat pumps, ambient temperature data set from solar potential study Hamburg is used as the heat source temperature. The sink temperature in this study is assumed to be 50°C [180].

$$COP = 6.81 - 0.121 \cdot (T_{sink} - T_{source}) + 0.00063 \cdot (T_{sink} - T_{source})^2 \tag{5.8}$$

T_{sink} sink temperature
T_{source} source temperature

In the context of this thesis, an electrical heaters is used as an additional heat source and assumed to operate with 100% efficiency. As the primary purpose of this electrical heater is to provide heating support, its size is not fixed to a specific value

5.6 Medium-Voltage Grid

As mentioned in previous chapters, the goal of this thesis to analyze the impact of residential heat pumps and PV on the electrical distribution grid in Hamburg. To fulfill this goal, georeferenced grid datasets are required. Generally these datasets are not publicly available, as DSOs (distribution system operators) are not required to publish infrastructure data [181], [182]. Two reasons are often cited to justify the lack of data availability, the security aspect [181], [183] and the economic aspect [181], [184].

In the literature, efforts have been made to produce synthetic MV grids in Germany using open data [182], [185]. Due to the scope of the project (whole Germany), the accuracy of the results is often lacking to correctly model a particular region (in this case, Hamburg). Figure 5.19 depicts the aforementioned problem.

In this thesis, the MV grid for Hamburg is approximated on the basis of SVG (scalable vector graphics) graphic provided by Stromnetz-Hamburg. As this graphic is no longer publicly available, archived version from June 2022 is used (Figure 5.20) [187].

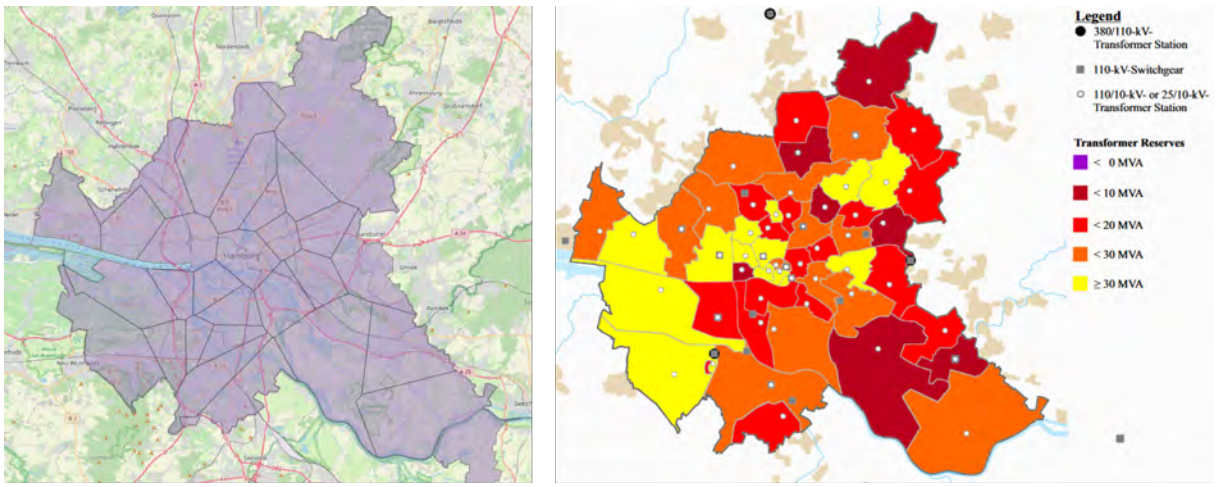

Figure 5.19: Comparison between MV grids of Hamburg [185], [186]. A represents synthetic MV grid from [185]. B represents transformer station areas on medium-voltage level in Hamburg [186]

Figure 5.20: MV grid of Hamburg [187]

Due to the characteristics of SVG graphics, a georeferencing process is required before this graphic can be used. For this purpose open source GIS (Geographical Information System) software QGIS is used. As SVG is not compatible with QGIS, this graphic is first converted to a CAD (computer aided design) drawing using AutoCAD. Using georeferenced administrative borders from ALKIS as control points,

this graphic is then georeferenced with the help of QGIS. The resulting georeferenced MV grid is shown in Figure 5.21. As the selection of control points needs to be done manually, inaccuracies within the individual areas of the MV grid are to be expected. Within this thesis, the grid areas of Altenwerder and Hausburch are assumed to have no residential building, as both of these zones comprise almost exclusively of port and industrial areas.

Due to the lack of additional grid information, such as transformers, no power flow analysis can be conducted within this work. The analysis of the effects of PV and heat pumps is therefore performed by analyzing the aggregated hourly electricity balance in each MV grid area.

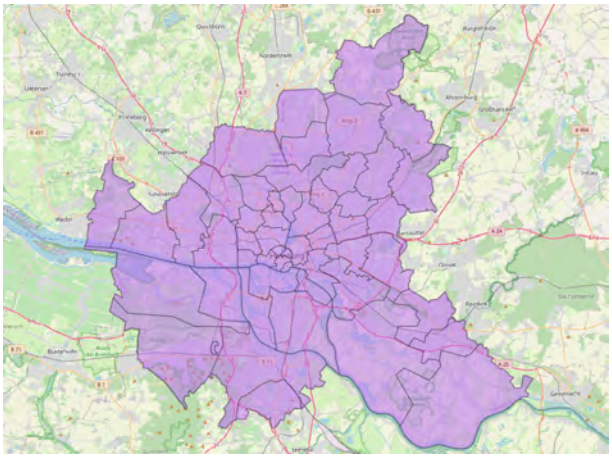

Figure 5.21: Approximated MV grid of Hamburg

5.7 District Heating Areas

As previously mentioned in Chapter 5.5.1, the assumed heating system of a building depends on the availability of district heating. In this thesis, district heating data set described in Chapter 4.6 is used. Figure 5.22 provides an overview of the district heating data set used in this thesis. As this thesis aims to only analyze the heating structure of residential buildings in Hamburg in its finished state, district heating is assumed to also be available for both district heating expansion and decentralized heating network areas. By combining this data set and the assumed location of the building (either using the georeferenced address for main and secondary buildings or building centroid for buildings with missing address), the heating system of each building can be determined based on the assumptions made in Chapter 5.5.1.

For two building blocks (109012 (A) and 319097 (B)) in Hamburg, no conclusion can be drawn regarding the availability of district heating due to data gaps. This problem is displayed in Figure 5.23. The pink colored areas represent building blocks provided by ALKIS, red rectangles represent building objects, and the purple, green, and gray colored areas represent the district heating data set. It can be clearly seen that for these two areas, no information can be drawn from the district heating data set due to data gaps. For case A (building block 109012), the assumption is made that district heating exists due to the availability of district heating in the surrounding building blocks. On the other hand, for case B (building

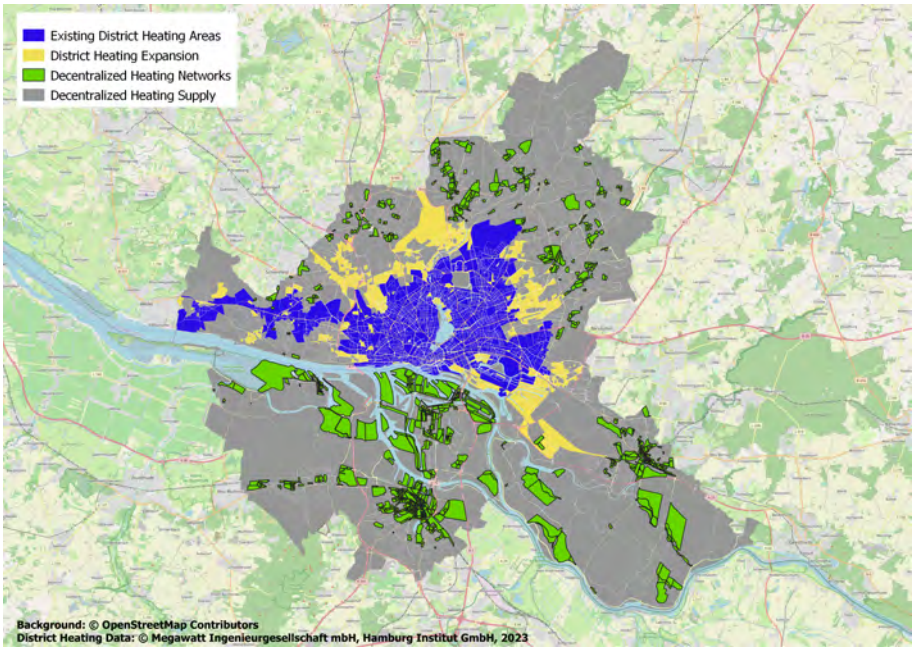

Figure 5.22: District heating areas per building block [122]

block 319097) no conclusion can be made, as more details are needed to estimate the linear heat density of this building block. The assumption is, therefore, made that decentralized heating supply are needed for this building block.

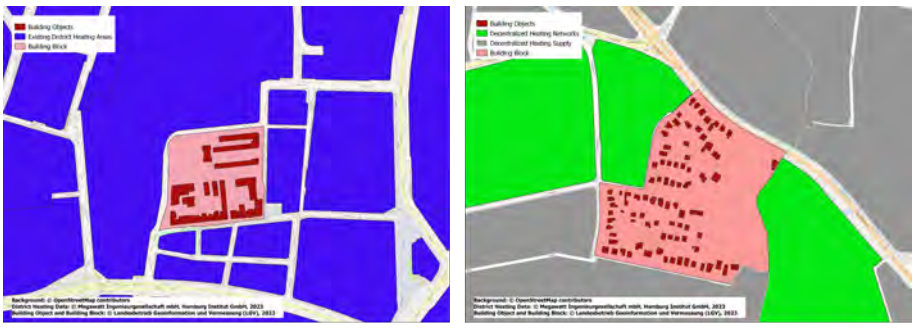

Figure 5.23: Data gap within the provided district heating data set [122]

5.8 Energy Optimization Model

In this section, the linear optimization model used to optimize the energy flow of each building is explained. Depending of the building energy system configuration, different optimization models are used. Following the aim of this thesis, the optimization models implemented in this thesis are designed to

only optimize the energy flow within the system from the point of view of the DSO. This leads to the optimization goal of peak reduction in both consumption from the grid and feed-in to the grid.

The chosen optimization model, however, can lead to unrealistically high total electricity demand. This occurs because the used optimization models do not consider the economic aspect of the energy system.Electrical energy from the grid is, therefore, considered free of charge. To make the model somewhat realistic, a secondary objective to minimize the total electricity demand is required. To reduce the complexity of this multi-objective optimization model, a constraint is introduced to limit the annual electricity demand [188].

In the following, each of the optimization models is described.

5.8.1 Buildings with District Heating and without PV System

As previously mentioned in Chapter 5.5, for buildings located in district heating areas, it is assumed that no thermal energy storage system exists within these buildings. Additionally, due to the non-existence of PV, no battery storage system exist in these buildings. Considering the lack of flexibility in the system, no optimization is done for this type of building.

5.8.2 Buildings without District Heating and without PV System

Figure 5.24 provides a representation of the energy system configuration assumed for buildings without a PV system that lie outside of the district heating network. The heat demand of the building has to be met using the available heating system. The resulting electricity demand is then fully provided by the electrical grid. As no PV system exists, no electricity is fed into the grid.

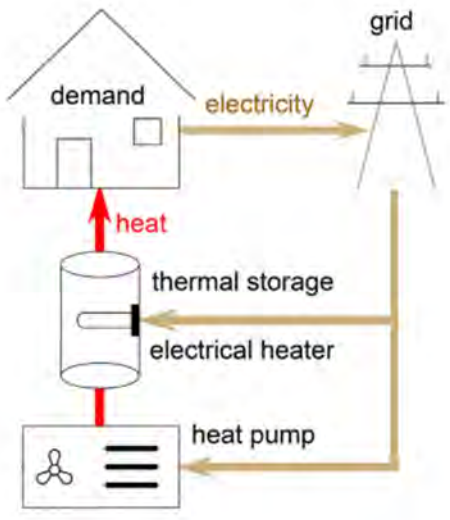

Figure 5.24: Buildings without district heating and without PV system. Adapted from [165]

Notations

The following indices, sets, variables and parameters of this model are defined below.

1. Indices
    - t - discrete time period
2. Sets
    - T - set of all discrete periods of time
3. Parameters
    - COP - coefficient of performance
    - W_{th} - heat demand
    - W_{el} - electricity demand
    - P_{hp} - maximum heat ouput of heat pump
    - $W_{TES,max}$ - maximum energy stored in thermal energy storage
    - $W_{el,limit}$ - maximum electricity demand allowed during optimization
    - $\eta_{TES,c}$ - thermal storage charge efficiency
    - $\eta_{TES,d}$ - thermal storage discharge efficiency
    - σ_{TES} - thermal storage daily self discharge rate
4. Variables
    - k_{hp} - heat pump utilization factor for heat demand
    - $k_{hp,c}$ - heat pump utilization factor for thermal storage
    - $W_{el,hp}$ - electricity demand from heat pump
    - $W_{el.heater}$ - heat supply from electrical heater
    - $W_{el.heater,c}$ - heat supply from electrical heater for thermal storage
    - W_{TES} - energy stored in thermal energy storage
    - $W_{TES,c}$ - energy charged into thermal energy storage
    - $W_{TES,d}$ - energy discharged from thermal energy storage
    - $W_{el,total}$ - total electricity demand
    - $W_{el,max,p}$ - peak electricity value in postive direction

Equations and Objective Function

In the following section, the equations and objective function (OF) used for this model are described.

Heat Balance The overall heat balance W_{th} of the building is defined by equation 5.9. The heat demand is met using the combination of an electrical heater, a heat pump and energy discharged from thermal energy storage.

$$W_{th}[t] = (k_{hp}[t] \cdot P_{hp} + W_{el.heater}[t] + W_{TES,d}[t] \cdot \eta_{TES,d}) \quad \forall t \in T \tag{5.9}$$

Thermal Energy Storage The constraints used to describe the behavior of thermal energy storage are shown in equations presented in this section. The energy stored at the start of the time step W_{TES} is calculated using the energy stored in the previous time step and the amount of energy charged into and discharged from the storage system. As this thesis assumes a constant daily self discharge rate regardless of the boundary condition, this value is divided by 24 to calculate the hourly self discharge rate. Furthermore, it is assumed that initially, no amount of thermal energy is stored in the storage system. This behavior is described in equation 5.10.

$$W_{TES}[t] = \begin{cases} 0, & \text{if } t = 0 \\ (W_{TES}[t-1] - W_{TES,d}[t-1] & \\ +W_{TES,c}[t-1]) \cdot (1 - \frac{\sigma_{TES}}{24}), & \forall t \in T \text{ and } t \neq 0 \end{cases} \tag{5.10}$$

To make sure that enough capacity is available for charge $W_{TES,c}$ and enough energy is available for discharge $W_{TES,d}$, two constraints (5.11 and 5.12) are introduced to the model. As this model utilizes only the amount of energy at each time step, no statement can made regarding the charge and discharge sequence of the thermal storage. To simplify this problem, the assumption is made that the amount of energy available for charge and discharged are limited by the heat amount stored at the beginning of the time step. Furthermore, the simplification that the thermal storage can be charged and discharged at the same time step is used. As heat losses are assumed for both charging and discharging of the thermal energy storage, this simplification may lead to a higher utilization of both heat pump and electrical heater. This is turn can increase the overall electrical demand for the specific time step. This possible inaccuracy within the model is accepted, as the goal of this work is not to provide a detailed calculation of the energy system but rather to analyze the effects on the electricity grid.

$$W_{TES,c}[t] \leq (W_{TES,max} - W_{TES}[t]) \quad \forall t \in T \tag{5.11}$$

$$W_{TES,d}[t] \leq W_{TES}[t] \quad \forall t \in T \tag{5.12}$$

The amount of heat charged into the thermal storage $W_{TES,c}$ is then calculated using the heat output available from heat pump $k_{hp,c}$ and electrical heater $W_{el.heater,c}$. On top of that, the charge efficiency $\eta_{TES,c}$ from table 5.12 is used. The mathematical formulation of this constraint is shown below (equation 5.13)

$$W_{TES,c}[t] = (k_{hp,c}[t] \cdot P_{hp} + W_{el.heater,c}[t]) \cdot \eta_{TES,c} \quad \forall t \in T \tag{5.13}$$

Heat Pump For heat pump, equation 5.14 is introduced to ensure that the sum of the utilization factors (k_{hp} and $k_{hp,c}$) is less than or equal to one. The total electricity demand for heat pump $W_{el,hp}$ is then calculated using the utilization factors, maximum heat output P_{hp}, and its COP (equation 5.15).

$$k_{hp}[t] + k_{hp,c}[t] \leq 1 \quad \forall t \in T \tag{5.14}$$

$$W_{el,hp}[t] = (k_{hp}[t] + k_{hp,c}[t]) \cdot \frac{P_{hp}}{COP[t]} \quad \forall t \in T \tag{5.15}$$

Electrical Balance To fully represent the overall electricity demand $W_{el,total}$ of the building, the electricity demand for heating purposes needs to be added to the electricity demand from auxiliary devices W_{el}.

$$W_{el,total}[t] = W_{el}[t] + W_{el,hp}[t] + W_{el.heater}[t] + W_{el.heater,c}[t] \quad \forall t \in T \tag{5.16}$$

As previously mentioned, equation 5.17 is used to limit the annual electrical demand to avoid turning this model into a multi-objective optimization model. $W_{el,limit}$ is total electricity demand for the building using the assumption that the heat demand is met using only heat pump and electrical heater.

$$\sum_{\forall t \in T} W_{el,total} \leq W_{el,limit} \tag{5.17}$$

The objective of this model is to minimize the maximum hourly electricity demand. As this type of problem is often infeasible for MILP (Mixed-Integer Linear Programming) solvers currently available in the market, a helper variable $W_{el,max,p}$ is utilized. This variable is used to store the highest hourly overall electricity demand within the whole time period T (equation 5.18). This variable can then be used to formulate the objective function 5.19.

$$W_{el,max,p} \geq W_{el,total}[t] \quad \forall t \in T \tag{5.18}$$

$$OF := min(W_{el,max,p}) \tag{5.19}$$

5.8.3 Buildings with District Heating and with PV System

In Figure 5.25, the energy system of a building with PV system that lies within district heating areas is shown. Due to the existence of PV system, the possibility of electricity being fed into the grid has to be considered. This change in behavior warrants an adjustment to the optimization model, as now the electricity peak in both positive (grid consumption) and negative (grid feed in) direction has to be considered.

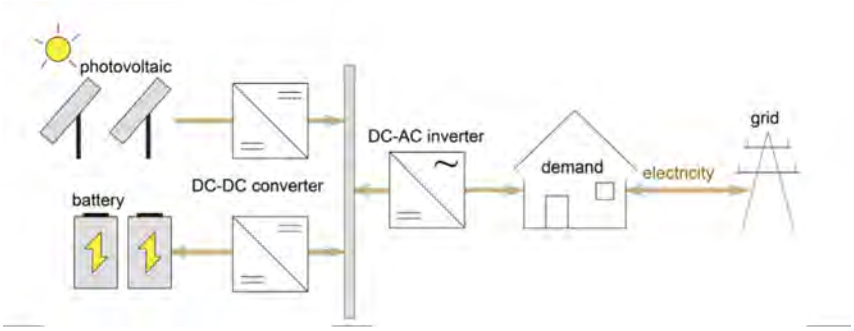

Figure 5.25: Buildings with district heating and with PV system. Adapted from [165]

Notations

The following indices, sets, variables and parameters of this model are defined below.

1. Indices
    - t - discrete time period
2. Sets
    - T - set of all discrete periods of time
3. Parameters
    - W_{el} - electricity demand
    - W_{pv} - PV generation
    - $W_{el,limit}$ - maximum electricity demand allowed during optimization
    - C_{BAT} - maximum battery capacity
    - η_{AC2BAT} - AC to battery efficiency
    - η_{PV2BAT} - PV to battery efficiency
    - η_{PV2AC} - PV to AC efficiency
    - η_{BAT2AC} - battery to AC efficiency
4. Variables
    - W_{BAT} - energy stored in battery
    - $W_{BAT,c}$ - energy charged into battery
    - $W_{BAT,d}$ - energy discharged from battery
    - $W_{pv,BAT}$ - PV generation for battery
    - $W_{pv,grid}$ - PV generation for grid feed in

- $W_{grid,BAT}$ - energy from the grid to charge battery
- $W_{el,total}$ - total electricity demand
- $W_{el,total,p}$ - total electricity demand in postive direction
- $W_{el,total,n}$ - total electricity demand in negative direction
- $W_{el,max,p}$ - peak electricity value in postive direction
- $W_{el,max,n}$ - peak electricity value in negative direction

Equations and Objective Function

In the following section, the equations and objective function (OF) used for this model are described.

Battery Storage In this section, the constraints used to model the behavior of battery storage is presented. Similar to assumptions used for thermal energy storage in Chapter 5.8.2, the battery is assume to be empty to start. The amount of electrical energy in the battery W_{BAT} available at a particular time step depends on the energy stored and the energy flow of the battery ($W_{BAT,c}$ and $W_{BAT,d}$) from the previous time step. The battery storage also considers a constant self discharge rate σ_{BAT} (battery daily self discharge rate). Equation 5.20 provides the mathematical formulation of the constraint used for the optimization model.

$$W_{BAT}[t] = \begin{cases} 0, & \text{if } t = 0 \\ (W_{BAT}[t-1] - W_{TES,d}[t-1] \\ +W_{BAT,c}[t-1]) \cdot (1 - \frac{\sigma_{BAT}}{24}), & \forall t \in T \text{ and } t \neq 0 \end{cases} \tag{5.20}$$

Using the same assumptions used for thermal storage system in equations 5.11 and 5.12, the amount of electricity available for charge $W_{BAT,c}$ and discharge $W_{BAT,d}$ is limited by the amount of energy available at the start of the time step. The simplification, which allows the battery to be charged and discharged in the same time step, is also used. This simplification may lead to larger losses within the battery storage system, potentially leading to reduced peak shaving potential due to lower energy stored in the battery system. Given that this work aims to provide only a qualitative assessment of the resulting situation, these inaccuracies are accepted.

$$W_{BAT,c}[t] \leq (C_{Bat} - W_{BAT}[t]) \quad \forall t \in T \tag{5.21}$$

$$W_{BAT,d}[t] \leq W_{Bat}[t] \quad \forall t \in T \tag{5.22}$$

Since no limitations is placed regarding the source of electricity to charge the battery, both PV $W_{pv,BAT}$ and electricity from the grid $W_{grid,BAT}$ can be utilized. For each of the energy paths, assumptions from Table 5.11 is used. The equation below shows how this constraint is implemented in this model.

$$W_{BAT,c}[t] = W_{pv,BAT}[t] \cdot \eta_{PV2BAT} + W_{grid,BAT}[t] \cdot \eta_{AC2BAT} \quad \forall t \in T \tag{5.23}$$

PV System As shown in Figure 5.25, the electricity generate from PV can either be used to charge the battery $W_{pv,BAT}$ or directly utilized $W_{pv,grid}$. Within this thesis no distinction is made between electricity used for demands in building and for grid feed in. This decision is made as from the point of view of DSO, both of these possibilities reduces the electricity taken from the grid.

$$W_{pv}[t] = W_{pv,BAT}[t] + W_{grid,BAT}[t] \quad \forall t \in T \tag{5.24}$$

Electrical Balance The total electricity demand $W_{el,total}$ of the building depends on the demand from auxiliary devices W_{el}, electricity from the grid to charge the battery $W_{grid,BAT}$, utilized PV generation $W_{pv,grid}$, and electricity discharged from battery $W_{BAT,d}$. The equation below shows how the constraint is formulated in this model.

$$W_{el,total}[t] = W_{el}[t] + W_{grid,BAT}[t] - W_{pv,grid}[t] \cdot \eta_{PV2AC} - W_{BAT,d} \cdot \eta_{BAT2AC} \quad \forall t \in T \tag{5.25}$$

As previously mentioned, a maximum value is used to limit the annual electricity demand of the building. For this purpose, the previously mentioned equation 5.17 is also implemented in this model

$$\sum_{\forall t \in T} W_{el,total} \leq W_{el,limit} \tag{5.17}$$

As PV generation exists in this system, the optimization model needs to adjusted to optimize the peak electricity demand in both positive (grid consumption) and negative (grid feed in) directions. To get the peak electricity demand in both directions, the total electricity demand $W_{el,total}$ is first split into its positive $W_{el,total,p}$ and negative $W_{el,total,n}$ components (equation 5.26). To avoid infeasibility problems for MILP solvers, helper variables $W_{el,max,p}$ and $W_{el,max,n}$ are used to get the absolute peak value for both directions.

$$W_{el,total}[t] = W_{e,total,p}[t] + W_{e,total,n}[t] \quad \forall t \in T \tag{5.26}$$

$$W_{el,max,p} \geq W_{e,total,p}[t] \quad \forall t \in T \tag{5.27}$$

$$W_{el,max,n} \geq (-W_{e,total,n}[t]) \quad \forall t \in T \tag{5.28}$$

To avoid turning the optimization model into a multi objective optimization model, the objective function is created using the linear weighted sum method [188], [189]. In this model, it is assumed that the effects of peak electricity demand, from the point of view of DSOs, are identical regardless of the direction. Thus, the weights used for both $W_{el,max,p}$ and $W_{el,max,n}$ are identical and can be neglected in the equation 5.29.

$$OF := min(W_{el,max,p} + W_{el,max,n}) \tag{5.29}$$

5.8.4 Buildings without District Heating and with PV System

The building energy system used for buildings within this category can be seen in Figure 5.17. The optimization model used for these buildings can be roughly seen as the combination of the optimization models used in Chapters 5.8.2 and 5.8.3. Nonetheless, adjustments are needed to model the connection between PV system and heat supply.

Notations

The following indices, sets, variables and parameters of this model are defined below.

1. Indices
    - t - discrete time period
2. Sets
    - T - set of all discrete periods of time
3. Parameters
    - W_{th} - heat demand
    - W_{el} - electricity demand
    - W_{pv} - PV generation
    - $W_{el,limit}$ - maximum electricity demand allowed during optimization
    - P_{hp} - maximum heat ouput of heat pump
    - COP - coefficient of performance
    - $W_{TES,max}$ - maximum energy stored in thermal energy storage
    - C_{BAT} - maximum battery capacity
    - η_{AC2BAT} - AC to battery efficiency
    - η_{PV2BAT} - PV to battery efficiency
    - η_{PV2AC} - PV to AC efficiency
    - η_{BAT2AC} - battery to AC efficiency
    - $\eta_{TES,c}$ - thermal storage charge efficiency
    - $\eta_{TES,d}$ - thermal storage discharge efficiency
    - σ_{TES} - thermal storage daily self discharge rate
4. Variables
    - k_{hp} - heat pump utilization factor for heat demand
    - $k_{hp,c}$ - heat pump utilization factor for thermal storage

- $W_{el.heater}$ - heat supply from electrical heater
- $W_{el.heater,c}$ - heat supply from electrical heater for thermal storage
- W_{TES} - energy stored in thermal energy storage
- $W_{TES,c}$ - energy charged into thermal energy storage
- $W_{TES,d}$ - energy discharged from thermal energy storage
- W_{BAT} - energy stored in battery
- $W_{BAT,c}$ - energy charged into battery
- $W_{BAT,d}$ - energy discharged from battery
- $W_{BAT,d,TES}$ - energy discharged from battery for thermal storage
- $W_{BAT,d,grid}$ - energy discharged from battery for electricity grid
- $W_{pv,BAT}$ - PV generation for battery
- $W_{pv,grid}$ - PV generation for grid feed in
- $W_{pv,TES}$ - PV generation for thermal storage
- $W_{grid,BAT}$ - energy from the grid to charge battery
- $W_{grid,TES}$ - energy from the grid to charge thermal storage
- $W_{el,total}$ - total electricity demand
- $W_{el,total,p}$ - total electricity demand in postive direction
- $W_{el,total,n}$ - total electricity demand in negative direction
- $W_{el,max,p}$ - peak electricity value in postive direction
- $W_{el,max,n}$ - peak electricity value in negative direction

Equations and Objective Function

In the following section, the equations and objective function (OF) used for this model are described.

Heat Balance To model the overall heat balance for buildings within this category, equation 5.9 is used without any adjustment, as the assumptions used for both models are identical.

$$W_{th}[t] = k_{hp}[t] \cdot P_{hp} + W_{el.heater}[t] + W_{TES,d}[t] \cdot \eta_{TES,d} \quad \forall t \in T \tag{5.9}$$

Thermal Energy Storage Identical to the constraints used in Chapter 5.8.2 to describe the energy level of the thermal energy storage W_{TES}, equation 5.10 is once again utilized. On top of that, equations 5.11 and 5.12 are needed to limit the amount of energy charged into and discharged from the thermal energy storage.

$$W_{TES}[t] = \begin{cases} 0, & \text{if } t = 0 \\ (W_{TES}[t-1] - W_{TES,d}[t-1] \\ +W_{TES,c}[t-1]) \cdot (1 - \frac{\sigma_{TES}}{24}), & \forall t \in T \text{ and } t \neq 0 \end{cases} \tag{5.10}$$

$$W_{TES,c}[t] \leq (W_{TES,max} - W_{TES}[t]) \quad \forall t \in T \tag{5.11}$$

$$W_{TES,d}[t] \leq W_{TES}[t] \quad \forall t \in T \tag{5.12}$$

For buildings in this category, adjustments are needed for the calculation of the heat amount charged into the thermal energy storage $W_{TES,c}$ to take the possibility of charging the thermal energy storage using PV into account. First the amount of electrical energy needed to charge the thermal energy storage is determined (equation 5.30). The electrical energy can come from battery storage $W_{BAT,d,TES}$, PV $W_{pv,TES}$, or the electricity grid $W_{grid,TES}$. Equation 5.31 is then used to calculate the amount of heat added into thermal energy storage.

$$k_{hp,c}[t] \cdot \frac{P_{hp}}{COP[t]} + W_{el.heater,c}[t] = \begin{array}{l} W_{BAT,d,TES}[t] \cdot \eta_{BAT2AC} + \\ W_{pv,TES}[t] \cdot \eta_{PV2AC} + \\ W_{grid,TES}[t] \end{array} \quad \forall t \in T \tag{5.30}$$

$$W_{TES,c}[t] = (k_{hp,c}[t] \cdot P_{hp} + W_{el.heater,c}[t]) \cdot \eta_{TES,c} \quad \forall t \in T \tag{5.31}$$

Heat Pump For heat pumps, equation 5.14 from Chapter 5.8.2 is used to ensure that the heat output of the heat pump does not exceed its maximum value.

$$k_{hp}[t] + k_{hp,c}[t] \leq 1 \quad \forall t \in T \tag{5.14}$$

Battery Storage As the system shown in Figure 5.17 does not offer the possibility to convert heat back to electricity, the constraints used in Chapter 5.8.3 regarding battery storage are once again used and shown below.

$$W_{BAT}[t] = \begin{cases} 0, & \text{if } t = 0 \\ (W_{BAT}[t-1] - W_{BAT,d}[t-1] \\ +W_{BAT,c}[t-1]) \cdot (1 - \frac{\sigma_{BAT}}{24}), & \forall t \in T \text{ and } t \neq 0 \end{cases} \tag{5.20}$$

$$W_{BAT,c}[t] \leq (C_{Bat} - W_{BAT}[t]) \quad \forall t \in T \tag{5.21}$$

$$W_{BAT,d}[t] \leq W_{Bat}[t] \quad \forall t \in T \tag{5.22}$$

$$W_{BAT,c}[t] = W_{pv,BAT}[t] \cdot \eta_{PV2BAT} + W_{grid,BAT}[t] \cdot \eta_{AC2BAT} \quad \forall t \in T \tag{5.23}$$

In addition to the aforementioned constraints, equation 5.32 is used to split the amount of electricity discharged $W_{BAT,d}$ from the battery depending on its usage.

$$W_{BAT,d}[t] = W_{BAT,d,grid}[t] + W_{BAT,d,TES}[t] \quad \forall t \in T \tag{5.32}$$

PV System For buildings within this category, the constraint described in equation 5.24 is extended to include the charging of thermal storage using PV. The equation used in this model is shown in equation 5.33.

$$W_{pv}[t] = W_{pv,BAT}[t] + W_{pv,TES}[t] + W_{grid,BAT}[t] \quad \forall t \in T \tag{5.33}$$

Electrical Balance For this category of buildings, a new constraint is formulated to calculate the total electricity demand $W_{el,total}$. Concerning the calculation of the total electricity demand $W_{el,total}$, only energy flows, that are visible from the point of view of DSO need to be considered. The resulting equation is shown below.

$$W_{el,total}[t] = \begin{aligned} & W_{el}[t] + (k_{hp}[t]) \cdot \frac{P_{hp}}{COP[t]} + W_{el.heater}[t] + \\ & W_{grid,BAT}[t] + W_{grid,TES}[t] - \\ & (W_{BAT,d,grid} \cdot \eta_{BAT2AC} + W_{pv,grid}[t] \cdot \eta_{PV2AC}) \end{aligned} \quad \forall t \in T \tag{5.34}$$

To limit the annual electricity demand, equation 5.17 is once again utilized.

$$\sum_{\forall t \in T} W_{el,total} \leq W_{el,limit} \tag{5.17}$$

Due to the existence of PV in buildings within this category, peak electricity demands in both positive and negative direction are to be optimized. For this reason, assumptions and methods used to formulate the objective function from Chapter 5.8.3 can once again be used (equations 5.26 - 5.29).

$$W_{el,total}[t] = W_{e,total,p}[t] + W_{e,total,n}[t] \quad \forall t \in T \tag{5.26}$$

$$W_{el,max,p} \geq W_{e,total,p}[t] \quad \forall t \in T \tag{5.27}$$

$$W_{el,max,n} \geq (-W_{e,total,n}[t]) \quad \forall t \in T \tag{5.28}$$

$$OF := min(W_{el,max,p} + W_{el,max,n}) \tag{5.29}$$

5.9 Software and Hardware Implementation

Due to the chosen spatial and temporal resolution of the methods used in this thesis, it is necessary to consider the software and hardware requirements. The following section provides a brief overview of the software implementation and the hardware utilized for this thesis. Subsequently, the total computational time required for the overall calculations using the methods described in Chapter 5 is presented

Software Implementation and Hardware

The models developed in this thesis are generated using the Python programming language in conjunction with a spatial database comprising PostgreSQL 12 and PostGIS 3. To solve the LP models, which are generated using optimization problem formulator Pyomo, outlined in Chapter 5.8, CPLEX 22.1.1 is used. The software is installed on a server with 128 GB of RAM and two Intel(R) Xeon(R) CPU E5-2630 v2 @ 2.60GHz (24 CPUs in total) running Linux Ubuntu 20.04.6 LTS.

Computational Time

The bulk of the computational time lies on the optimization of every single residential building (229,119 buildings) in Hamburg. To address the single-thread limitation of Python, multiprocessing is used to parallelize the calculation process. To avoid instabilities on the server, only 20 out of the 24 CPUs are utilized for the calculation. In total, approximately 80 to 85 hours of runtime are needed to complete the calculation. It is worth noting that the LP models used in this thesis are not yet optimized, leaving room for potential improvements in runtime.

6 Plausibility Check

Within this chapter, plausibility checks are conducted to estimate the extent of errors made using the presented method. Due to the lack of data availability, plausibility checks can only be done for a number of generated datasets. In the context of this work, the plausibility checks are done using only publicly available datasets.

6.1 Reference Area Plausibility

As the methods presented in chapter 5 are mostly based on the reference living area of the buildings, a plausibility check of the calculated reference area provides a good first estimation of the errors. The plausibility check for reference area is based on methods used in [128].

For this purpose, a data set from the Hamburg statistics office containing average residential living space per city district is used. Since the values for residential living space from this statistics are calculated based on results of the 2011 German census, deviations from real situation are to be expected [190]. Nonetheless this statistic still provides the best guess for residential living area situation in Hamburg.

Figure 6.1 shows the result of the correlation analysis. From the figure, it can be seen that the estimated reference residential area fits relatively well with the values calculated using the statistics. The estimated residential living area shows in total an overestimation by 0.2% compared to the statistics.

Despite the good correlation between the aggregated values, significant deviations may still occur at the building level. Table 6.1 presents the descriptive statistics for the estimated reference area on the building level. From this table, it is clear that using the methods described in the previous chapter may lead to unrealistic values. Outlier values, such as 107,668 m^2 of residential living area, are mainly caused due to the heterogeneity of buildings classified within the same ALKIS code [128]. This maximum value points to a large shopping center in Hamburg, the *Einkaufscenter Jenfeld*. For this building object, the code 1120 (*Wohngebäude mit Handel und Diestleistungen*) is assigned. To correctly model this building, a significantly lower share has to be manually assigned. Due to the amount of building objects considered in this thesis (229,169 building objects in total), manual assignment of residential share percentage for each building is deemed unrealistic.

Considering the aim of this thesis is to analyze the interplay between the modeled components on the MV level, the errors made at the building level are accepted. Additionally, at the time of writing, there exists no other data set other than ALKIS that offers sufficient spatial resolution and detailed information.

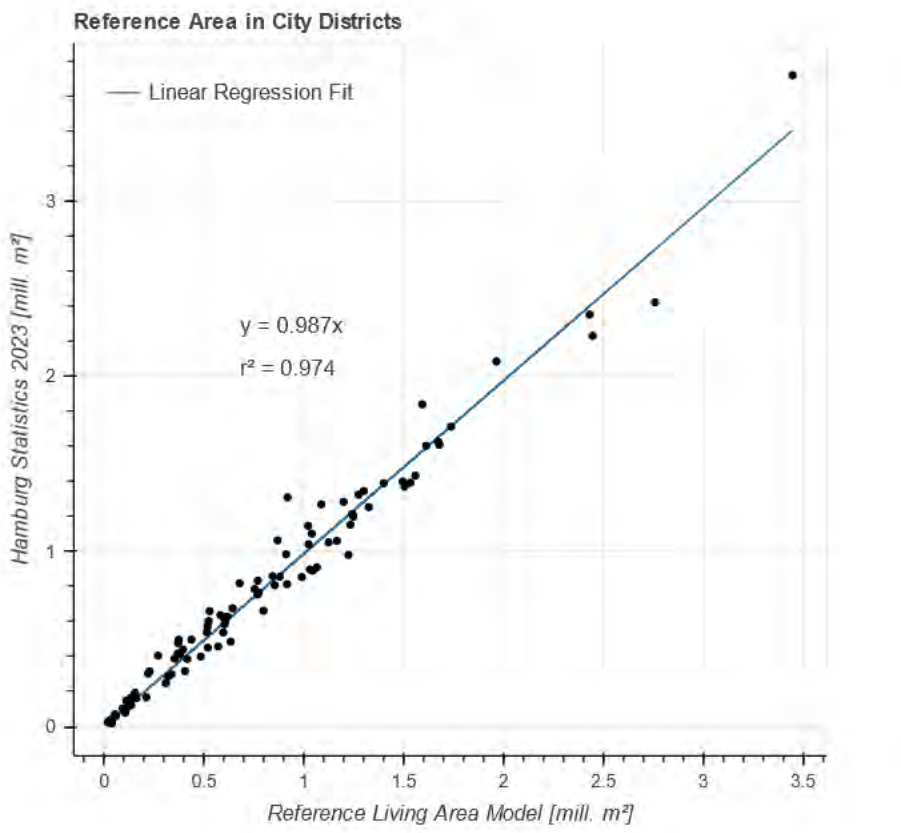

Figure 6.1: Correlation between calculated reference living area and statistics at city district level

Table 6.1: Descriptive statistics of estimated residential living area

Attribute	Value [m^2]
Mean	331
Median	109
Min	1
Max	107668
Standard Deviation	834
99th Percentile	3254

6.2 Heat Demand Plausibility

Due to the lack of available data set, the plausibility check for the annual heat demand is only done at the NUTS-1 level. For this plausibility check, the methods described in [126], [128] are implemented in this thesis. As no measurement data of annual heat demand is available, the reference value for comparison has to be calculated using the available statistics.

The first statistics used in this thesis to estimate the annual residential heat demand are energy consumption statistics according to its sector and fuel types, provided by the Hamburg statistics office [191]–[194]. Due to the way this statistics is put together, the amount of energy used per fuel type for private households in Hamburg can be determined.

As the aforementioned statistics does not provide any information regarding the end usage of the fuel types, additional further data set is needed to translate the fuel types into heat demand (space heating and domestic heat water). For this reason, country wide statistics from AGEB (Working Group on Energy Balances - *Arbeitsgemeinschaft Energiebilanzen e.V.*) are used [195], [196]. Using the assumption that the values from this country wide statistics are also applicable to Hamburg, the portion of energy used for space heating and domestic hot water for each fuel type can be estimated [126], [128]. It is however important to note that the heating systems used in Hamburg differ significantly from the average country wide heating system. [16].

Since this thesis utilizes TABULA to estimate the annual heat demand for each building type, the annual heat demands calculated from the statistics need to be corrected for weather conditions. The weather correction is done for space heating using degree days method [126], [128], with relevant weather data generated with IWU degree days tool using assumptions from Table 5.6 [136].

The approximated heat demand for Hamburg is shown in Table 6.2. In this table, the values for three latest available years are provided. The calculated annual heat demand using TABULA is finally compared to the average annual demand for years 2019-2021. From the results in Table 6.3, it can be concluded that the model used in this thesis is plausible. It is nonetheless important to note that the values calculated from the energy statistics provide only an approximation and should therefore be approached with care.

Table 6.2: Weather corrected annual heat demand of Hamburg based on [136], [192]–[196]

Year	Fuel Type	Fuel Amount [GWh]	End Use Split		Degree-days / Long Term Average	Results	
			Space Heating	Domestic Hot Water		Space Heating [GWh]	Domestic Hot Water [GWh]
2019	Oil	2107	83.7%	15.4%	2729 / 2937	1898	324
	Gas	4139	78.3%	21.2%		3488	878
	Electricity	3160	5.9%	11.4%		201	360
	District Heating	2842	90.5%	9.5%		2768	270
	Coal	6	100%	0%		6	0

	Renewables	408	88.1%	11.9%		387	49
2020	Oil	1670	83.9%	15.4%	2630 / 2937	1565	257
	Gas	4134	78.3%	21.2%		3615	876
	Electricity	3136	5.9%	11.4%		207	357
	District Heating	2770	90.5%	9.5%		2800	263
	Coal	5	100%	0%		5	0
	Renewables	443	87.7%	12.3%		434	54
2021	Oil	1334	83.6%	15.3%	3088 / 2937	1060	204
	Gas	4551	78.3%	21.2%		3389	965
	Electricity	3176	5.9%	11.4%		178	362
	District Heating	3244	90.5%	9.5%		2792	308
	Coal	5	100%	0%		5	0
	Renewables	451	88.8%	11.2%		381	51

Table 6.3: Comparison of total estimated heat demand and energy statistics

Source	Heat Demand [GWh]
Three Year Average	10253
Heat Demand Model	10274

6.3 Heat Time Series Plausibility

The assessment of the hourly heat demand time series presented in this thesis is done by comparing its hourly values to the SLP for gas at the NUTS-1 level [137]. This gas load profile has also often been used as a proxy for heat demand profile [125]. To ensure that the SLP is comparable with the calculated load profile, the SLP is scaled to the same annual demand as the calculated profile. Figure 6.2 visualizes the comparison between the profiles. From this figure, the similarity between both profiles at the NUTS-1 level can be observed. In the statistical analysis provided in Table 6.4, it can seen that both of these profiles are relatively similar.

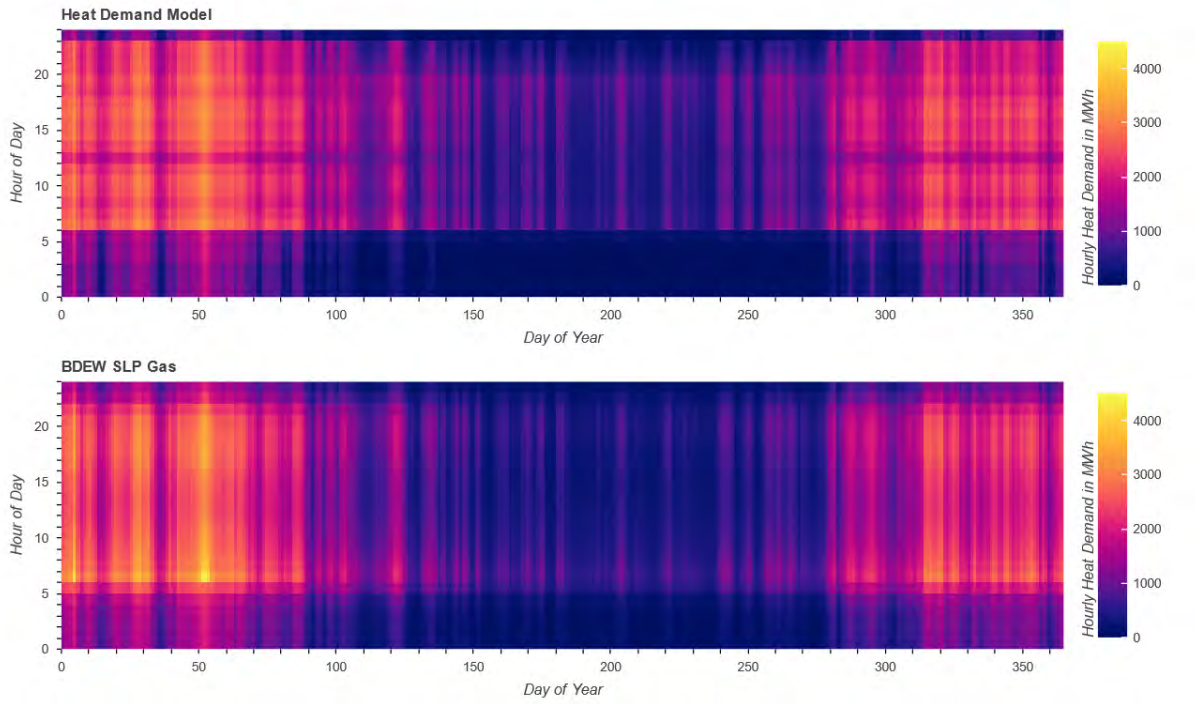

Figure 6.2: Comparison between VDEW dynamic household load profile [155] and electricity demand model

Table 6.4: Statistical overview of the hourly standard load profile gas from BDEW [155] and heat demand model. All Values in MWh

Source	Mean	Median	Min	Max	Standard Deviation
Standard Load Profile	1173	971	21	4401	835
Heat Demand Model	1173	983	12	3358	842

6.3.1 Heating System Sizing Plausibility

To estimate whether the chosen method for the sizing of heat pump is suitable for the purpose of this thesis, the annual FLH (full load hour) is calculated for each of the heat pumps. Table 6.5 provides a statistical overview of the FLH values.

Table 6.5: Descriptive statistics of heat pump full load hours

Attribute	Value [kW]
Mean	2365
Median	2265
Min	536
Max	11478
Standard Deviation	928
10th Percentile	1294
25th Percentile	1729
75th Percentile	2758
90th Percentile	3308

To better evaluate the calculated FLH values, different reference values from the literature are shown in Table 6.6. Disregarding the outliers, the computed FLH values demonstrate a relatively good correlation when compared to the reference values obtained from the literature.

Table 6.6: Reference full load hours

Type	FLH	Source
EFH	2100	[197]
MFH	2000	[197]
Assumed average value	1800	[198]
Large-scale heat pump	3000	[49]

In the literature, the size of the thermal energy storage is typically calculated using a mathematical optimization [176], [199] or dimensioned directly based on its boundary conditions [200]. As both of these methods require a comprehensive analysis for each building object, no plausibility check is therefore carried out for thermal energy storage sizing method.

6.4 Electricity Demand Plausibility

As no publicly available data set for annual electricity demand for residential sector is available, this value needs to be estimated using available statistics. For this reason, statistics regarding energy usage per fuel type depending are once again used, together with country wide statistics from AGEB [192]–[196]. Similar to the annual heat demand, the electricity demand estimated using this model is compared the the average electricity demand of the three last available years from the statistics. This result is presented in Table 6.7. The model used in this thesis overestimates the electricity demand by roughly 5.6% and is acceptable for the scope of this thesis. It is once again crucial to emphasize that the value used for comparison is derived out of statistics and provides only an approximation.

Table 6.7: Comparison of total estimated electricity demand and energy statistics

Source	Electricity Demand [GWh]
Three Year Average	2611
Electricity Demand Model	2757

6.5 Electricity Time Series Plausibility

To assess the plausibility of the generated hourly electricity time series, a comparison is made with the SLP. Due to the lack of measurement data, this comparison is made at NUTS-1 level instead of the city district level. The annual demand of the SLP is scaled to 2757 GWh to match the electricity demand model used in this thesis. In the following Figure 6.3 the comparison is shown. Parallel to the trend mentioned in Chapter 5.3.6, a similar pattern can be observed. While the peaks in demand align in time, considerable difference in magnitude can be observed.

Considering that the SLP are based on measurements made in the 1980s and 1980s, the difference in peak values also fit with the technological of the household appliances since the development of the profiles [125], [148]. Nowadays, electrical appliances typically have considerably lower standby energy consumption, which can result in lower energy consumption during the night [125], [201]. Furthermore, this work utilizes a set of 2511 load profiles instead of 100,000 profiles (Chapter 5.3.1), which may contribute to peak values occurring at specific time steps. Considering these factors, this deviation is deemed acceptable, as one of the goals of the electrical demand model is not to recreate the values of SLP but rather to introduce variance to the load profiles.

To better describe the difference, Table 6.8 provides a statistical overview for both hourly profiles. From the statistical analysis, it can be seen that the electricity demand model generates higher peak values with higher standard deviations.

Table 6.8: Statistical overview of the hourly load profile from VDEW dynamic household standard load profile and electricity demand model. All Values in MWh

Source	Mean	Median	Min	Max	Standard Deviation
Standard Load Profile	315	329	102	732	134
Electricity Demand Model	315	297	55	956	211

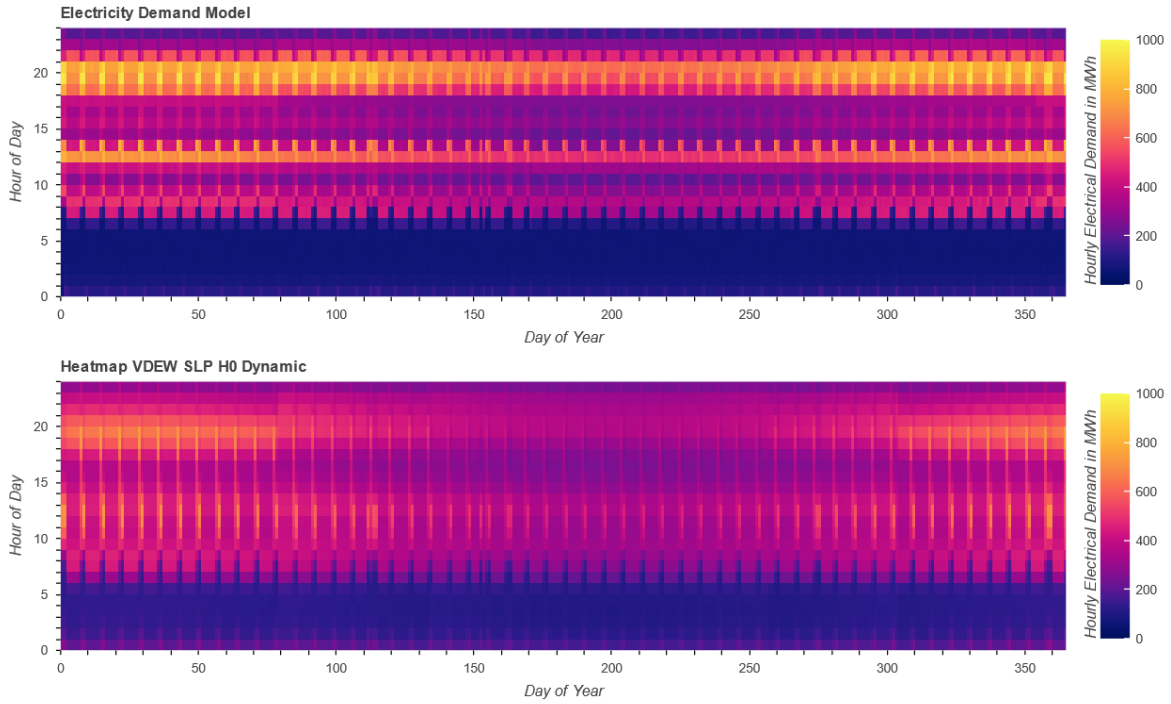

Figure 6.3: Comparison between VDEW dynamic household load profile [155] and electricity demand model

7 Results and Discussion

In this chapter, the assumptions and results generated using the methods described in the previous chapter are presented and discussed. It starts by showcasing the outcomes of the optimization model and concludes with a discussion of the generated results.

7.1 Results

In this section, the results generated from the methods described in chapter 5 are presented. As a result of the chosen spatial and temporal resolution used in this thesis, the calculation resulted in a large amount of data. The evaluation of the generated results is therefore done in aggregated form. In the following, results on different aggregation levels are shown.

7.1.1 Results based on Building Energy System Configuration

To better understand the hourly electricity demand resulting from the different combinations of technologies, the results are first aggregated based on the building energy system configuration.

Buildings with District Heating and without PV System

As previously mentioned in Chapter 5.8.1, no flexibility options exist for buildings in this category. In total, 7,906 building objects are classified within this category. In Figure 7.1, the hourly electricity demand profile is shown together with the SLP. From this comparison it is once again clear that while the shape of the profile is relatively similar, the difference in magnitudes is relatively significant.

From Figure 7.1, it can also be seen that the peak electricity demand for this building type come during the winter times. The seasonal variation in electricity demand can also be clearly observed. To help evaluate the peak hourly electricity demand in relation to its profile, FLH is once again used. For the quantification of the peak demand, FLH is calculated by dividing the total electricity demand by the peak hourly electricity demand. Using this definition, a value of 2807 h can be calculated. For SLP on the other hand, a value of 3765 h can be calculated for FLH. Compared to SLP, the modeled electricity demand is therefore shown to have a considerable higher volatility.

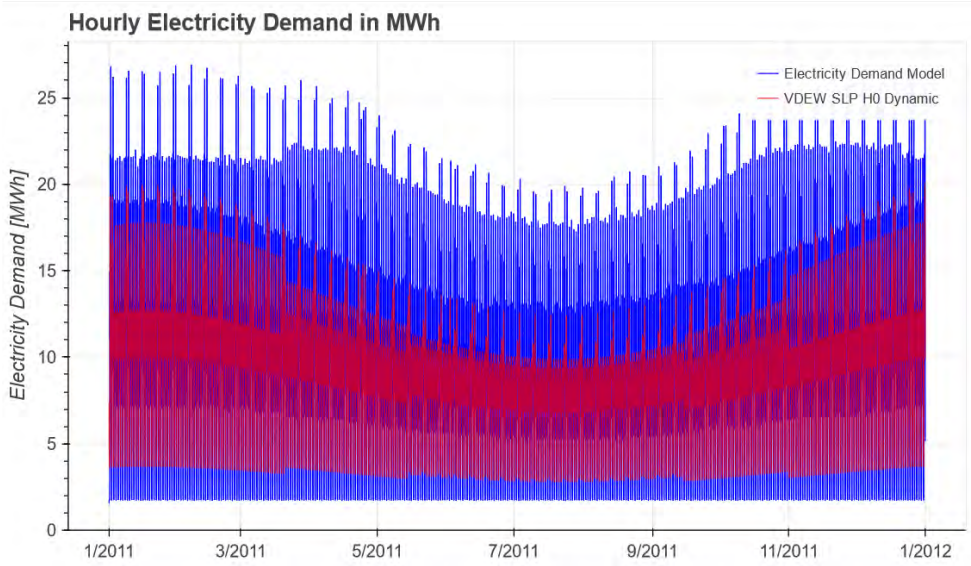

Figure 7.1: Hourly electricity demand profile in MWh for buildings with district heating and without PV system

Buildings without District Heating and without PV System

Using the methodology presented in this thesis, 31,408 building objects can be classified into this category. In Figure 7.2, the hourly electricity demand profile is shown.

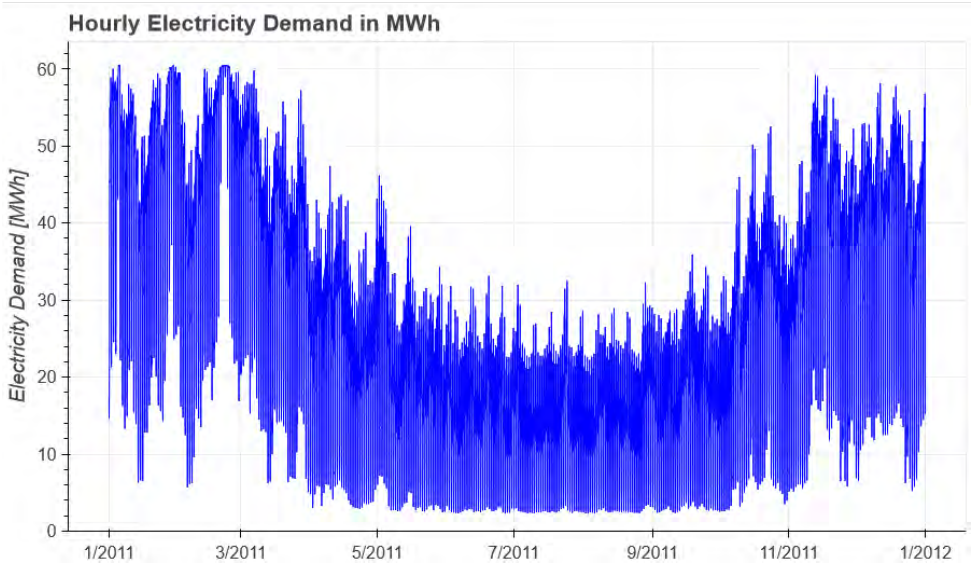

Figure 7.2: Hourly electricity demand profile in MWh for buildings without district heating and without PV system

Similar to the previous building category, the peak electricity demand occurs in winter. This outcome aligns with expected result, considering that the building's heat demand is supplied through a combination of heat pump, electrical heater, and thermal energy storage. From the aggregated electricity demand time series, a FLH of 3,759 hours can be calculated. This relatively high value is partly attributed to the capability of thermal energy storage, which allows for the partial decoupling of heat generation and heat consumption.

To better understand the role of thermal energy storage for the reduction of peak electricity demand, the average storage level and the normalized demand for both electricity and heat is presented in Figure 7.3. The normalized demands reveal that the highest electricity demands occur during times of peak heat demands (marked with a black rectangle). Concurrently, a sharp increase in storage level is observed within this time frame. This sharp increase demonstrates the load-shifting capability of a thermal storage system, effectively reducing peak demand and flattening the demand profile. Additionally, the consistently low average storage level throughout the considered period provides an indication that the thermal storage sizing method described in chapter 5.5.3 may be unsuitable for the purpose of this thesis.

As described in Chapter 5.5.3, the size of the electrical heater is not fixed but rather calculated as a part of the LP model. The results show that for 1,135 building objects, no additional electrical heater is required for the heating supply. For the rest, a ratio between the size of the heat pump and electrical heater is calculated by dividing the heating load of the heat pump by the size of the electrical heater. Table 7.1 provides a statistical overview of the calculated ratios. From the statistics, it is clear that the required electrical heaters for this building category are considerably smaller compared to the heat pumps.

Table 7.1: Descriptive statistics of the ratio between heat pump and electrical heater for buildings without district heating and without PV system

Attribute	Ratio [-]
Mean	3.86
Median	2.64
Min	0.33
Max	3098
Standard Deviation	31.84
10th Percentile	1.75
25th Percentile	2.11
75th Percentile	3.66

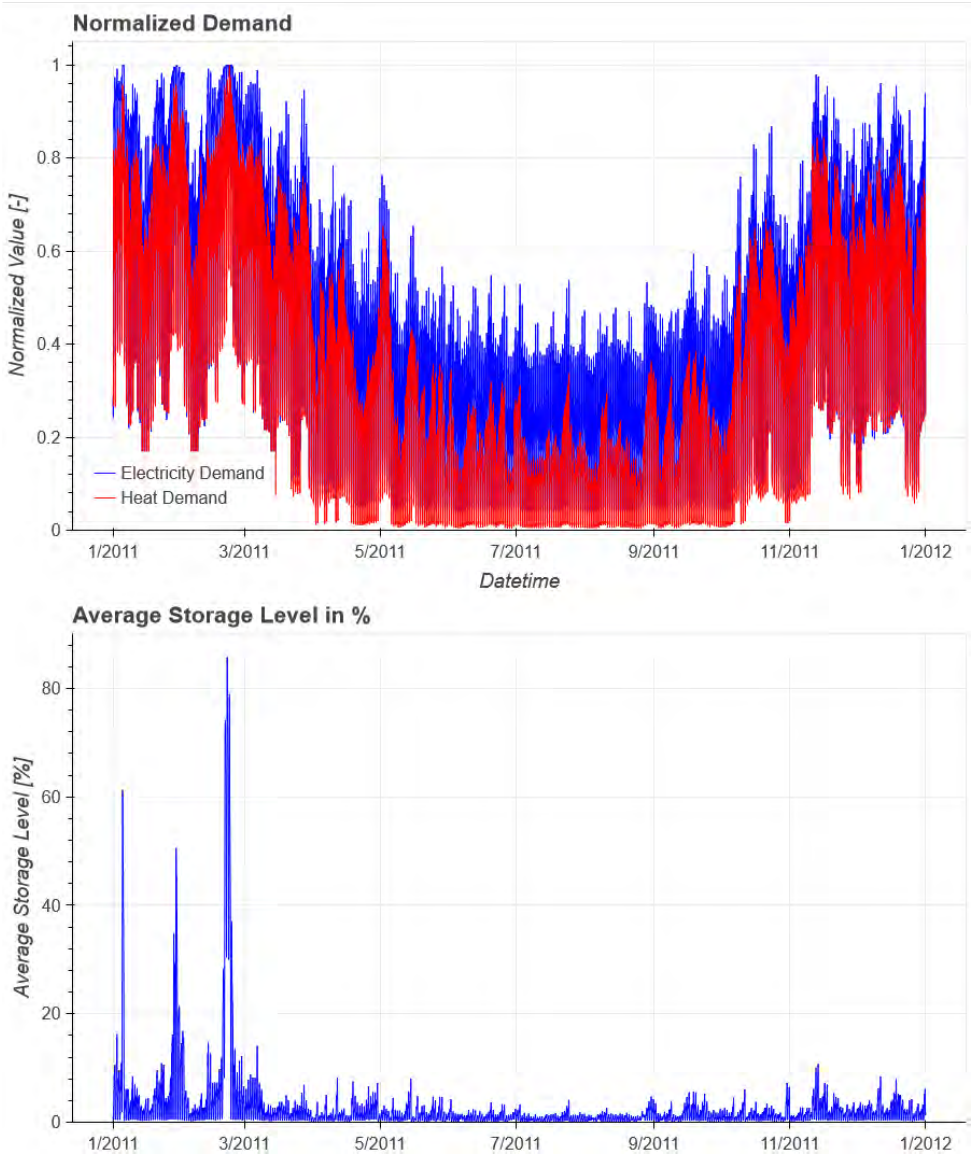

Figure 7.3: Average thermal storage level in % and the normalized energy demand for buildings without district heating and PV system.

Buildings with District Heating and with PV System

The flexibility in these types of buildings is represented by the presence of battery storage in the PV system. In this category, a total of 54,095 building objects can be identified. In Figure 7.4, the hourly electricity demand profile is shown.

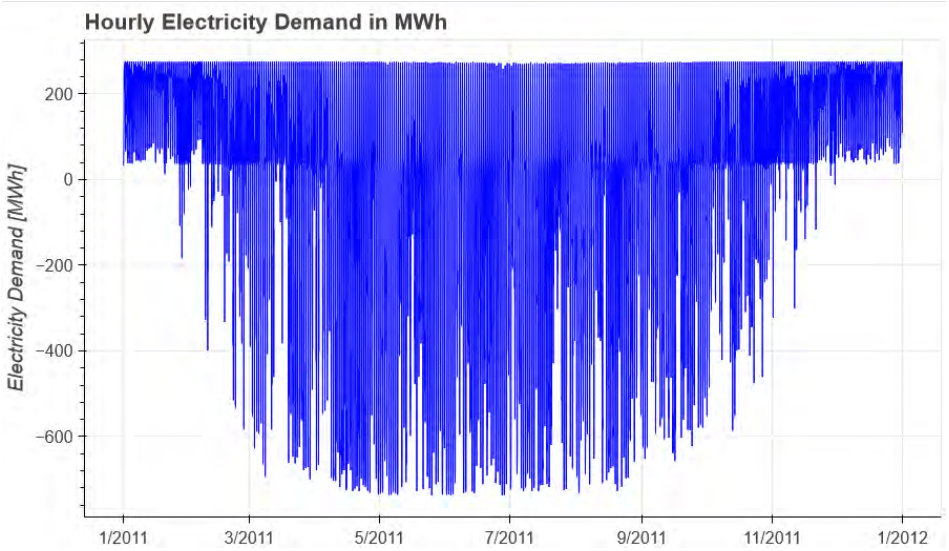

Figure 7.4: Hourly electricity demand profile in MWh for buildings with district heating and PV system

Due to the presence of PV within the system, electricity demand in both the positive direction (referring to energy taken from the grid) and the negative direction (referring to energy fed into the grid) can be observed. From the hourly values, it is clear that the peak electricity demand in the negative direction is significantly larger than the peak demand in the positive direction. On top of that the expected seasonal variation of electricity generation from PV is also clearly shown.

Furthermore, it can be seen that the peak electricity demands in the positive direction can be flattened, while huge variations can be seen in the negative direction. To better analyze the flatness of the demand profiles, the electricity demands are sorted in descending order and displayed in Figure 7.5. From this figure, it is also clear that for the majority of the time, electricity is required from the grid, while roughly 25% of the time electricity is fed into the grid. Annually, the amount of energy required from the grid is higher than the total energy fed into the grid.

To assess the flatness of the electricity demand profile, FLH is once again used. Due to the bidirectionality of the demand profile, FLH is calculated for its positive, negative, and absolute values. The consideration of the absolute values is made due to the assumption that, from the DSO point of view, the effects of the demand profile are identical regardless of its direction. In the following, the FLH values are presented.

- Negative FLH: 1183 h
- Positive FLH: 3483 h
- Absolute FLH: 2486 h

Based on the calculated FLH values and Figure 7.5, it can be assumed that the electricity fed into the grid may pose significant challenges in maintaining grid stability.

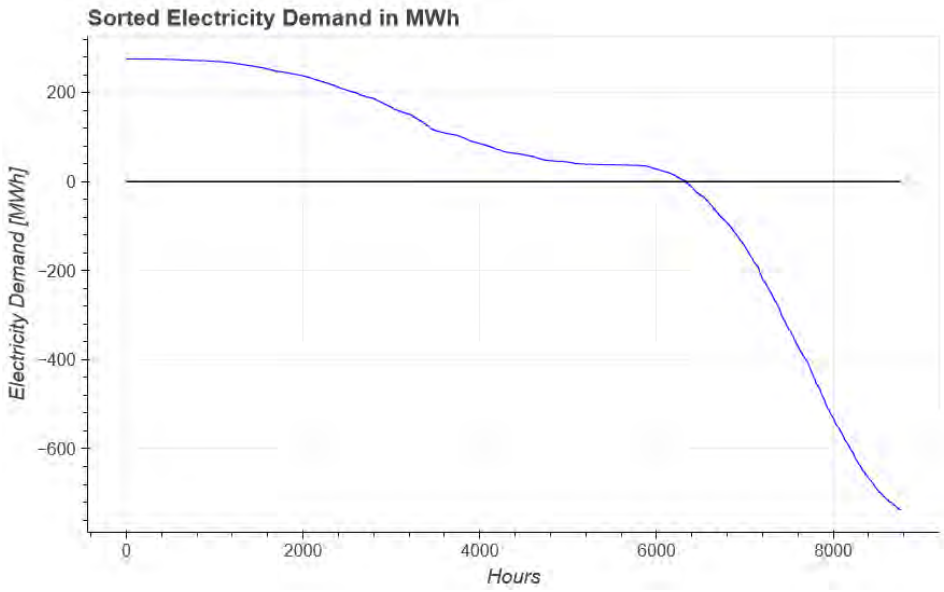

Figure 7.5: Hourly electricity demand profile in MWh sorted in descending order for buildings with district heating and PV system

To better understand the role of battery storage for buildings in this category, the average level of the battery storage is provided in Figure 7.6. As opposed to the seasonal variation of the electricity generation from PV, a continuous utilization throughout the year can be observed. This highlights the potential of battery storage to both flatten and reduce the peak demands.

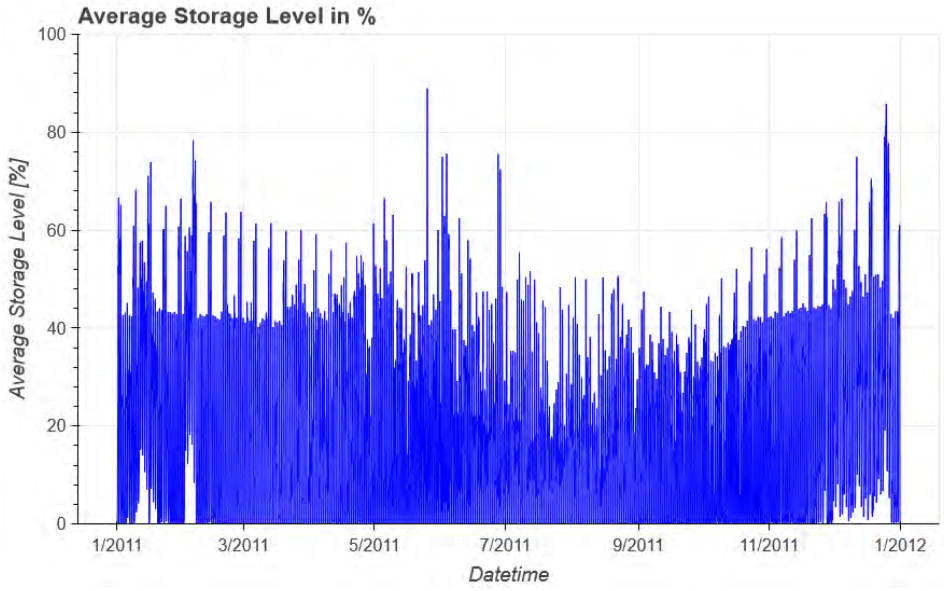

Figure 7.6: Average battery storage level in % for buildings with district heating and PV system.

However, Figure 7.6 does not provide any indication regarding the battery sizing method. To address this, the average battery levels are sorted in descending order and presented in Figure 7.7. The figure reveals that on average, for the majority of the time, the battery storage is not highly utilized. Based on this result, it is reasonable to assume that the chosen sizing method slightly overestimates the size of the battery storage. Choosing a smaller battery, however, would adversely impact the reduction and flattening potential of the battery. A more detailed sizing of the battery would require a more in-depth consideration of additional factors, such as economic feasibility, which is beyond the scope of this work. As a result, this possible overestimation is accepted.

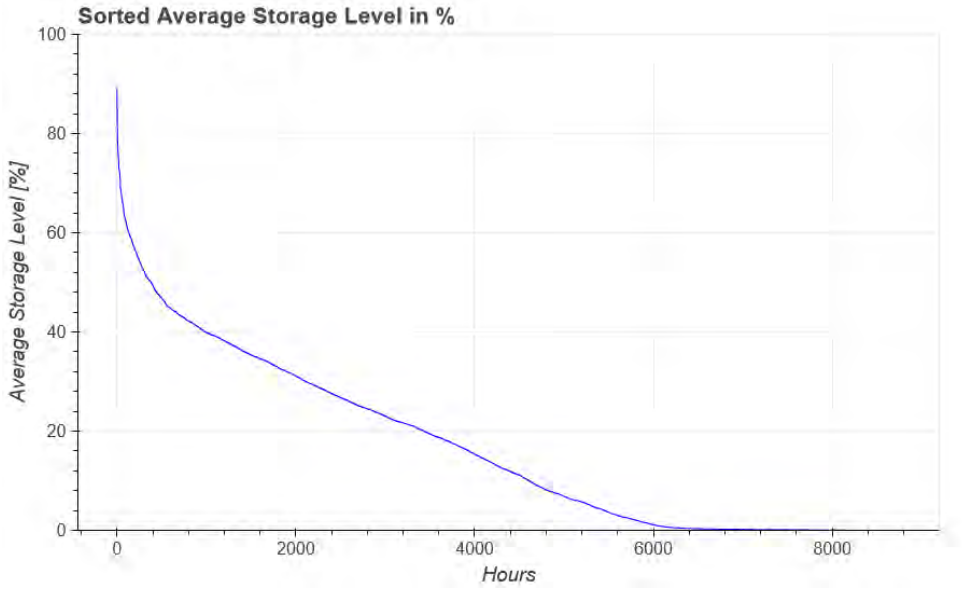

Figure 7.7: Average battery storage level in % sorted in descending order for buildings with district heating and PV system.

Buildings without District Heating and with PV System

This category represents buildings with the highest flexibility options available. The presence of both thermal energy storage and battery storage offers the opportunity for both load shifting and peak reduction of electricity demand by coupling both sectors together. A total of 135,760 building objects are calculated within this category. In Figure 7.8, the hourly electricity demand profile is shown.

In contrast to the previous categories, the hourly peak electricity demands in both positive direction (537 MWh) and negative direction (524 MWh) are similar. This indicates a considerable improvement compared to building objects without thermal storage and with a PV system, where the hourly peak electricity demand in the negative direction is roughly 2.7 times higher than its positive counterparts (Figure 7.4).

Figure 7.9 displays the electricity demands sorted in descending order. Once again, it can be observed that roughly 25% of the time, electricity is fed into the grid. Despite the similarity in peak values,

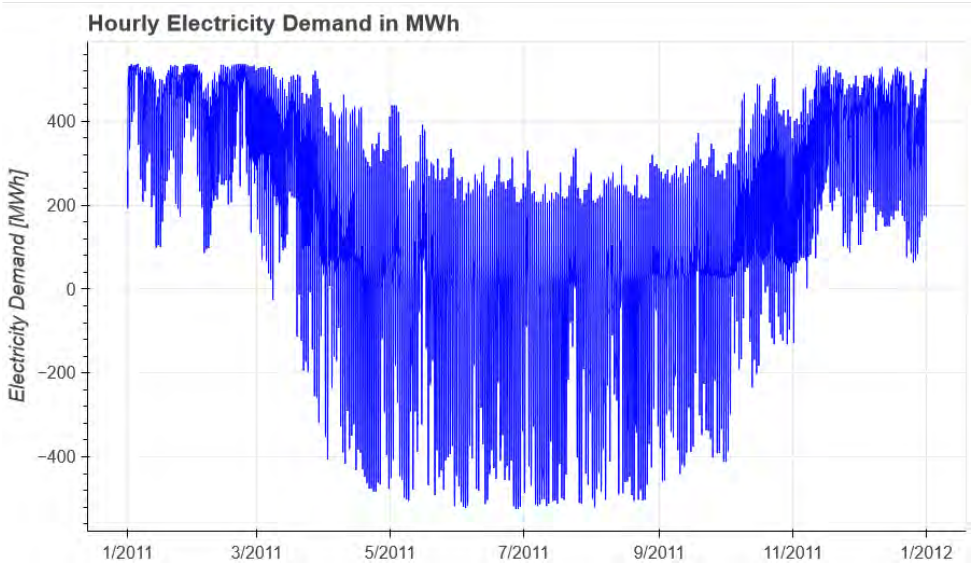

Figure 7.8: Hourly electricity demand profile in MWh for buildings without district heating and with PV system

the slope of sorted negative values is higher, which shows the volatility of the amount of residual PV generation fed into the grid.

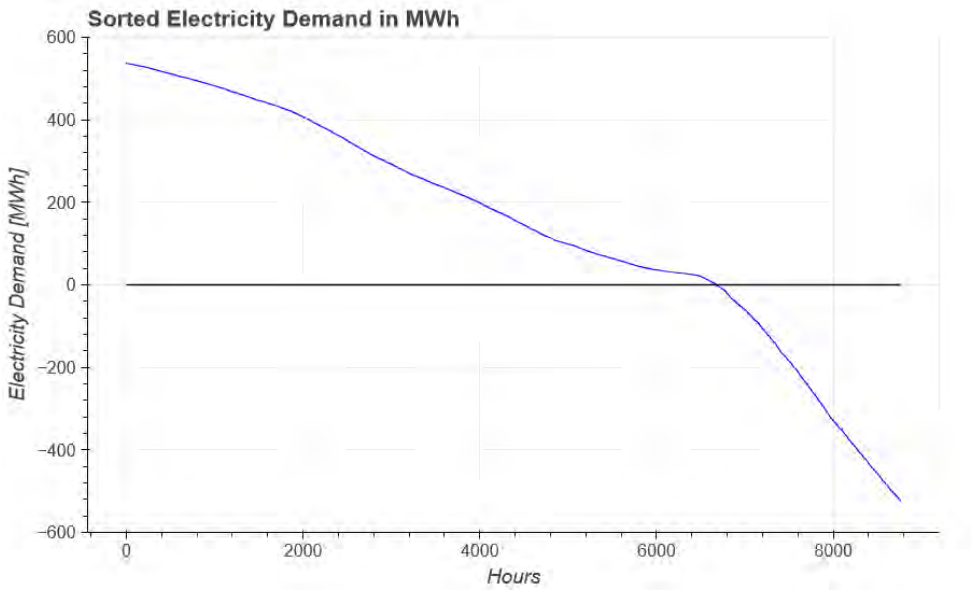

Figure 7.9: Hourly electricity demand profile in MWh sorted in descending order for buildings without district heating and with PV system

Similar to the other building categories, FLH is also employed here to better understand the generated electricity demand profile. Once again, FLH is calculated for positive, negative, and absolute values. The

values are presented as follows:

- Negative FLH: 995 h
- Positive FLH: 3313 h
- Absolute FLH: 4285 h

At the first glance, both the negative and positive FLH do not offer any noticeable improvement compared to the previous category (with district heating and PV system). However, when examining the absolute FLH, a significant improvement is evident. The absolute FLH value hints at the potential benefits of sector coupling for the electricity grid.

To better understand the effects of both thermal and battery storage, the average storage level of both flexibility options is shown in Figure 7.10. It can be observed that both thermal and battery storage are used in tandem throughout the year. Interestingly, the highest average storage level for thermal storage is reached during the summer. As thermal storage system allows the decoupling of heat generation and heat demand, residual loads coming from PV generation can be used to charge the thermal storage using the combination of heat pump and electrical heater, which can be discharged to fulfill heat demand at a later time. Based on this principle, the potential of thermal storage to help smoothen the electricity feed-in profile can be highlighted.

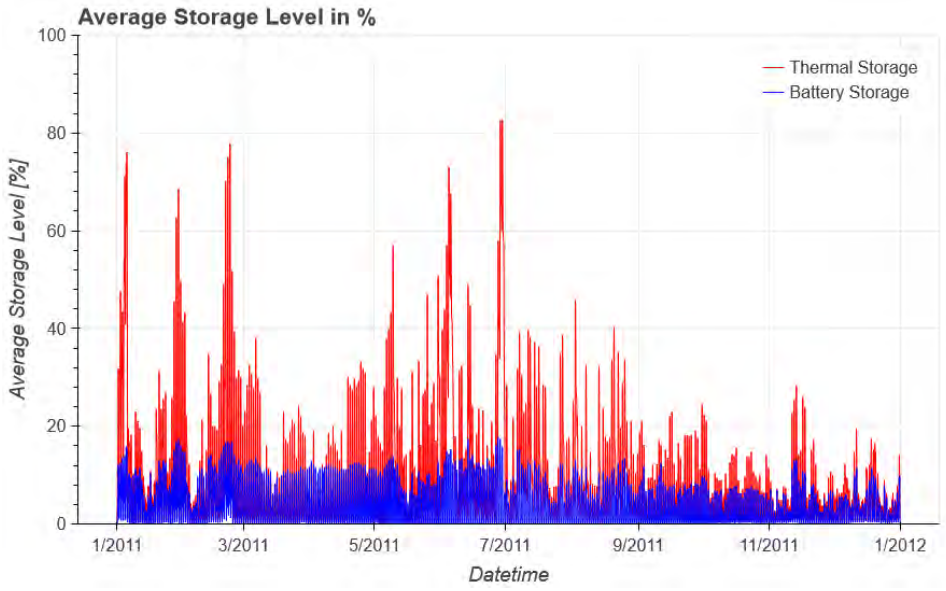

Figure 7.10: Average battery storage level in % for buildings without district heating and with PV system.

To asses the size of the required additional electrical heater, the ratio between the heating load of the heat pump and the size of the electrical heater is calculated. Table 7.2 provides a statistical overview of the calculated ratios. From the statistics, it can be seen, that for more than half of the buildings within this building category, electrical heaters are dimensioned to be bigger than the heating load of the pump (ratio smaller than 1).

Table 7.2: Descriptive statistics of the ratio between heat pump and electrical heater for buildings without district heating and with PV system

Attribute	Ratio [-]
Mean	1.02
Median	0.82
Min	0.08
Max	46.62
Standard Deviation	0.73
10th Percentile	0.37
25th Percentile	0.54
75th Percentile	1.27

Compared to the statistics presented in Table 7.1, this building type exhibits a considerably larger size of electrical heater. The need for a larger electrical heater can be attributed to the presence of PV within the system. This effect is illustrated in Figure 7.11, where the normalized output of the electrical heater for buildings with PV and without PV is depicted. From this figure, it is evident that the electrical heater provides an additional flexibility option during the summer to reduce the amount of electricity fed into the grid.

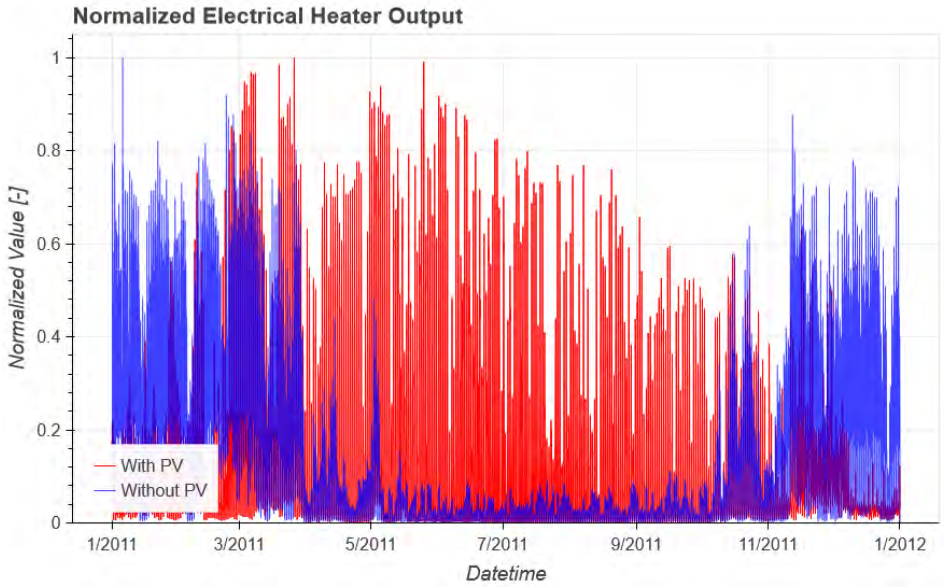

Figure 7.11: Normalized heat output from electrical heater

7.1.2 Results on NUTS-1 Level

To analyze the effects of different building energy system configurations for the region of Hamburg, the results are aggregated at the NUTS-1 level. The resulting aggregated hourly electricity demand profile is presented in Figure 7.12. It is evident that the overall peak hourly electricity demand occurs during the summer, highlighting the potential and challenges arising from PV generation. With 1,243 MWh, the maximum hourly feed-in is roughly 1.4 times higher than the highest hourly electricity required from the grid.

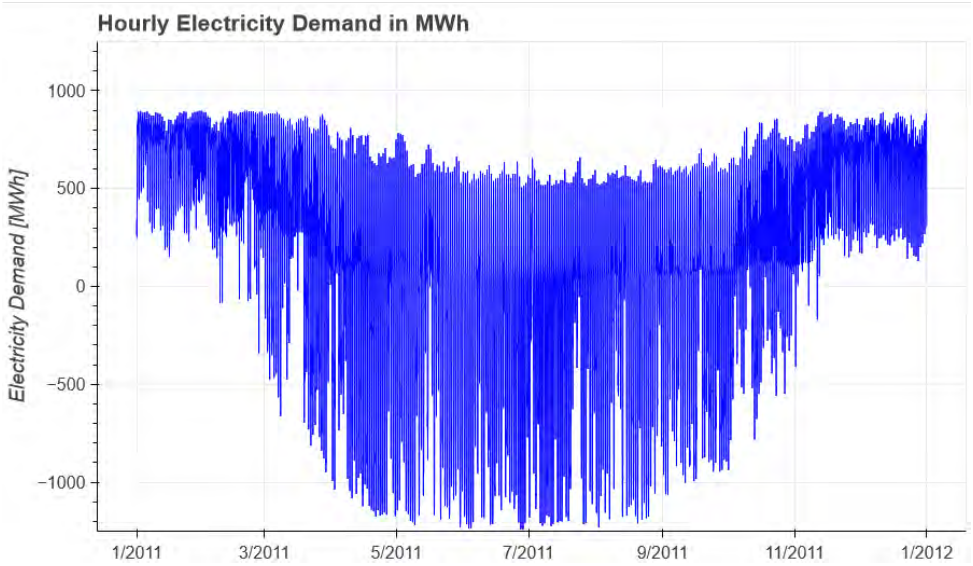

Figure 7.12: Hourly electricity demand profile in MWh for Hamburg

However, an analysis of the annual electricity demands paints a relatively different picture. The yearly electricity demand totals 1,648 GWh, indicating a roughly 40% reduction compared to the baseline annual electricity demand of 2,757 GWh (see Chapter 6.4). Despite the disproportionate feed-in in the summer (Figure 7.12), a relatively good absolute FLH value of 3417 h can still be calculated. Figure 7.13 illustrates, once again, that roughly one-fourth of the time, electricity is fed into the grid.

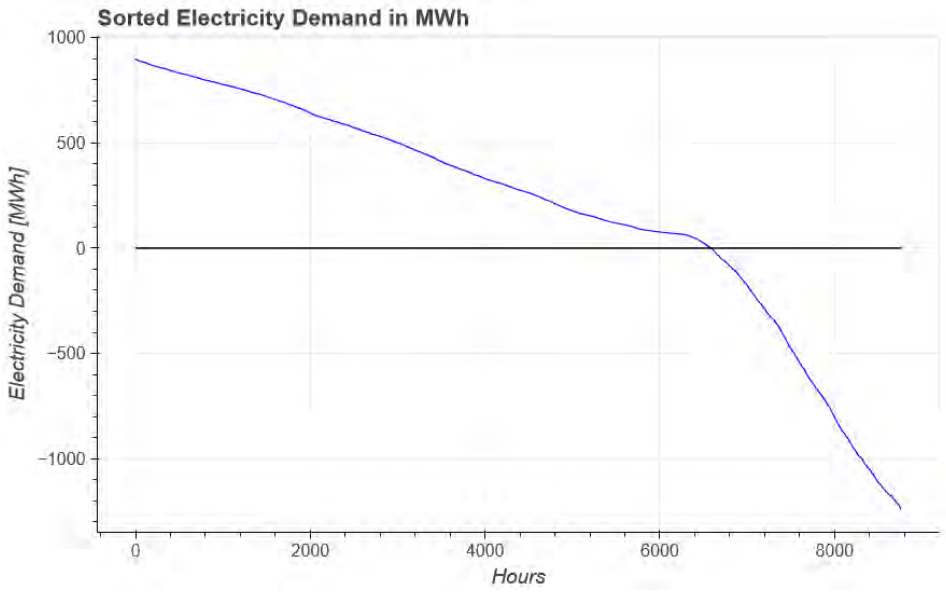

Figure 7.13: Hourly electricity demand profile in MWh sorted in descending order for Hamburg

7.1.3 Results on Medium-Voltage Grid Level

As previously mentioned in Chapter 3.4.3, the optimization results are aggregated based on the MV grid to provide a simple assessment of grid congestion on the lower voltage levels. As electricity demand varies for each MV grid, the comparison between the grid areas are done using two indicators, namely: absolute FLH and ratio between hourly peak demand in positive direction and negative direction.

In Figure 7.14, the FLH values of each grid area is shown. As Altenwerder and Hausbruch are assumed to have no residential area (see Chapter 5.6), both of these areas are not shown in this figure. A low FLH corresponds to a relatively volatile electricity demand profile with high peak values with high FLH refers to area with relatively flat electricity demand. It can be seen that high FLH values (represented by darker shade of green) are located mostly outside of the city center. In addition to FLH, the ratio between the peak demands is calculated for each grid area (Figure 7.15) to evaluate the proportion of the residual feed-in coming from PV generation. This ratio is calculated by dividing the peak hourly electricity required from the grid by the peak residual PV feed-in. As the ratios here represent the proportion of the peak demands, values closer to 1 are considered ideal for the electricity grid. Similar to Figure 7.14, the best ratios are mostly located on the outskirts of the city. Additionally, it can be also seen that in grid areas with a relatively low FLH, the peak electricity feed-ins are often disproportionately larger than its counterparts (low ratio). Additionally it is evident that grid areas with relatively similar peak demands (represented by ratio close to 1) are also associated with comparatively good FLH values.

From Figures 7.15 and 7.14, it is evident that the detrimental effects of PV generation are not evenly distributed. Within this work, this discrepancy is primarily attributed to the absence of a heat pump, electrical heater, and thermal energy storage. This is further supported by Figure 7.16, illustrating the overlap between MV grid areas and district heating areas. Using this figure, a correlation between grid areas with widespread connection of district heating and low FLH and ratio can be established.

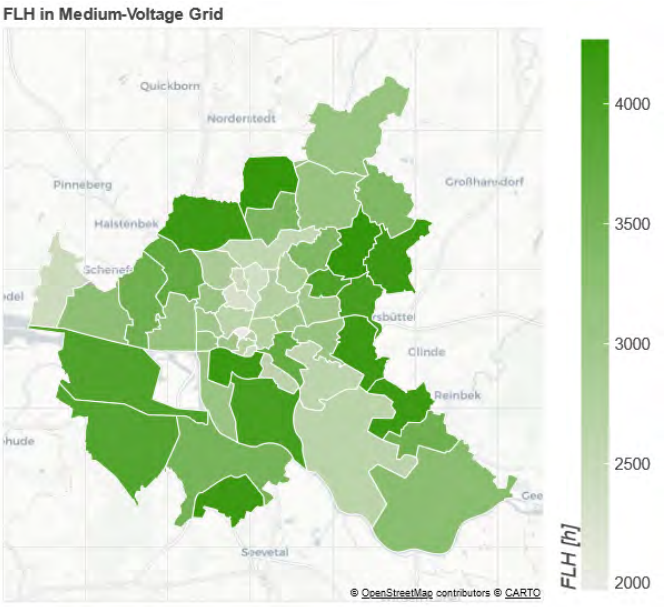

Figure 7.14: FLH in Medium-Voltage Grid Areas

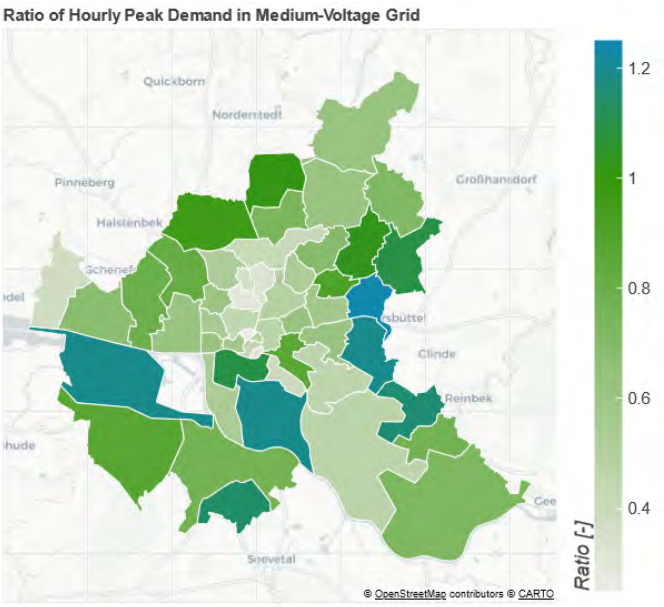

Figure 7.15: Ratio between hourly peak demands in Medium-Voltage Grid Areas

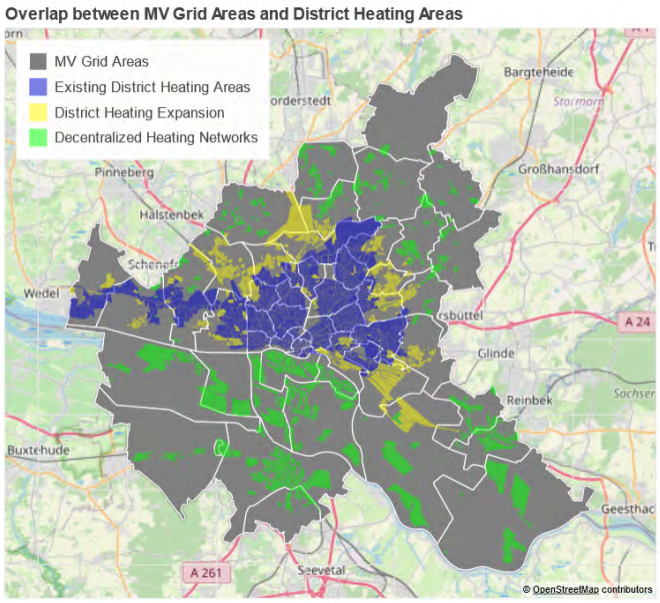

Figure 7.16: Overlap between MV grid areas and district heating areas [122]

7.2 Discussion

In this section, the results from different aggregation levels presented in Chapter 7.1 are discussed further, along with an assessment of the practical implications of these findings.

7.2.1 Discussion of Results

Results based on Building Energy System Configuration

To compare the results of the different building energy system configurations from Chapter 7.1.1, FLH is utilized as an indicator. Due to the presence of PV within the system, absolute values are employed to ensure comparability of the calculated values.

- SLP : 3765 h
- with district heating and without PV : 2807 h
- without district heating and without PV : 3759 h
- with district heating and with PV : 2486 h
- without district heating and with PV : 4285 h

The lowest FLH is calculated for building objects with only PV system, highlighting the seasonal variation and volatility of PV generation profile. Even with the presence of battery storage system, situations may occur in which the peak electricity demand in the negative direction is significantly larger than its positive counterparts (Figure 7.4).

Figure 7.8 demonstrates that the electrification of heat demand using a heat pump, electrical heater, and thermal storage could provide a considerable improvement. This enhancement is also noticeable in terms of FLH, showcasing the potential of sector coupling to help stabilize the grid. Figure 7.10 further supports this, illustrating that both battery and thermal energy storage work in tandem to improve the electricity demand profile. Even in the absence of a PV system, a relatively high FLH (3759 h) can be calculated, which highlights the compatibility between heat pump, electrical and thermal energy storage to maintain a relatively stable electricity demand profile. This is further supported by the comparison with SLP, where the FLH value from SLP can only be reached when heat pump, electrical heater, and thermal storage are available in the system.

Results on NUTS-1 Level

In Hamburg, in spite of the electrification of heat demand for 73% of all residential building objects, a reduction of approximately 40% compared to the baseline annual electricity demand can be observed. This can be attributed to the huge potential of PV in residential buildings. It is therefore reasonable to assume that the electrification of heat demand using the aforementioned building energy system configurations is plausible. From Figure 7.12, it is clear that the potential detrimental effects of disproportionate electricity feed-in from residual PV generation during the summer must be addressed to ensure the stability of the electricity grid.

Results on Medium-Voltage Grid Level

As previously mentioned, residential PV systems are mostly connected to lower voltage levels of the distribution grid. This therefore highlights the need for an analysis of the electricity flow on the lower voltage levels. Due to the availability of the data set, this analysis is done using aggregated results on MV level. From Figures 7.15 and 7.14, it can be seen that the highest volatility of the electricity demand profile is located within the city center. It is also important to note that these grid areas correspond highly with areas, where a heating supply from district heating is to be expected. Due to the lack of flexibility options (no thermal storage and electric heating available), these areas can be seen as having the highest risk of grid congestion.

7.2.2 Practical Implications

Out of the presented results, several practical implications can be derived.

Energy System Planning

To ensure a climate-neutral and economical heating system, a strategic approach is required. District heating is often highlighted as one of the key technologies to achieve this goal. However, the widespread use of district heating could potentially lead to a decrease in flexibility options within the system. In a transformed energy system, where heat and electricity are closely coupled, a reduction in flexibility could adversely affect the electricity grid. This effect can be intensified by the high penetration of renewable generation sources (see Figure 7.15 and 7.14 for example). For this reason, the impact a heating system can have on the electricity grid, and vice versa, should always be considered in the pathway towards a transformed energy system [202]. This need is further highlighted by the introduction of WPG (Heat Planning Act - *Wärmeplanungsgesetz*), which obligates the federal states to establish heat transformation plans towards climate neutrality.

Obstacles for Residential Flexibility Options

Within the current landscape of energy sector, constant electricity tariffs are used for the majority of customers. Due to the rising electricity prices along the years, these fixed tariffs make it financially attractive to utilize the self generated electricity and have proven to be an important driver for the expansion and acceptance of renewable energy (rooftop PV in particular). This current scheme however provides no financial incentive for individual household consumers to adjust their demand profile for the benefit of the electrical grid [203].

Beside the lack of financial incentives, a number of current regulatory obstacles also has to be addressed to effectively integrate flexibility into the electricity grid. One typical example is the limitation placed on battery storage system, where the EEG (Renewable Energy Act - *Erneuerbare-Energien-Gesetz*) is applied. In these batteries, only green energy (energy from the corresponding renewable sources) may be stored. If gray electricity (electricity from the grid) is stored alongside green electricity, all of the electricity charged in the battery is automatically considered as gray electricity. Concretely this means

that storage systems from the innovation tenders cannot be charged using electricity from the grid, even if it is financially viable to do [204]–[206]

Therefore, systematic changes within the energy sector has to occur before the full potential of flexibility options can be fully realized for the grid.

8 Conclusion and Outlook

The following section summarizes the results of this work and highlights possible changes and extensions to the methods used in this work.

8.1 Conclusion

Within the scope of this work, a method has been developed to analyze the potential and impact of PV and heat pumps in a highly electrified and coupled energy system for every residential building in Hamburg. Given the scope of this work, the model employed in this thesis is considerably simplified, focusing mainly on technical aspects such as efficiency.

The results presented in this work lead to the conclusion that a highly electrified heating system for residential buildings, based on heat pumps, electrical heaters, and PV, is feasible. However, to avoid detrimental effects on the electricity grid, a considerable amount of flexibility is required within the system to prevent short-term disproportionate load peaks in both positive (energy taken from the grid) and negative (energy fed into the grid) directions. Additionally, a high adoption rate of rooftop PV systems may introduce new challenges in the form of highly volatile and seasonal bidirectional electricity flow.

The aggregated results on the MV grid further demonstrate potential challenges that may arise due to the combination of district heating and high PV penetration in residential areas. Since there is no option to couple the electricity and heat sectors, the seasonal volatility of PV becomes more predominant. This highlights the need for a specific strategic approach for each individual area to ensure a smooth integration of these CO_2-friendly technologies. Despite the promising potential of heat pumps and PVs, substantial changes to the current frameworks of the energy market are required to fully realize the potential of these technologies for the benefit of the electricity grid.

Furthermore, this work demonstrates that the analysis of every residential building in Hamburg (a total of 229,119 buildings) at an hourly resolution is generally feasible. Given the extensive data generated by this type of analysis, attention should be paid to meaningfully interpret the results. Particular care must also be taken to ensure that the input data sets are of adequate quality, as the analysis results heavily depend on the quality of the data. All in all, using the methodology developed in this thesis, the objectives laid out in Chapter 1.1 can be fulfilled to varying degrees.

8.2 Outlook

In this thesis a wide range of different methods is used. Consequently, a plethora of assumptions and simplifications are made during the development of the model to ensure it fits the scope of this work.

In the following, a set of limitations of the presented method that can be addressed in future work are discussed.

8.2.1 Quality of Datasets

As briefly mentioned in Chapter 4.7, the datasets used in this work differ in terms of quality. Since the quality of the results directly correlates with the quality of the input data, considerations should be made regarding the 2022 German census (not yet published at the time of writing this work) and the 3D city model of Hamburg in LoD3 (which does not yet cover the entire region of Hamburg) [112], [113], [118]

8.2.2 Economical Aspects

As this work aims to only analyze the effects of heat pumps and PV on the finished state, the economic viability of the chosen technologies is neglected. In reality, the adoption of a technology is highly dependent on the economic viability of such solution.

8.2.3 Sizing Method

Within this work, both battery storage and thermal storage systems are sized using a generalized method (Chapter 5.5). However, from Chapter 7.1, a trend of oversizing for both of these storage systems can be observed. In future work, other sizing methods, such as VDI 4657 Part 3 and VDI 4645, should be considered. Since these methods may result in smaller storage sizes, reducing their potential to reduce peak loads, it is important to further investigate the effects they can have on the electricity grid.

8.2.4 PV Generation Model

Within this work, the methodology used to calculate the PV generation time series is described in Chapter 5.4). Due to the emergence of LoD3 datasets for Hamburg, the model used in this thesis can be be further enhanced. Compared to LoD2, the LoD3 data set provides a significant improvement, offering information regarding roof constructions, such as dormers and chimneys, as well as roof textures [118].

8.2.5 Consideration of Commercial and Industrial Load Profile

The electrical grid consists not only of residential loads, but also of commercial and industrial loads. As this work only consider residential buildings, the analysis shown in this thesis provides an incomplete picture of the electricity grid. While PV generation in residential sector may cause a challenge due to its seasonal variation, this problem may prove to be insignificant when electricity demands from commercial and industrial sources are taken into account.

8.2.6 Consideration of Other Heating Technologies

For regions without a connection to district heating, the heating technologies within this work are limited to air source heat pump and electrical heater, narrowing down the scope of this work. To ensure the best suitable option is used, other CO_2-friendly heating technologies, such as hybrid or solar thermal collector, should be considered in future work.

8.2.7 Power Flow Analysis

Within this work, possibility of grid congestion is approximated using both the FLH and ratio between the peak electricity demands. Assuming the availability of required data sets of grid infrastructures, power flow analysis should be done to correctly assess the risks of grid congestion caused by widespread decentralized PV systems and increased heat pump integration.

Bibliography

[1] Intergovernmental Panel on Climate Change, *Urgent climate action can secure a liveable future for all*, Press release, 2023-03-20. [Online]. Available: https://www.ipcc.ch/report/ar6/syr/downloads/press/IPCC_AR6_SYR_PressRelease_en.pdf (visited on 2023-10-27).

[2] Bundesregierung. "Climate Change Act 2021. Intergenerational contract for the climate". (), [Online]. Available: https://www.bundesregierung.de/breg-de/schwerpunkte/klimaschutz/climate-change-act-2021-1936846 (visited on 2023-10-27).

[3] Umweltbundesamt. "Indicator: Greenhouse gas emissions". (2023), [Online]. Available: https://www.umweltbundesamt.de/en/data/environmental-indicators/indicator-greenhouse-gas-emissions#at-a-glance (visited on 2023-12-27).

[4] Deutsche Braunkohlen-Industrie-Verein (DEBRIV). "Strommix 1990-2021". (2022-04), [Online]. Available: https://braunkohle.de/medium/strommix-2007-2017/ (visited on 2023-12-10).

[5] Statistisches Bundesamt (Destatis). "Stromerzeugung im 1. Halbjahr 2023: 11,4 % weniger Strom als im Vorjahreszeitraum". (2023), [Online]. Available: https://www.destatis.de/DE/Presse/Pressemitteilungen/2023/09/PD23_351_43312.html (visited on 2023-11-26).

[6] C. Rullán Lemke, D. John, N. Tedjosantoso, M. Kaltschmitt, and H. Schäfers, *Solarpotenzialstudie für Hamburg. nicht nur Schietwetter in Hamburg! Typologisierung von Fallbeispielen und Ableitung von Handlungsempfehlungen*, 2023-03. [Online]. Available: %7Bhttps://www.erneuerbare-energien-hamburg.de/de/service/downloads.html?page_c8=2&file=files/eehh-website/upload/eehh/over_all/downloads/2023/03/EEHH-Solarpotenzialstudie.pdf%7D (visited on 2023-11-14).

[7] H. Wirth, *Gutachten Energetische Quartiersentwicklung*, Fraunhofer ISE, 2023. [Online]. Available: https://www.ise.fraunhofer.de/content/dam/ise/en/documents/publications/studies/recent-facts-about-photovoltaics-in-germany.pdf (visited on 2023-11-30).

[8] B. Uzum, A. Onen, H. M. Hasanien, and S. M. Muyeen, "Rooftop solar pv penetration impacts on distribution network and further growth factors—a comprehensive review", *Electronics*, vol. 10, no. 1, p. 55, 2020-12, ISSN: 2079-9292. DOI: 10.3390/electronics10010055. [Online]. Available: http://dx.doi.org/10.3390/electronics10010055.

[9] F. Peprah, S. Gyamfi, M. Amo-Boateng, and E. Effah-Donyina, "Impact assessment of grid tied rooftop pv systems on lv distribution network", *Scientific African*, vol. 16, e01172, 2022-07, ISSN: 2468-2276. DOI: 10.1016/j.sciaf.2022.e01172. [Online]. Available: http://dx.doi.org/10.1016/j.sciaf.2022.e01172.

[10] M. Dwortzan. “Reducing industrial carbon emissions”. (2021), [Online]. Available: https://news.mit.edu/2021/reducing-emissions-decarbonizing-industry-0721 (visited on 2023-12-20).

[11] J. Wettengel. “2022 emissions reduction too little to put germany on track for 2030 target”. (2023), [Online]. Available: https://www.cleanenergywire.org/news/2022-emissions-reduction-too-little-put-germany-track-2030-target (visited on 2023-12-20).

[12] Behörde für Umwelt, Klima, Energie und Agrarwirtschaft (BUKEA). “Bilanz des Statistikamtes Nord für 2021. CO2-Emissionen in Hamburg”. (), [Online]. Available: https://www.hamburg.de/co2-bilanz-hh/ (visited on 2023-12-20).

[13] Umweltbundesamt. “Energieverbrauch privater Haushalte”. (2023), [Online]. Available: https://www.umweltbundesamt.de/daten/private-haushalte-konsum/wohnen/energieverbrauch-privater-haushalte#endenergieverbrauch-der-privaten-haushalte (visited on 2023-11-26).

[14] Statistisches Bundesamt (Destatis). “Energy consumption for housing, by area of energy use, 2021”. (2024), [Online]. Available: https://www.destatis.de/EN/Themes/Society-Environment/Environment/Environmental-Economic-Accounting/_Graphic/_Interactive/energy-consumption-housing.html (visited on 2024-01-02).

[15] Statistisches Bundesamt (Destatis). “Energy consumption for housing, by energy source”. (2024), [Online]. Available: https://www.destatis.de/EN/Themes/Society-Environment/Environment/Environmental-Economic-Accounting/_Graphic/_Interactive/energy-consumption-housing-energy.html (visited on 2024-01-02).

[16] Bundesverband der Energie- und Wasserwirtschaft (bdew), *Wie heizt Deutschland?*, de, 2023. [Online]. Available: https://www.bdew.de/media/documents/BDEW_Heizungsmarkt_2023_Langfassung_final_28.11.2023_korrigiert.pdf (visited on 2023-12-14).

[17] SolarPower Europe, *Solar Powers Heat 2023*, 2023. [Online]. Available: https://api.solarpowereurope.org/uploads/0523_SPE_Solar_Heating_report_09_mr_98b11ef7ab.pdf?updated_at=2023-03-09T06:13:41.408Z (visited on 2023-12-27).

[18] thermondo. “Thermondo teilt Ergebnisse aus Befragung und Daten aus 2.500 Wärmepumpen-Installationen: Wärmepumpe nach GEG-Beschluss beste Option im Altbau”. (2023), [Online]. Available: https://www.thermondo.de/unternehmen/presse/pressemitteilungen/thermondo-teilt-Ergebnisse-aus-Befragung-und-Installations-Daten/ (visited on 2023-12-27).

[19] Umweltbundesamt. “Marktdaten: Wohnen”. (2022), [Online]. Available: https://www.umweltbundesamt.de/daten/private-haushalte-konsum/konsum-produkte/gruene-produkte-marktzahlen/marktdaten-bereich-wohnen#wohnflache-pro-einwohnerin-gestiegen (visited on 2023-12-27).

[20] A. Rinaldi, M. C. Soini, K. Streicher, M. K. Patel, and D. Parra, "Decarbonising heat with optimal pv and storage investments: A detailed sector coupling modelling framework with flexible heat pump operation", *Applied Energy*, vol. 282, p. 116 110, 2021-01, ISSN: 0306-2619. DOI: 10.1016/j.apenergy.2020.116110. [Online]. Available: http://dx.doi.org/10.1016/j.apenergy.2020.116110.

[21] A. Rinaldi, S. Yilmaz, M. K. Patel, and D. Parra, "What adds more flexibility? an energy system analysis of storage, demand-side response, heating electrification, and distribution reinforcement", *Renewable and Sustainable Energy Reviews*, vol. 167, p. 112 696, 2022-10, ISSN: 1364-0321. DOI: 10.1016/j.rser.2022.112696. [Online]. Available: http://dx.doi.org/10.1016/j.rser.2022.112696.

[22] A. Pena-Bello, P. Schuetz, M. Berger, J. Worlitschek, M. K. Patel, and D. Parra, "Decarbonizing heat with pv-coupled heat pumps supported by electricity and heat storage: Impacts and trade-offs for prosumers and the grid", *Energy Conversion and Management*, vol. 240, p. 114 220, 2021-07, ISSN: 0196-8904. DOI: 10.1016/j.enconman.2021.114220. [Online]. Available: http://dx.doi.org/10.1016/j.enconman.2021.114220.

[23] Z. Wang, M. B. Luther, M. Amirkhani, C. Liu, and P. Horan, "State of the art on heat pumps for residential buildings", *Buildings*, vol. 11, no. 8, p. 350, 2021-08, ISSN: 2075-5309. DOI: 10.3390/buildings11080350. [Online]. Available: http://dx.doi.org/10.3390/buildings11080350.

[24] Bundesministerium für Wirtschaft und Klimaschutz (BMWK). "7. Energieforschungsprogramm der Bundesregierung". (2018), [Online]. Available: https://www.bmwk.de/Redaktion/DE/Publikationen/Energie/7-energieforschungsprogramm-der-bundesregierung.html (visited on 2023-11-22).

[25] B. Munzel, M. Reiser, and K. Steinbacher, *Flexibilitätspotenziale und Sektorkopplung. Synthesebericht 1 des SINTEG Förderprogramms*, Studie im Auftrag des BMWK, 2022. [Online]. Available: https://www.bmwk.de/Redaktion/DE/Publikationen/Sinteg/synthesebericht-1-flexibilitatspotenziale-und-sektorkopplung.pdf?__blob=publicationFile&v=1 (visited on 2023-12-28).

[26] W. Beba, O. Arendt, L. Süthoff, *et al.*, *Abschlussbericht zum SINTEG-Schaufenster New 4.0 Norddeutsche Energiewende 4.0 : Laufzeit des Vorhabens: 01.12.2016-31.03.2021, Berichtszeitraum: 01.12.2016-31.03.2021*, Hamburg, 2021. DOI: 10.2314/KXP:1774183781. [Online]. Available: https://www.tib.eu/de/suchen/id/TIBKAT%5C%3A1774183781.

[27] Reiner Lemoine Institut (RLI). "Egon". (), [Online]. Available: https://reiner-lemoine-institut.de/en/egon/ (visited on 2023-11-14).

[28] Reiner Lemoine Institut (RLI). "Ego^n open and cross-sectoral planning of transmission and distribution grids". (), [Online]. Available: https://ego-n.org/ (visited on 2023-11-14).

[29] C. Büttner, K. Esterl, I. Cußmann, C. Epia, J. Amme, and A. Nadal, "Influence of flexibility options on the german transmission grid — a sector-coupled mid-term scenario", 2023. DOI: 10.2139/ssrn.4442243. [Online]. Available: http://dx.doi.org/10.2139/ssrn.4442243.

[30] H.-P. Tetens, S. Günther, K. Esterl, C. Epia, and B. Schachler, *Abschlussworkshop ego^n. Komplexitätsexplosion und -reduktion*, 2023. [Online]. Available: https://ego-n.org/presentations/2023_eGon_Abschluss-WS_Session_I-B_Komplexitaetsreduktion.pdf (visited on 2023-10-25).

[31] M. Röck, M. R. M. Saade, M. Balouktsi, *et al.*, "Embodied ghg emissions of buildings – the hidden challenge for effective climate change mitigation", *Applied Energy*, vol. 258, p. 114 107, 2020-01, ISSN: 0306-2619. DOI: 10.1016/j.apenergy.2019.114107. [Online]. Available: http://dx.doi.org/10.1016/j.apenergy.2019.114107.

[32] X. Yang, M. Hu, N. Heeren, *et al.*, "A combined gis-archetype approach to model residential space heating energy: A case study for the netherlands including validation", *Applied Energy*, vol. 280, p. 115 953, 2020-12, ISSN: 0306-2619. DOI: 10.1016/j.apenergy.2020.115953. [Online]. Available: http://dx.doi.org/10.1016/j.apenergy.2020.115953.

[33] L. G. Swan and V. I. Ugursal, "Modeling of end-use energy consumption in the residential sector: A review of modeling techniques", *Renewable and Sustainable Energy Reviews*, vol. 13, no. 8, pp. 1819–1835, 2009-10, ISSN: 1364-0321. DOI: 10.1016/j.rser.2008.09.033. [Online]. Available: http://dx.doi.org/10.1016/j.rser.2008.09.033.

[34] J. Dong, Y. Schwartz, A. Mavrogianni, I. Korolija, and D. Mumovic, "A review of approaches and applications in building stock energy and indoor environment modelling", *Building Services Engineering Research and Technology*, vol. 44, no. 3, pp. 333–354, 2023-03, ISSN: 1477-0849. DOI: 10.1177/01436244231163084. [Online]. Available: http://dx.doi.org/10.1177/01436244231163084.

[35] L. Frayssinet, L. Merlier, F. Kuznik, J.-L. Hubert, M. Milliez, and J.-J. Roux, "Modeling the heating and cooling energy demand of urban buildings at city scale", *Renewable and Sustainable Energy Reviews*, vol. 81, pp. 2318–2327, 2018-01, ISSN: 1364-0321. DOI: 10.1016/j.rser.2017.06.040. [Online]. Available: http://dx.doi.org/10.1016/j.rser.2017.06.040.

[36] C. Deb, F. Zhang, J. Yang, S. E. Lee, and K. W. Shah, "A review on time series forecasting techniques for building energy consumption", *Renewable and SustainablDe Energy Reviews*, vol. 74, pp. 902–924, 2017-07, ISSN: 1364-0321. DOI: 10.1016/j.rser.2017.02.085. [Online]. Available: http://dx.doi.org/10.1016/j.rser.2017.02.085.

[37] J. Von Appen, J. Haack, and M. Braun, "Erzeugung zeitlich hochaufgelöster Stromlastprofile für verschiedene Haushaltstypen", 2014-01.

[38] A. Mastrucci, A. Marvuglia, U. Leopold, and E. Benetto, "Life cycle assessment of building stocks from urban to transnational scales: A review", *Renewable and Sustainable Energy Reviews*, vol. 74, pp. 316–332, 2017-07, ISSN: 1364-0321. DOI: 10.1016/j.rser.2017.02.060. [Online]. Available: http://dx.doi.org/10.1016/j.rser.2017.02.060.

[39] A. Brown, A. Foley, D. Laverty, S. McLoone, and P. Keatley, "Heating and cooling networks: A comprehensive review of modelling approaches to map future directions", *Energy*, vol. 261, p. 125 060, 2022-12, ISSN: 0360-5442. DOI: 10.1016/j.energy.2022.125060. [Online]. Available: http://dx.doi.org/10.1016/j.energy.2022.125060.

[40] T. Loga, B. Stein, N. Diefenbach, and R. Born, *Deutsche Wohngebäudetypologie: Beispielhafte Maßnahmen zur Verbesserung der Energieeffizienz von typischen Wohngebäuden*, de, 2015. [Online]. Available: https://www.episcope.eu/downloads/public/docs/brochure/DE_TABULA_TypologyBrochure_IWU.pdf.

[41] *Tabula calculation method – energy use for heating and domestic hot water*, 2013-01. [Online]. Available: https://www.episcope.eu/downloads/public/docs/report/TABULA_CommonCalculationMethod.pdf.

[42] Hamburger Energiewerke. "Wie funktioniert Fernwärme?" (), [Online]. Available: https://www.hamburger-energiewerke.de/wissen-themen/fernwaerme/wie-funktioniert-fernwaerme (visited on 2023-12-01).

[43] I. Sarbu, M. Mirza, and E. Crasmareanu, "A review of modelling and optimisation techniques for district heating systems", *International Journal of Energy Research*, 2019-05, ISSN: 1099-114X. DOI: 10.1002/er.4600. [Online]. Available: http://dx.doi.org/10.1002/er.4600.

[44] P. Konstantin and M. Konstantin, *Praxisbuch der Fernwärme- und Fernkälteversorgung: Systeme, Netzaufbauvarianten, Kraft-Wärme- und Kraft-Wärme-Kälte-Kopplung, Kostenstrukturen und Preisbildung*. Springer Berlin Heidelberg, 2022, ISBN: 9783662643433. DOI: 10.1007/978-3-662-64343-3. [Online]. Available: http://dx.doi.org/10.1007/978-3-662-64343-3.

[45] Agentur für Erneuerbare Energien (AEE), *Fernwärmeerzeugung nach Energieträgern in Deutschland 2020*, 2021. [Online]. Available: https://www.unendlich-viel-energie.de/mediathek/grafiken/fernwaermeerzeugung-nach-energietraegern-in-deutschland-2020 (visited on 2023-12-01).

[46] Wärme Hamburg. "Primärenergiefaktor und CO_2-Emissionen - Bestwerte für die Fernwärme". (), [Online]. Available: https://waerme.hamburg/fernwaermesystem/primaerenergiefaktor (visited on 2023-12-01).

[47] I. Dochev, I. Peters, H. Seller, and G. K. Schuchardt, "Analysing district heating potential with linear heat density. a case study from hamburg.", *Energy Procedia*, vol. 149, pp. 410–419, 2018-09, ISSN: 1876-6102. DOI: 10.1016/j.egypro.2018.08.205. [Online]. Available: http://dx.doi.org/10.1016/j.egypro.2018.08.205.

[48] T. Nussbaumer, S. Thalmann, A. Jenni, and J. Ködel, *Handbook on planning of district heating networks*, 2020. [Online]. Available: https://www.verenum.ch/Dokumente/Handbook-DH_V1.0.pdf (visited on 2023-12-01).

[49] N. Thamling, N. Langreder, D. Rau, *et al.*, *Gutachten Perspektive der Fernwärme: Maßnahmenprogramm 2030 Aus- und Umbau städtischer Fernwärme als Beitrag einer sozial-ökologischen Wärmepolitik*, de, Arbeitsgemeinschaft Fernwärme (AGFW), 2020. [Online]. Available: https://www.hamburg-institut.com/wp-content/uploads/2021/06/AGFW_Perspektive_der_Fernwaerme_2030_final.pdf (visited on 2023-11-30).

[50] M. Sandrock, V. Bürger, J. Mundt, and N. Jaeschke, *Entwicklungsszenarien für neue Klimaziele: Szenario b*, de, Behörde für Umwelt, Klima, Energie und Agrarwirtschaft (BUKEA), 2022. [Online]. Available: https://www.hamburg.de/contentblob/16782034/9bd290f51dad11b7199146ed7918423e/data/d-szenarien-szenariob.pdf (visited on 2023-11-30).

[51] V. Quaschning, *Understanding renewable energy systems*, 2., überarb. Aufl. London: Earthscan, 2016, p. 406, ISBN: 978-1-138-78196-2. [Online]. Available: http://www.volker-quaschning.de/publis/regen_e/index.php.

[52] I. Sarbu and C. Sebarchievici, "Solar-assisted heat pumps", in *Solar Heating and Cooling Systems*. Elsevier, 2017, pp. 347–410. DOI: 10.1016/b978-0-12-811662-3.00009-8. [Online]. Available: http://dx.doi.org/10.1016/B978-0-12-811662-3.00009-8.

[53] T. C. P. on Heat Pumping Technologies (HPT TCP). "How does a heat pump work?" (), [Online]. Available: https://heatpumpingtechnologies.org/market-technology/heat-pump-work/ (visited on 2023-12-01).

[54] Wright Renewable Heating. "Air source heat pumps". (), [Online]. Available: https://www.wrightrenewableheating.co.uk/air-source-heat-pumps/ (visited on 2023-12-15).

[55] T. C. P. on Heat Pumping Technologies (HPT TCP). "Efficiency and heat pumping application". (), [Online]. Available: https://heatpumpingtechnologies.org/market-technology/efficiency-heat-pumps/ (visited on 2023-12-01).

[56] ETG Taskforce Wärmemarkt, *Potenziale für Strom im Wärmemarkt bis 2050*, de, VDE ETG Energietechnik, 2015. [Online]. Available: https://docplayer.org/24584807-Potenziale-fuer-strom-im-waermemarkt-bis-2050.html (visited on 2023-11-30).

[57] A. A. Kebede, T. Kalogiannis, J. Van Mierlo, and M. Berecibar, "A comprehensive review of stationary energy storage devices for large scale renewable energy sources grid integration", *Renewable and Sustainable Energy Reviews*, vol. 159, p. 112 213, 2022-05, ISSN: 1364-0321. DOI: 10.1016/j.rser.2022.112213. [Online]. Available: http://dx.doi.org/10.1016/j.rser.2022.112213.

[58] I. Stadler and A. Hauer, "Thermische energiespeicher", in *Energiespeicher - Bedarf, Technologien, Integration*. Springer Berlin Heidelberg, 2017, pp. 579–618, ISBN: 9783662488935. DOI: 10.1007/978-3-662-48893-5_10. [Online]. Available: http://dx.doi.org/10.1007/978-3-662-48893-5_10.

[59] M. Mamun, M. Islam, M. Hasanuzzaman, and J. Selvaraj, "Effect of tilt angle on the performance and electrical parameters of a pv module: Comparative indoor and outdoor experimental investigation", *Energy and Built Environment*, vol. 3, no. 3, pp. 278–290, 2022-07, ISSN: 2666-1233. DOI: 10.1016/j.enbenv.2021.02.001. [Online]. Available: http://dx.doi.org/10.1016/j.enbenv.2021.02.001.

[60] P. Takács, J. Slíz-Balogh, Á. Horváth, D. Horváth, I. M. Jánosi, and G. Horváth, "How the morning-afternoon cloudiness asymmetry affects the energy-maximizing azimuth direction of fixed-tilt monofacial solar panels", *Royal Society Open Science*, vol. 9, no. 4, 2022-04, ISSN: 2054-5703. DOI: 10.1098/rsos.211948. [Online]. Available: http://dx.doi.org/10.1098/rsos.211948.

[61] F. Saeed and A. Zohaib, "Quantification of losses in a photovoltaic system: A review", in *The 2nd International Electronic Conference on Applied Sciences*, ser. ASEC 2021, MDPI, 2021-10. DOI: 10.3390/asec2021-11200. [Online]. Available: http://dx.doi.org/10.3390/ASEC2021-11200.

[62] A. M. Khalid, I. Mitra, W. Warmuth, and V. Schacht, "Performance ratio – crucial parameter for grid connected pv plants", *Renewable and Sustainable Energy Reviews*, vol. 65, pp. 1139–1158, 2016-11, ISSN: 1364-0321. DOI: 10.1016/j.rser.2016.07.066. [Online]. Available: http://dx.doi.org/10.1016/j.rser.2016.07.066.

[63] R. Khezri, A. Mahmoudi, and H. Aki, "Optimal planning of solar photovoltaic and battery storage systems for grid-connected residential sector: Review, challenges and new perspectives", *Renewable and Sustainable Energy Reviews*, vol. 153, p. 111 763, 2022-01, ISSN: 1364-0321. DOI: 10.1016/j.rser.2021.111763. [Online]. Available: http://dx.doi.org/10.1016/j.rser.2021.111763.

[64] BMWK. "Durchschnittlichen EEG-Vergütung von Photovoltaikanlagen in Deutschland in den Jahren 2000 bis 2022 (in Euro-Cent pro Kilowattstunde) [graph]". (2022-03), [Online]. Available: https://de.statista.com/statistik/daten/studie/173265/umfrage/durchschnittliche-eeg-verguetung-von-photovoltaikanlagen-seit-2009/ (visited on 2023-11-11).

[65] Bundesnetzagentur, *Strompreise für Haushaltskunden in Deutschland in den Jahren 2013 bis 2023 (in Euro-Cent pro Kilowattstunde) [graph]*, 2023-11. [Online]. Available: https://de.statista.com/statistik/daten/studie/154908/umfrage/strompreise-fuer-haushaltskunden-seit-2006/ (visited on 2023-12-11).

[66] A. M. Ershad, F. Ueckerdt, R. C. Pietzcker, A. Giannousakis, and G. Luderer, "A further decline in battery storage costs can pave the way for a solar pv-dominated indian power system", *Renewable and Sustainable Energy Transition*, vol. 1, p. 100 006, 2021-08, ISSN: 2667-095X. DOI: 10.1016/j.rset.2021.100006. [Online]. Available: http://dx.doi.org/10.1016/j.rset.2021.100006.

[67] Our World In Data, 2021-04. [Online]. Available: https://ourworldindata.org/battery-price-decline (visited on 2023-12-15).

[68] BloombergNEF. "Lithium-ion battery price worldwide from 2013 to 2023 (in 2023 u.s. dollars per kilowatt-hour) [graph]". (2023-11), [Online]. Available: https://www.statista.com/statistics/883118/global-lithium-ion-battery-pack-costs/ (visited on 2023-12-15).

[69] B. Wrålsen, V. Prieto-Sandoval, A. Mejia-Villa, R. O'Born, M. Hellström, and B. Faessler, "Circular business models for lithium-ion batteries - stakeholders, barriers, and drivers", *Journal of Cleaner Production*, vol. 317, p. 128 393, 2021-10, ISSN: 0959-6526. DOI: 10.1016/j.jclepro.2021.128393. [Online]. Available: http://dx.doi.org/10.1016/j.jclepro.2021.128393.

[70] D. Pelegov and J. Pontes, "Main drivers of battery industry changes: Electric vehicles—a market overview", *Batteries*, vol. 4, no. 4, p. 65, 2018-12, ISSN: 2313-0105. DOI: 10.3390/batteries4040065. [Online]. Available: http://dx.doi.org/10.3390/batteries4040065.

[71] Fraunhofer ISI, *Alternative Battery Technologies Roadmap 2030+*, 2023-09. [Online]. Available: https://www.isi.fraunhofer.de/content/dam/isi/dokumente/cct/2023/abt-roadmap.pdf (visited on 2023-12-11).

[72] A. J. Schwab, *Elektroenergiesysteme: Smarte Stromversorgung im Zeitalter der Energiewende*. Springer Berlin Heidelberg, 2022, ISBN: 9783662647745. DOI: 10.1007/978-3-662-64774-5. [Online]. Available: http://dx.doi.org/10.1007/978-3-662-64774-5.

[73] European Parliamentary Research Service (EPRS), *Understanding electricity markets in the eu*, 2016-11. [Online]. Available: https://www.europarl.europa.eu/RegData/etudes/BRIE/2016/593519/EPRS_BRI(2016)593519_EN.pdf (visited on 2023-12-01).

[74] ENTSO-E. "Regional groups". (2018), [Online]. Available: https://docstore.entsoe.eu/about-entso-e/system-operations/regional-groups/Pages/default.aspx (visited on 2023-12-05).

[75] Bundesministerium für Wirtschaft und Klimaschutz (BMWK). "Das deutsche Strom-Verteilernetz". (), [Online]. Available: https://www.bmwk.de/Redaktion/EN/Infografiken/Energie/verteilernetz.html (visited on 2023-11-22).

[76] Forschungszentrum Jülich. "Übertragungsnetz". (), [Online]. Available: https://www.enargus.de/pub/bscw.cgi/d14617-2/*/*/%5C%c3%5C%9cbertragungsnetz?op=Wiki.getwiki (visited on 2023-12-15).

[77] K. Heuck, K.-D. Dettmann, and D. Schulz, *Elektrische Energieversorgung: Erzeugung, Übertragung und Verteilung elektrischer Energie für Studium und Praxis*. Springer Fachmedien Wiesbaden, 2013, ISBN: 9783834821744. DOI: 10.1007/978-3-8348-2174-4. [Online]. Available: http://dx.doi.org/10.1007/978-3-8348-2174-4.

[78] Forschungszentrum Jülich. "Verteilnetz". (), [Online]. Available: https://www.enargus.de/pub/bscw.cgi/d13442-2/*/*/Verteilnetz?op=Wiki.getwiki (visited on 2023-12-15).

[79] Bundesnetzagentur. "Monitoringbericht 2023". (2023-11), [Online]. Available: https://data.bundesnetzagentur.de/Bundesnetzagentur/SharedDocs/Mediathek/Monitoringberichte/MonitoringberichtEnergie2023.pdf (visited on 2023-12-05).

[80] Stromnetz Hamburg. "Täglich für Hamburg im Einsatz". (), [Online]. Available: https://www.stromnetz-hamburg.de/ueber-uns/aufgaben/verteilungsnetzbetreiber (visited on 2023-12-10).

[81] EnBW. "Transport". (), [Online]. Available: https://www.enbw.com/energie-entdecken/verteilung-und-transport/stromnetz/ (visited on 2023-12-15).

[82] G. Brunekreeft, M. Buchmann, C. Dänekas, *et al.*, "Germany's way from conventional power grids towards smart grids", in *Regulatory Pathways For Smart Grid Development in China*. Springer Fachmedien Wiesbaden, 2015, pp. 45–78, ISBN: 9783658084639. DOI: 10.1007/978-3-658-08463-9_4. [Online]. Available: http://dx.doi.org/10.1007/978-3-658-08463-9_4.

[83] C. Weber, D. Möst, and W. Fichtner, *Economics of Power Systems: Fundamentals for Sustainable Energy*. Springer International Publishing, 2022, ISBN: 9783030977702. DOI: 10.1007/978-3-030-97770-2. [Online]. Available: http://dx.doi.org/10.1007/978-3-030-97770-2.

[84] Forschungszentrum Jülich. "Mittelspannung". (), [Online]. Available: https://www.energus.de/pub/bscw.cgi/d7528-2/*/*/Mittelspannung?op=Wiki.getwiki (visited on 2023-12-15).

[85] Forschungszentrum Jülich. "Niederspannung". (), [Online]. Available: https://www.energus.de/pub/bscw.cgi/d8085-2/*/*/Niederspannung?op=Wiki.getwiki (visited on 2023-12-15).

[86] Council of European Energy Regulators (CEER) and Energy Community Regulatory Board (ECRB), *7th Benchmarking Report on the Quality of Electricity and Gas Supply*, 2022. [Online]. Available: https://www.ceer.eu/documents/104400/-/-/e19caae8-95cf-f048-0664-0720228881bb (visited on 2023-12-01).

[87] Erdiwansyah, Mahidin, H. Husin, Nasaruddin, M. Zaki, and Muhibbuddin, "A critical review of the integration of renewable energy sources with various technologies", *Protection and Control of Modern Power Systems*, vol. 6, no. 1, 2021-02, ISSN: 2367-0983. DOI: 10.1186/s41601-021-00181-3. [Online]. Available: http://dx.doi.org/10.1186/s41601-021-00181-3.

[88] Bundesnetzagentur, *Flexibility in the electricity system*, 2017. [Online]. Available: https://www.bundesnetzagentur.de/SharedDocs/Downloads/EN/Areas/ElectricityGas/FlexibilityPaper_EN.pdf?__blob=publicationFile&v=1 (visited on 2023-12-16).

[89] P. Neetzow, "The effects of power system flexibility on the efficient transition to renewable generation", *Applied Energy*, vol. 283, p. 116 278, 2021-02, ISSN: 0306-2619. DOI: 10.1016/j.apenergy.2020.116278. [Online]. Available: http://dx.doi.org/10.1016/j.apenergy.2020.116278.

[90] L. P. C. Do, Š. Lyócsa, and P. Molnár, "Residual electricity demand: An empirical investigation", *Applied Energy*, vol. 283, p. 116 298, 2021-02, ISSN: 0306-2619. DOI: 10.1016/j.apenergy.2020.116298. [Online]. Available: http://dx.doi.org/10.1016/j.apenergy.2020.116298.

[91] P. Liu and F. Trieb, "Cost comparison of thermal storage power plants and conventional power plants for flexible residual load coverage", *Journal of Energy Storage*, vol. 56, p. 106 027, 2022-12, ISSN: 2352-152X. DOI: 10.1016/j.est.2022.106027. [Online]. Available: http://dx.doi.org/10.1016/j.est.2022.106027.

[92] Agora Energiewende, *Flexibility in thermal power plants – with a focus on existing coal-fired power plants*, 2017. [Online]. Available: https://www.agora-energiewende.de/fileadmin/Projekte/2017/Flexibility_in_thermal_plants/115_flexibility-report-WEB.pdf (visited on 2023-12-01).

[93] IRENA, *Innovation landscape brief: Flexibility in conventional power plants*, 2019. [Online]. Available: https://www.irena.org/-/media/Files/IRENA/Agency/Publication/2019/Sep/IRENA_Flexibility_in_CPPs_2019.pdf?la=en&hash=AF60106EA083E492638D8FA9ADF7FD099259F5A1 (visited on 2023-12-01).

[94] H. Weyer, F. Müsgens, F.-D. Drake, *et al.*, "Grid congestion as a challenge for the electricity system options for a future market design. position paper", 2021. [Online]. Available: https://en.acatech.de/publication/grid-congestion-as-a-challenge-electricity-system/ (visited on 2023-12-01).

[95] M. Titz, S. Pütz, and D. Witthaut, "Identifying drivers and mitigators for congestion and redispatch in the german electric power system with explainable ai", *Applied Energy*, vol. 356, p. 122 351, 2024-02, ISSN: 0306-2619. DOI: 10.1016/j.apenergy.2023.122351. [Online]. Available: http://dx.doi.org/10.1016/j.apenergy.2023.122351.

[96] N. Brinkel, L. Visser, T. AlSkaif, and W. van Sark, "Avoiding low-voltage grid congestion using smart charging of electric vehicles based on day-ahead probabilistic photovoltaic forecasts", in *2021 International Conference on Smart Energy Systems and Technologies (SEST)*, IEEE, 2021-09. DOI: 10.1109/sest50973.2021.9543447. [Online]. Available: http://dx.doi.org/10.1109/SEST50973.2021.9543447.

[97] I. B. Majeed and N. I. Nwulu, "Impact of reverse power flow on distributed transformers in a solar-photovoltaic-integrated low-voltage network", *Energies*, vol. 15, no. 23, p. 9238, 2022-12, ISSN: 1996-1073. DOI: 10.3390/en15239238. [Online]. Available: http://dx.doi.org/10.3390/en15239238.

[98] M. Zeman, "Developing the future electricity grid", *Europhysics News*, vol. 52, no. 5, pp. 32–35, 2021, ISSN: 1432-1092. DOI: 10.1051/epn/2021505. [Online]. Available: http://dx.doi.org/10.1051/epn/2021505.

[99] M. I. Henderson, D. Novosel, and M. L. Crow, "Electric power grid modernization trends, challenges, and opportunities", in *IEEE, Nov*, 2017.

[100] P. D. Lund, J. Lindgren, J. Mikkola, and J. Salpakari, "Review of energy system flexibility measures to enable high levels of variable renewable electricity", *Renewable and Sustainable Energy Reviews*, vol. 45, pp. 785–807, 2015-05, ISSN: 1364-0321. DOI: 10.1016/j.rser.2015.01.057. [Online]. Available: http://dx.doi.org/10.1016/j.rser.2015.01.057.

[101] L. Herc, A. Pfeifer, and N. Duić, "Optimization of the possible pathways for gradual energy system decarbonization", *Renewable Energy*, vol. 193, pp. 617–633, 2022-06, ISSN: 0960-1481. DOI: 10.1016/j.renene.2022.05.005. [Online]. Available: http://dx.doi.org/10.1016/j.renene.2022.05.005.

[102] T. A. Reddy and G. P. Henze, *Applied Data Analysis and Modeling for Energy Engineers and Scientists*. Springer International Publishing, 2023, ISBN: 9783031348693. DOI: 10.1007/978-3-031-34869-3. [Online]. Available: http://dx.doi.org/10.1007/978-3-031-34869-3.

[103] F. Hillier and G. Lieberman, *ISE introduction to operations research*, 11th ed. Columbus, OH: McGraw-Hill Education, 2020-03.

[104] A. Koop and H. Moock, *Lineare Optimierung – eine anwendungsorientierte Einführung in Operations Research: Mit Python-Programmen*. Springer Berlin Heidelberg, 2023, ISBN: 9783662663875. DOI: 10.1007/978-3-662-66387-5. [Online]. Available: http://dx.doi.org/10.1007/978-3-662-66387-5.

[105] A. Fattahi, J. Sijm, and A. Faaij, "A systemic approach to analyze integrated energy system modeling tools: A review of national models", *Renewable and Sustainable Energy Reviews*, vol. 133, p. 110 195, 2020-11, ISSN: 1364-0321. DOI: 10.1016/j.rser.2020.110195. [Online]. Available: http://dx.doi.org/10.1016/j.rser.2020.110195.

[106] IBM. “What does CPLEX do?” (2022-12), [Online]. Available: https://www.ibm.com/docs/en/icos/22.1.1?topic=cplex-what-does-do (visited on 2023-12-15).

[107] M. Macmillan, K. Eurek, W. Cole, and M. D. Bazilian, “Solving a large energy system optimization model using an open-source solver”, *Energy Strategy Reviews*, vol. 38, p. 100 755, 2021-11, ISSN: 2211-467X. DOI: 10.1016/j.esr.2021.100755. [Online]. Available: http://dx.doi.org/10.1016/j.esr.2021.100755.

[108] H. Mittelmann. “Benchmarking optimization softare a (Hi)Strory”. (), [Online]. Available: https://plato.asu.edu/talks/euro2019.pdf (visited on 2023-12-15).

[109] M. Parzen, J. Hall, J. Jenkins, and T. Brown, “Optimization solvers: The missing link for a fully open-source energy system modelling ecosystem.”, 2022. DOI: 10.5281/ZENODO.6409432. [Online]. Available: https://zenodo.org/record/6409432.

[110] R. Schreiber and K. Dworzak, *Zensus 2011: Durchführung der Wiederholungsbefragung*, 2012. [Online]. Available: https://www.zensus2011.de/SharedDocs/Downloads/DE/Publikationen/Aufsaetze_Archiv/2012_07_BY_Durchfuehrung_der_Wiederholungsbefragung.pdf?__blob=publicationFile&v=2 (visited on 2023-11-25).

[111] Statistisches Bundesamt (Destatis), *Ergebnisse des Zensus 2011*. [Online]. Available: https://ergebnisse2011.zensus2022.de/datenbank/online/ (visited on 2023-11-24).

[112] Bundesministerium des Innern und für Heimat (BMI). “Zensus 2022”. (2023), [Online]. Available: https://www.bmi.bund.de/DE/themen/moderne-verwaltung/statistik/zensus-2022/zensus-2022-node.html (visited on 2023-11-25).

[113] Statistisches Bundesamt (Destatis). “Welche Ergebnisse wird es geben?” (), [Online]. Available: https://www.zensus2022.de/DE/Ergebnisse/_inhalt.html (visited on 2023-11-26).

[114] Arbeitsgemeinschaft der Vermessungsverwaltungen der Länder der Bundesrepublik Deutschland (AdV). “Authoritative Real Estate Cadastre Information System (ALKIS®)”. (2015), [Online]. Available: https://www.adv-online.de/Products/Real-Estate-Cadastre/ALKIS/ (visited on 2023-11-25).

[115] Landesbetrieb Geoinformation und Vermessung (LGV), *Alkis - ausgewählte Daten Hamburg*, 2023. [Online]. Available: https://metaver.de/trefferanzeige?docuuid=DC71F8A1-7A8C-488C-AC99-23776FA7775E#detail_links (visited on 2023-11-26).

[116] Landesbetrieb Geoinformation und Vermessung (LGV), *Anweisung LGV 01/2015 über die Datenhaltung, Erhebung und Fortführung im Amtlichen Liegenschaftskatasterinformationssystem (ALKIS)*, de, 2015-07. [Online]. Available: https://daten.transparenz.hamburg.de/Dataport.HmbTG.ZS.Webservice.GetRessource100/GetRessource100.svc/1661832a-9978-404e-b3c9-fd0b97685dda/Akte_622.690-13_01.pdf (visited on 2023-11-12).

[117] Open Geospatial Consortium (OGC), *OGC City Geography Markup Language (CityGML) 3.0 Conceptual Model Users Guide*, 2021. [Online]. Available: http://www.opengis.net/doc/UG/CityGML-user-guide/3.0 (visited on 2023-10-22).

[118] Landesbetrieb Geoinformation und Vermessung (LGV). “3D Stadtmodell. Hamburgs neues 3D Stadtmodell”. (), [Online]. Available: https://www.hamburg.de/bsw/geodaten-des-lgv/7615476/3d-stadtmodell/ (visited on 2023-07-26).

[119] Landesbetrieb Geoinformation und Vermessung (LGV). “3D Stadtmodell. 3D-Gebäudemodelle”. (), [Online]. Available: https://www.hamburg.de/bsw/geodaten-des-lgv/17116664/3d-gebaeudemodelle/ (visited on 2023-07-26).

[120] I. Cußmann, *Data bundle for egon-data: A transparent and reproducible data processing pipeline for energy system modeling*, version 0.8, Zenodo, 2022-06. DOI: 10.5281/zenodo.6630616. [Online]. Available: https://doi.org/10.5281/zenodo.6630616.

[121] Megawatt Ingenieurgesellschaft mbH. “Machbarkeitsstudie „Klimaneutrales Wohnen in Hamburg“ veröffentlicht”. (), [Online]. Available: https://megawatt.de/blog/2023/04/06/machbarkeitsstudie-klimaneutrales-wohnen-in-hamburg-veroeffentlicht/ (visited on 2023-11-30).

[122] Megawatt Ingenieurgesellschaft mbH and Hamburg Institut GmbH, *Gutachten Energetische Quartiersentwicklung*, de, Behörde für Stadtentwicklung und Wohnen (BSW), 2023. [Online]. Available: https://www.hamburg.de/contentblob/17123654/ea66cb263aa13705ae3263dfe00c210a/data/klimaschutzziele-wohngebaeude-megawatt.pdf (visited on 2023-11-30).

[123] F. Arnold, K. Enders, T. Gniechwitz, *et al.*, *Umsetzungsorientierte Machbarkeitsstudie zur Erreichung der Klimaschutzziele im Bereich der Wohngebäude in Hamburg : Ergebnisbericht der projektbeteiligten Gutachterinnen und Gutachter*, de, Behörde für Stadtentwicklung und Wohnen (BSW), 2023. [Online]. Available: https://www.hamburg.de/contentblob/17012714/497dd54349da726739e02eb93e7b6de5/data/klimaschutzziele-wohngebaeude.pdf (visited on 2023-11-30).

[124] N. Gerhardt, D. Böttger, T. Trost, *et al.*, *Analyse eines europäischen -95%- Klimazielszenarios über mehrere Wetterjahre*, 2017. [Online]. Available: https://publica-rest.fraunhofer.de/server/api/core/bitstreams/08403917-e801-4d82-96b5-b51c3f9ff6d0/content (visited on 2023-11-30).

[125] C. Büttner, J. Amme, J. Endres, A. Malla, B. Schachler, and I. Cußmann, “Open modeling of electricity and heat demand curves for all residential buildings in germany”, *Energy Informatics*, vol. 5, no. S1, 2022-09. DOI: 10.1186/s42162-022-00201-y. [Online]. Available: https://doi.org/10.1186/s42162-022-00201-y.

[126] I. Dochev, “Urban Building Energy Modelling with Combinatorial Optimisation and Microsimulation. Application and Policy Analysis for Hamburg, Germany”, Ph.D. dissertation, 2023. DOI: 10.34712/142.42. [Online]. Available: https://repos.hcu-hamburg.de/handle/hcu/914.

[127] Behörde für Umwelt und Energie (BuE), *Wärmekataster Handbuch*, de. [Online]. Available: https://www.hamburg.de/contentblob/8679336/abfc99dc53a6f145a9daa7c93a259ce4/data/d-handbuch.pdf (visited on 2023-11-12).

[128] I. Dochev, H. Seller, and I. Peters, “Assigning energetic archetypes to a digital cadastre and estimating building heat demand. an example from hamburg, germany”, *Environmental and Climate Technologies*, vol. 24, no. 1, pp. 233–253, 2020-01. DOI: 10.2478/rtuect-2020-0014. [Online]. Available: https://doi.org/10.2478/rtuect-2020-0014.

[129] Insitut Wohnen und Umwelt (IWU). “”TABULA” - EU-Project”. (), [Online]. Available: https://www.iwu.de/1/research/gebaeudebestand/tabula-en/ (visited on 2023-11-12).

[130] European Union, *Directive 2012/27/EU of the European Parliament and the Council of 25 october 2012 on Energy Efficiency, Amending Directives 2009/125/EC and 2010/30/EU and Repealing Directives 2004/8/EC and 2006/32/EC*, 2012. [Online]. Available: https://eur-lex.europa.eu/legal-content/EN/TXT/PDF/?uri=CELEX:02012L0027-20200101&from=NL.

[131] I. Dochev, H. Seller, I. Peters, A.-L. Tschirschwitz, J. Schiewe, and E. Köhler, *Abschlussbericht zum Verbundprojekt: GEWISS - GEografisches Wärme- Informations- und SimulationsSystem: Projektlaufzeit: 01.07.2014 bis 31.12.2019*, de, 2020. DOI: 10.2314/KXP:1780128819. [Online]. Available: https://www.tib.eu/suchen/id/TIBKAT:1780128819/.

[132] D. Heidenthaler, Y. Deng, M. Leeb, *et al.*, “Automated energy performance certificate based urban building energy modelling approach for predicting heat load profiles of districts”, *Energy*, vol. 278, p. 128 024, 2023-09. DOI: 10.1016/j.energy.2023.128024. [Online]. Available: https://doi.org/10.1016/j.energy.2023.128024.

[133] *Richtlinie über Flächen für die Feuerwehr*, de, 2011-02. [Online]. Available: https://www.hamburg.de/contentblob/152976/538e6a7ea84452fdb30ed42c3a68fa6d/data/7-4-feuerwehrflaechen-juli-1998).pdf (visited on 2023-11-12).

[134] *Energy efficiency of buildings - calculation of the net, final and primary energy demand for heating, cooling, ventilation, domestic hot water and lighting - part 1: General balancing procedures, terms and definitions, zoning and evaluation of energy sources*, Norm, DIN V 18599-1, 2018-09.

[135] *Characteristic consumption values for buildings - characteristic heating-energy, electrical-energy and water consumption values*, Norm, VDI 3807 Blatt 2, 2014-11.

[136] Insitut Wohnen und Umwelt (IWU), *Gradtagzahlen-deutschland*, 2023. [Online]. Available: https://www.iwu.de/fileadmin/tools/gradtagzahlen/Gradtagzahlen-Deutschland.xlsx (visited on 2023-11-14).

[137] BDEW/VKU/GEODE, *Leitfaden “Abwicklung von Standardlastprofilen Gas”*, 2022. [Online]. Available: https://www.bdew.de/media/documents/20220331_LF_SLP_Gas_KoV_XIII_3Qo7qMf.pdf (visited on 2023-11-14).

[138] M. Hellwig, “Entwicklung und Anwendung parametrisierter Standard-Lastprofile”, de, Ph.D. dissertation, Technische Universität München, 2003, p. 152.

[139] M. Hinterstocker, B. Eberl, and S. von Roon, *Weiterentwicklung des Standardlastprofilverfahrens Gas*, de, 2015. [Online]. Available: https://www.ffe.de/wp-content/uploads/2022/08/Studie_Weiterentwicklung-SLP-Gas_FfE.pdf (visited on 2023-11-14).

[140] G. M. Huebner, M. McMichael, D. Shipworth, M. Shipworth, M. Durand-Daubin, and A. Summerfield, “Heating patterns in english homes: Comparing results from a national survey against common model assumptions”, *Building and Environment*, vol. 70, pp. 298–305, 2013-12. DOI: 10.1016/j.buildenv.2013.08.028. [Online]. Available: https://doi.org/10.1016/j.buildenv.2013.08.028.

[141] A. Malla, "Generation of high spatial and temporal resolution heat demand profiles for germany", en, 2021. [Online]. Available: https://ego-n.org/theses/2021_MA_Malla_Heat_demand_profiles.pdf.

[142] S. R. Drauz, "Synthesis of a heat and electrical load profile for single and multi-family houses used for subsequent performance tests of a multi-component energy system", en, 2016. DOI: 10.13140/RG.2.2.13959.14248. [Online]. Available: http://rgdoi.net/10.13140/RG.2.2.13959.14248.

[143] oemof Developer Group, *The oemof demandlib (oemof.demandlib)*, 2023. [Online]. Available: https://demandlib.readthedocs.io/en/latest/index.html (visited on 2023-11-15).

[144] F. Gotzens, B. Gillessen, S. Burges, *et al.*, "Demandregio - harmonisierung und entwicklung von verfahren zur regionalen und zeitlichen auflösung von energienachfragen", de, 2020. DOI: 10.34805/FFE-119-20. [Online]. Available: https://openaccess.ffe.de/10.34805/ffe-119-20.

[145] A. Bruckmeier, F. Böing, M. Hinterstocker, *et al.*, "Teilbericht Basisdaten: "Projekt MONA 2030: Grundlage für die Bewertung von netzoptimierenden Maßnahmen: Teilbericht Basisdaten"", de, 2017. [Online]. Available: https://www.ffe.de/wp-content/uploads/2021/10/20180403_MONA_2030_Teilbericht_Basisdaten.pdf.

[146] P. Esslinger and R. Witzmann, "Entwicklung und Verifikation eines stochastischen Verbraucherlastmodells für Haushalte", presented at the 12. Symposium Energieinnovation Graz, 2012.

[147] G. Kerber, "Aufnahmefähigkeit von niederspannungsverteilnetzen für die einspeisung aus photovoltaikkleinanlagen", dissertation, Technische Üniversität München, 2011. [Online]. Available: https://mediatum.ub.tum.de/doc/998003/998003.pdf (visited on 2023-11-01).

[148] H. Meier, C. Fünfgeld, T. Adam, and B. Schieferdecker, "Repräsentative VDEW-Lastprofile", *VDEW, Frankfurt (Main)*, 1999.

[149] *Number of adults by sex, age groups, number of children, age of youngest child and household composition (1 000). (2023)*, [Data set]. [Online]. Available: http://data.europa.eu/88u/dataset/hzscauqugm4ysghf0okna (visited on 2023-11-15).

[150] E. Pajares, R. M. Nieto, L. Meng, and G. Wulfhorst, "Population disaggregation on the building level based on outdated census data", *ISPRS International Journal of Geo-Information*, vol. 10, no. 10, p. 662, 2021-10. DOI: 10.3390/ijgi10100662. [Online]. Available: https://doi.org/10.3390/ijgi10100662.

[151] M. Heinrichs, D. Krajzewicz, R. Cyganski, and A. von Schmidt, "Disaggregated car fleets in microscopic travel demand modelling", *Procedia Computer Science*, vol. 83, pp. 155–162, 2016. DOI: 10.1016/j.procs.2016.04.111. [Online]. Available: https://doi.org/10.1016/j.procs.2016.04.111.

[152] Statistisches Bundesamt (Destatis), *Personen: Alter (11 Altersklassen) - Größe des privaten Haushalts - Typ des privaten Haushalts (nach Familien/Lebensform)*, 2011. [Online]. Available: https://ergebnisse2011.zensus2022.de/datenbank//online?operation=table&code=1000A-3016&bypass=true&levelindex=0&levelid=1700057588826#abreadcrumb (visited on 2023-11-15).

[153] Statistisches Bundesamt (Destatis), *Datensatzbeschreibung "Haushalte im 100 Meter-Gitter"*, 2018. [Online]. Available: https://www.zensus2011.de/SharedDocs/Downloads/DE/Pressemitteilung/DemografischeGrunddaten/Datensatzbeschreibung_Haushalt_100m_Gitter.xlsx?__blob=publicationFile&v=2 (visited on 2023-11-15).

[154] Statistisches Bundesamt (Destatis). "Data protection in the 2011 census". (2020), [Online]. Available: https://www.zensus2011.de/SharedDocs/AktuellesEN/Data_protection_in_the_2011_census.html (visited on 2023-11-24).

[155] C. Fünfgeld and R. Tiedemann, "Anwendung der repräsentative VDEW-Lastprofile step - by - step", *VDEW, Frankfurt (Main)*, 2000.

[156] Behörde für Gesundheit und Verbraucherschutz (BGV), "Bericht zum Demografie-Konzept Hamburg 2030", de, 2019. [Online]. Available: https://www.hamburg.de/contentblob/12032286/0880e17d6ef77aab152751b988daf47f/data/download-fortschreibung-demografiekonzept-hamburg2030.pdf (visited on 2023-11-18).

[157] Statistisches Amt für Hamburg und Schleswig-Holstein, "Struktur der Haushalte in den Hamburger Stadtteilen 2022. Auswertung auf Basis des Melderegisters", de, 2023. [Online]. Available: https://www.statistik-nord.de/fileadmin/Dokumente/Statistische_Berichte/bevoelkerung/A_I_11_j_H/A_I_11_j22_HH.pdf (visited on 2023-11-18).

[158] Bundesverband der Energie- und Wasserwirtschaft (bdew). "Energieeffizienz. faq zum Thema Energieeffizienz – in den Bereichen Private Haushalte, Industrie und Gewerbe und Kommunen". de. (2023), [Online]. Available: https://www.bdew.de/presse/pressemappen/faq-energieeffizienz/#Wie%5C%20hat%5C%20sich%5C%20der%5C%20Stromverbrauch%5C%20von%5C%20Haushalten%5C%20in%5C%20den%5C%20vergangenen%5C%20Jahren%5C%20entwickelt? (visited on 2023-11-14).

[159] A. Labetski, S. Vitalis, F. Biljecki, K. Arroyo Ohori, and J. Stoter, "3D building metrics for urban morphology", *International Journal of Geographical Information Science*, vol. 37, no. 1, pp. 36–67, 2023. DOI: 10.1080/13658816.2022.2103818.

[160] Behörde für Umwelt, Klima, Energie und Agrarwirtschaft (BUKEA). "Gesetzesentwurf vorgelegt Klimaschutzstärkungsgesetz". de. (2023), [Online]. Available: https://www.hamburg.de/klimaschutzgesetz/17322294/hamburgischesklimaschutzgesetz/ (visited on 2023-11-14).

[161] Behörde für Umwelt, Klima, Energie und Agrarwirtschaft (BUKEA). "Klimafreundliche Energie Photovoltaik ist Pflicht in Hamburg". de. (2023), [Online]. Available: https://www.hamburg.de/energielotsen/beratung/15147914/faqs-photovoltaikanlagen-pflicht/ (visited on 2023-11-14).

[162] Fraunhofer Institute for Solar Energy Systems (ISE), *Photovoltaics report*, 2023. [Online]. Available: https://www.ise.fraunhofer.de/content/dam/ise/de/documents/publications/studies/Photovoltaics-Report.pdf (visited on 2023-11-20).

[163] F. Omar, *A gray-box model of a two-stage heat pump for electrical load forecasting in a single-family residence*, en, 2023. DOI: https://doi.org/10.6028/NIST.TN.2249. [Online]. Available: https://tsapps.nist.gov/publication/get_pdf.cfm?pub_id=936410.

[164] X. Zhang, M. Lovati, I. Vigna, *et al.*, "A review of urban energy systems at building cluster level incorporating renewable-energy-source (res) envelope solutions", *Applied Energy*, vol. 230, pp. 1034–1056, 2018-11, ISSN: 0306-2619. DOI: 10.1016/j.apenergy.2018.09.041. [Online]. Available: http://dx.doi.org/10.1016/j.apenergy.2018.09.041.

[165] D. Coppitters, W. De Paepe, and F. Contino, "Robust design optimization of a photovoltaic-battery-heat pump system with thermal storage under aleatory and epistemic uncertainty", *Energy*, vol. 229, p. 120 692, 2021-08, ISSN: 0360-5442. DOI: 10.1016/j.energy.2021.120692. [Online]. Available: http://dx.doi.org/10.1016/j.energy.2021.120692.

[166] S. P. Koko, "Optimal battery sizing for a grid-tied solar photovoltaic system supplying a residential load: A case study under south african solar irradiance", *Energy Reports*, vol. 8, pp. 410–418, 2022-08, ISSN: 2352-4847. DOI: 10.1016/j.egyr.2022.02.183. [Online]. Available: http://dx.doi.org/10.1016/j.egyr.2022.02.183.

[167] R. G. Charles, M. L. Davies, P. Douglas, I. L. Hallin, and I. Mabbett, "Sustainable energy storage for solar home systems in rural sub-saharan africa – a comparative examination of lifecycle aspects of battery technologies for circular economy, with emphasis on the south african context", *Energy*, vol. 166, pp. 1207–1215, 2019-01, ISSN: 0360-5442. DOI: 10.1016/j.energy.2018.10.053. [Online]. Available: http://dx.doi.org/10.1016/j.energy.2018.10.053.

[168] R. Luthander, J. Widén, D. Nilsson, and J. Palm, "Photovoltaic self-consumption in buildings: A review", *Applied Energy*, vol. 142, pp. 80–94, 2015-03, ISSN: 0306-2619. DOI: 10.1016/j.apenergy.2014.12.028. [Online]. Available: http://dx.doi.org/10.1016/j.apenergy.2014.12.028.

[169] W. Cole and K. Akash, *Cost projections for utility-scale battery storage: 2023 update*, 2023. [Online]. Available: https://www.nrel.gov/docs/fy23osti/85332.pdf (visited on 2023-11-20).

[170] B. Boeckl and T. Kienberger, ""sizing of pv storage systems for different household types"", *Journal of Energy Storage*, vol. 24, p. 100 763, 2019-08, ISSN: 2352-152X. DOI: 10.1016/j.est.2019.100763. [Online]. Available: http://dx.doi.org/10.1016/j.est.2019.100763.

[171] N. Orth, J. Weniger, L. Meissner, I. Lawaczeck, and V. Quaschning, *Stromspeicher-inspektion 2022*, 2022. [Online]. Available: https://solar.htw-berlin.de/wp-content/uploads/HTW-Stromspeicher-Inspektion-2022.pdf (visited on 2023-11-22).

[172] Bundesministerium für Wirtschaft und Klimaschutz (BMWK). "Erneuerbares Heizen – Gebäudeenergiegesetz (GEG). häufig gestellte Fragen (FAQ)". (2023), [Online]. Available: https://www.energiewechsel.de/KAENEF/Redaktion/DE/FAQ/GEG/faq-geg.html (visited on 2023-11-22).

[173] D. Fischer, K. B. Lindberg, H. Madani, and C. Wittwer, "Impact of pv and variable prices on optimal system sizing for heat pumps and thermal storage", *Energy and Buildings*, vol. 128, pp. 723–733, 2016-09, ISSN: 0378-7788. DOI: 10.1016/j.enbuild.2016.07.008. [Online]. Available: http://dx.doi.org/10.1016/j.enbuild.2016.07.008.

[174] A. Franco and F. Fantozzi, "Optimal sizing of solar-assisted heat pump systems for residential buildings", *Buildings*, vol. 10, no. 10, p. 175, 2020-10, ISSN: 2075-5309. DOI: 10.3390/buildings10100175. [Online]. Available: http://dx.doi.org/10.3390/buildings10100175.

[175] T. Beck, H. Kondziella, G. Huard, and T. Bruckner, "Optimal operation, configuration and sizing of generation and storage technologies for residential heat pump systems in the spotlight of self-consumption of photovoltaic electricity", *Applied Energy*, vol. 188, pp. 604–619, 2017-02, ISSN: 0306-2619. DOI: 10.1016/j.apenergy.2016.12.041. [Online]. Available: http://dx.doi.org/10.1016/j.apenergy.2016.12.041.

[176] P. Benalcazar, "Sizing and optimizing the operation of thermal energy storage units in combined heat and power plants: An integrated modeling approach", *Energy Conversion and Management*, vol. 242, p. 114 255, 2021-08, ISSN: 0196-8904. DOI: 10.1016/j.enconman.2021.114255. [Online]. Available: http://dx.doi.org/10.1016/j.enconman.2021.114255.

[177] oemof Developer Group, *Stratified thermal storage*, 2023. [Online]. Available: https://oemof-thermal.readthedocs.io/en/latest/stratified_thermal_storage.html (visited on 2023-11-15).

[178] T. Bruckner, *Benutzerhandbuch deeco — version 1.0*, de, 2001. DOI: 10.5281/ZENODO.5148149. [Online]. Available: https://zenodo.org/record/5148149.

[179] T. Brown, D. Schlachtberger, A. Kies, S. Schramm, and M. Greiner, "Synergies of sector coupling and transmission reinforcement in a cost-optimised, highly renewable european energy system", *Energy*, vol. 160, pp. 720–739, 2018-10, ISSN: 0360-5442. DOI: 10.1016/j.energy.2018.06.222. [Online]. Available: http://dx.doi.org/10.1016/j.energy.2018.06.222.

[180] M. Lämmle, C. Bongs, J. Wapler, *et al.*, "Performance of air and ground source heat pumps retrofitted to radiator heating systems and measures to reduce space heating temperatures in existing buildings", *Energy*, vol. 242, p. 122 952, 2022-03, ISSN: 0360-5442. DOI: 10.1016/j.energy.2021.122952. [Online]. Available: http://dx.doi.org/10.1016/j.energy.2021.122952.

[181] W. Medjroubi, U. P. Müller, M. Scharf, C. Matke, and D. Kleinhans, "Open data in power grid modelling: New approaches towards transparent grid models", *Energy Reports*, vol. 3, pp. 14–21, 2017-11, ISSN: 2352-4847. DOI: 10.1016/j.egyr.2016.12.001. [Online]. Available: http://dx.doi.org/10.1016/j.egyr.2016.12.001.

[182] J. Amme, G. Pleßmann, J. Bühler, L. Hülk, E. Kötter, and P. Schwaegerl, "The ego grid model: An open-source and open-data based synthetic medium-voltage grid model for distribution power supply systems", *Journal of Physics: Conference Series*, vol. 977, p. 012 007, 2018-02, ISSN: 1742-6596. DOI: 10.1088/1742-6596/977/1/012007. [Online]. Available: http://dx.doi.org/10.1088/1742-6596/977/1/012007.

[183] Bundesamt für Sicherheit in der Informationstechnik (BSI). (), [Online]. Available: https://www.bsi.bund.de/DE/Themen/KRITIS-und-regulierte-Unternehmen/Kritische-Infrastrukturen/Allgemeine-Infos-zu-KRITIS/allgemeine-infos-zu-kritis_node.html (visited on 2023-11-24).

[184] J. Egerer, C. Gerbaulet, R. Ihlenburg, *et al.*, "Electricity sector data for policy-relevant modeling: Data documentation and applications to the german and european electricity markets", eng, Berlin, DIW Data Documentation 72, 2014. [Online]. Available: http://hdl.handle.net/10419/95950.

[185] U. P. Müller, B. Schachler, W.-D. Bunke, *et al.*, *Netzebenenübergreifendes Planungsinstrument - zur Bestimmung des optimalen Netz- und Speicherausbaus in Deutschland - integriert in einer OpenEnergyPlatform : Open_ego : Projektabschlussbericht : Open_ego : Projektzeitaum: 01.08.2015 . 31.10.2018*, Flensburg, 2019. DOI: 10.2314/KXP:1676027963. [Online]. Available: https://www.tib.eu/de/suchen/id/TIBKAT%7B%5C%%7D3A1676027963.

[186] M. Schumann, M. Meyer, M. Dietmannsberger, and S. Detlef, "Demands on the electrical grid due to electromobility in hamburg", in *Proceedings of the 1st E-Mobility Power System Integration Symposium, Berlin, Germany*, vol. 23, 2017. [Online]. Available: https://openhsu.ub.hsu-hh.de/handle/10.24405/5342.

[187] Stromnetz Hamburg. "Übersicht der Umspannwerksreserven (2022)". (), [Online]. Available: https://www.energieportal-hamburg.de/uw-reserven (visited on 2022-06-22).

[188] "Multi-objective linear programming", in *Multi-Criteria Decision Analysis via Ratio and Difference Judgement*, F. A. Lootsma, Ed. Boston, MA: Springer US, 1999, pp. 229–257, ISBN: 978-0-585-28008-0. DOI: 10.1007/978-0-585-28008-0_10. [Online]. Available: https://doi.org/10.1007/978-0-585-28008-0_10.

[189] C. Bazgan, S. Ruzika, C. Thielen, and D. Vanderpooten, "The power of the weighted sum scalarization for approximating multiobjective optimization problems", *Theory of Computing Systems*, vol. 66, no. 1, pp. 395–415, 2021-11, ISSN: 1433-0490. DOI: 10.1007/s00224-021-10066-5. [Online]. Available: http://dx.doi.org/10.1007/s00224-021-10066-5.

[190] Statistisches Amt für Hamburg und Schleswig-Holstein, "Hamburger Stadtteil-Profile. Berichtsjahr 2022", de, 2023. [Online]. Available: https://www.statistik-nord.de/fileadmin/Dokumente/NORD.regional/Stadtteilprofile2023.xlsx (visited on 2023-11-18).

[191] Statistisches Amt für Hamburg und Schleswig-Holstein, *Energiebilanz und CO2-Bilanzen für Hamburg*, de, 2023. [Online]. Available: https://www.statistik-nord.de/zahlen-fakten/umwelt-energie/energie/dokumentenansicht/product/3381/energie-und-co2-bilanzen-fuer-hamburg-361?cHash=4201529a752424c94a05eb3c4ae751ea (visited on 2023-11-18).

[192] Statistisches Amt für Hamburg und Schleswig-Holstein, *Energiebilanz und CO2-Bilanzen für Hamburg 2019*, de, 2023. [Online]. Available: https://www.statistik-nord.de/fileadmin/Dokumente/Sonderver%C3%B6ffentlichungen/Energie-_und_CO2-Bilanz_Hamburg/EB_CO2_HH_2019.xlsx (visited on 2023-11-18).

[193] Statistisches Amt für Hamburg und Schleswig-Holstein, *Energiebilanz und CO2-Bilanzen für Hamburg 2020*, de, 2023. [Online]. Available: https://www.statistik-nord.de/fileadmin/Dokumente/Sonderver%C3%B6ffentlichungen/Energie-_und_CO2-Bilanz_Hamburg/EB_CO2_HH_2020.xlsx (visited on 2023-11-18).

[194] Statistisches Amt für Hamburg und Schleswig-Holstein, *Energiebilanz und CO2-Bilanzen für Hamburg 2021*, de, 2023. [Online]. Available: https://www.statistik-nord.de/fileadmin/Dokumente/Sonderver%C3%B6ffentlichungen/Energie-_und_CO2-Bilanz_Hamburg/EB_CO2_HH_2021.xlsx (visited on 2023-11-18).

[195] Arbeitsgemeinschaft Energiebilanzen e.V. (AGEB), *Anwendungsbilanzen zur Energiebilanz Deutschland: Endenergieverbrauch nach Energieträgern und Anwendungszwecken*, de, 2020. [Online]. Available: https://ag-energiebilanzen.de/wp-content/uploads/2020/10/ageb_20v_v1.pdf (visited on 2023-11-26).

[196] Arbeitsgemeinschaft Energiebilanzen e.V. (AGEB), *Anwendungsbilanzen zur Energiebilanz Deutschland: Endenergieverbrauch nach Energieträgern und Anwendungszwecken*, de, 2023. [Online]. Available: https://ag-energiebilanzen.de/wp-content/uploads/2023/01/AGEB_21p2_V3_20221222.pdf (visited on 2023-11-26).

[197] Dimplex, *Projektierungshandbuch: Projektierungs- und Installationshandbuch. wärmepumpen für Heizen und Warmwasserbereitung*, 2022. [Online]. Available: https://dimplex.de/sites/default/files/20220913_Projektierungshandbuch_de.pdf (visited on 2023-11-30).

[198] STIEBEL ELTRON GmbH & Co. KG, *Planung und Installation: Luft-Wasser-Wärmepumpen, Sole-Wasser–Wärmepumpen, Wasser-Wasser-Wärmepumpen*, 2021. [Online]. Available: https://www.stiebel-eltron.de/content/dam/ste/de/de/products/downloads/Planungsunterlagen/Planungshandbuch/Planungshandbuch_EE_Waermepumpen.pdf (visited on 2023-11-25).

[199] M. Geraedts, J. Alpizar-Castillo, L. Ramirez-Elizondo, and P. Bauer, "Optimal sizing of a community level thermal energy storage system", in *2022 IEEE 21st Mediterranean Electrotechnical Conference (MELECON)*, IEEE, 2022-06. DOI: 10.1109/melecon53508.2022.9842945. [Online]. Available: http://dx.doi.org/10.1109/MELECON53508.2022.9842945.

[200] *Heating systems with heat pumps in single and multi-family houses planning, construction, operation*, Norm, VDI 4655, 2023-04.

[201] Umweltbundesamt. "Energieeffiziente Produkte". (2023), [Online]. Available: https://www.umweltbundesamt.de/daten/private-haushalte-konsum/konsum-produkte/energieeffiziente-produkte#stromverbrauch-der-haushalte (visited on 2023-12-27).

[202] GEF Ingenieur AG, Institut für Energie- und Umweltforschung gGmbH (ifeu), and badenova-Gruppe, *Masterplan wärme freiburg 2030*, Stadt Freiburg im Breisgau - Umweltschutzamt, 2021. [Online]. Available: https://www.freiburg.de/pb/site/Freiburg/get/params_E-1496368127/2021233/Masterplan_Waerme_Freiburg%5C%202030_barrierearm.pdf (visited on 2023-12-10).

[203] Agora Energiewende and Forschungsstelle für Energiewirtschaft e. V., *Haushaltsnahe Flexibilitäten nutzen. wie Elektrofahrzeuge, Wärmepumpen und Co. die Stromkosten für alle senken können.* de, 2023. [Online]. Available: https://www.agora-energiewende.de/fileadmin/Projekte/2023/2023-14_DE_Flex_heben/A-EW_315_Flex_heben_WEB.pdf (visited on 2023-12-27).

[204] Geschäftsstelle der Plattform Klimaneutrales Stromsystem (PKNS), *Bericht über die Arbeit der Plattform Klimaneutrales Stromsystem (PKNS)*, 2023. [Online]. Available: https://www.bmwk.de/Redaktion/DE/Downloads/P-R/erster-bericht-ueber-die-arbeit-der-pkns.pdf?__blob=publicationFile&v=4 (visited on 2023-12-27).

[205] Bundesministerium für Wirtschaft und Klimaschutz (BMWK), *Stromspeicher-strategie. Handlungsfelder und Maßnahmen für eine anhaltende Ausbaudynamik und optimale Systemintegration von Stromspeichern*, 2023. [Online]. Available: https://www.bmwk.de/Redaktion/DE/Downloads/S-T/stromspeicherstrategie-231208.pdf?__blob=publicationFile&v=2 (visited on 2023-12-27).

[206] M. Willuhn. "BMWK legt Stromspeicherstrategie zur Konsultation vor". (2023), [Online]. Available: https://www.pv-magazine.de/2023/12/18/bmwk-legt-stromspeicherstrategie-zur-konsultation-vor/ (visited on 2023-12-27).

Appendices

A.1 Digital Appendices

The following additional content can be found on the accompanying storage medium:

MA_Package.zip This zip data contains the codes developed in this work, structured as a Python package. It can be installed as a standalone library.

configuration.yml This file contains a nested dictionary with the configuration settings to be used during the calculation. The settings also include connection parameters for the database connections. This file is intended to be used in conjunction with the developed Python package.

datasets.yml This file contains a nested dictionary with the configuration settings for a portion of the required datasets. It is intended to be used in conjunction with the developed Python package.

TABULA_HH_2023.xlsx This file contains the specific heat consumption for different building archetypes (Table 5.7) calculated using the TABULA reference method and climate parameters shown in Table 5.6.

1000A-3016.csv This file contains the required household information from the 2011 German Census for Hamburg (NUTS-1). Currently, this data set cannot be automatically downloaded from the census database.

Workflow.ipynb In this file, the sequence of functions used for the developed methodology is provided. It is intended to be used in conjunction with the developed Python package. Additionally, within the file, further information regarding external datasets used in this work is provided. To use this file, either JupyterLab or Jupyter Notebook is required.

Results.zip This zip data contains the raw data required to generate the figures shown in Chapter 7.

Erklärung zur selbstständigen Bearbeitung einer Abschlussarbeit

Hiermit versichere ich, dass ich die vorliegende Arbeit ohne fremde Hilfe selbständig verfasst und nur die angegebenen Hilfsmittel benutzt habe. Wörtlich oder dem Sinn nach aus anderen Werken entnommene Stellen sind unter Angabe der Quellen kenntlich gemacht.

Ort	Datum	Unterschrift im Original